Parametric Analysis of Permanent Mould Material EN31 Steel using Ball End Solid Rotating Core Magnetorheological Finishing Process

A Dissertation Submitted
In Partial Fulfillment of the Requirements
for the Degree of

Master of Engineering
in
Production Engineering

By

Sahil Maan

to the

MECHANICAL ENGINEERING DEPARTMENT
THAPAR UNIVERSITY, PATIALA

July, 2016

CERTIFICATE

I hereby declare that the thesis entitled "**Parametric analysis of permanent mould material EN31 using ball end solid rotating core magnetorheological finishing process**" is an authentic record of my study carried out as requirements for the award of the degree of **Master of Engineering** in **Production Engineering** at **Thapar University, Patiala** under the supervision of **Dr. Anant Kumar Singh**, Assistant Professor, Mechanical Engineering Department, Thapar University, Patiala during July, 2016. The matter embodied in this report has not been submitted in partial or full to any other university or institute for the award of any degree.

Date: 15-07-2016

Sahil Maan

It is certified that the above statement made by the student is correct to the best of my/our knowledge and belief.

15/07/2016

Dr. Anant Kumar Singh
Assistant Professor
Mechanical Engineering Department
Thapar University, Patiala - 147004

Countersigned by

Dr. S. K. Mohapatra
Sr. Professor & Head
Mechanical Engineering Department
Thapar University, Patiala - 14700

Dr. S. S. Bhatia
Dean of Academic Affairs
Thapar University, Patiala - 147004

Dedicated

to

My Mother

who taught me

to

read and write

Acknowledgements

I would like to express a deep sense of gratitude and thank profusely to my thesis guide **Dr. Anant Kumar Singh** for his sincere & invaluable guidance and suggestions which inspired me to submit thesis report in the present form. I would also like to thank all the faculty and staff members of mechanical engineering department for their intellectual support and unyielding encouragement.

(Sahil Maan)

Abstract

Most plastic products are produced by the process of permanent mould casting as it is the most efficient and economical process. In some plastic product applications, aesthetics and surface topography play a vital role and in such cases the surface roughness of the permanent mould directly affects the final product. For such plastic products, those are to be produced by the process of permanent mould casting, the permanent mould being used, should have its surface roughness value as low as possible. EN31 is one of the most widely used materials for permanent mould manufacturing. Being hard, the mould manufactured using EN31 material is very tough to finish. The existing traditional process for finishing the moulds using die grinders make the process of finishing a very tedious task. Recently developed ball end magnetorheological finishing process has demonstrated its feasibility in finishing of flat as well as 3D surfaces of various materials. In the present work, its potential advantages have been used to finish hardened EN31 steel. The response surface method has been used to obtain the optimized parameters that can be used for finishing of hardened EN31 material. For the experimentation, the ball end solid rotating core magnetorheological finishing process has been used. The effects of five different variable parameters, that are, current, tool rotation, feed, abrasive concentration and carbonyl iron particles concentration on the percentage change in roughness value have been examined. Each variable parameter has 5 levels and these levels were decided on the basis of previous literature and preliminary experimentation conducted. Current was varied from 1 A to 5 A, tool rotation from 700 rpm to 2300 rpm, feed from 10 mm/min to 50 mm/min, abrasive concentration from 10 % to 30 % and CIP concentration from 10% to 30%. It was observed that maximum contribution was given by CIPs followed by tool rotation, abrasive concentration, current and feed. The minimum average roughness value obtained was 30 nm at 2A current, 1900 rpm tool rotation speed, 40 mm/min feed rate, 25 vol. % abrasive concentration and 25 vol. % CIP concentration in a given time of 60 minutes. After parametric optimization, the average surface roughness obtained was 24 nm at 2A current, 2300 rpm tool rotation, 50 mm/min feed, 15 vol. % abrasive concentration and 30 vol. % CIP concentration in just 40 minutes. Scanning electron microscope was also used for studying the surface morphology.

Contents

List of Figures

List of Tables

Nomenclature

R_a = Average roughness value

R_z = Average distance between the highest peak and the lowest valley in each sampling length

R_q = Root mean square value

Ra_i = Initial average roughness value

Ra_f = Final average roughness value

ΔR_a = change in average roughness value

$\% \Delta R_a$ = Percentage change in roughness

Greek Symbols

μ = Micro

Acronyms

I = Current

N = Rotation speed of tool core

F = Feed rate

A = Abrasive concentration

C = Carbonyl iron particle concentration

RMS = Root mean square

DoF = Degree of freedom

2FI = Two factor interaction

S.D = Standard deviation

C.V = Coefficient of variance

C.I = Confidence interval

VIF = Variance inflection factor

CIP = Carbonyl iron particles

AFM = Abrasive flow machining

CMP = Chemo mechanical polishing

MAF = Magnetic abrasive finishing

MRF = Magnetorheological finishing

MFP = Magnetic float polishing

MJF = Magnetorheological jet finishing

MRAFF = Magnetorheological abrasive flow finishing

BEMRF = Ball end magnetorheological finishing

MRP = Magnetorheological polishing

MRR = Material removal rate

SEM = Scanning electron microscope

SPI = Society of plastic industries

RSM = Response surface method

ANOVA= Analysis of Variance

Chapter 1

Introduction

1.1 Introduction

Surface roughness is the deviation of surface from the ideal flat. As it is know that there is nothing perfect in this world, hence in this context one can imply that roughness of a surface can never be eliminated but can only be reduced. The process of reducing the surface roughness of a material is called surface finishing. The requirement of the extent of surface finishing can be different for everyone. For a permanent mould manufacturer the extent or the level of surface finishing process required could be very high; however for a spanner manufacturer the surface finishing process required could be of very low level. The extent to which the roughness of surface is reduced by various processes can be categorized broadly as traditional and advanced finishing processes.

1.2 Traditional Finishing Processes

There are various traditional finishing processes such as honing, lapping, grinding etc. are commonly implied in the industries. The traditional finishing processes are not well suited for obtaining high level of finishing because of the constraint of size and profile of the material, the absence of control of forces exerted by the tool during finishing and the heat generated during the process. Grinding, lapping and honing are few of the several traditional finishing processes.

1.2.1 Grinding Process

Grinding is one of the easiest available among various machining processes for finishing of the different types of material and which can also be difficult to machine by any other finishing processes ranging from simple rubber to the hardest material [Khanna and Lal, 2010]. Grinding is based on the mechanism of relative motion between workpiece and abrasive particles of the grinding wheel, Fig. 1.1.

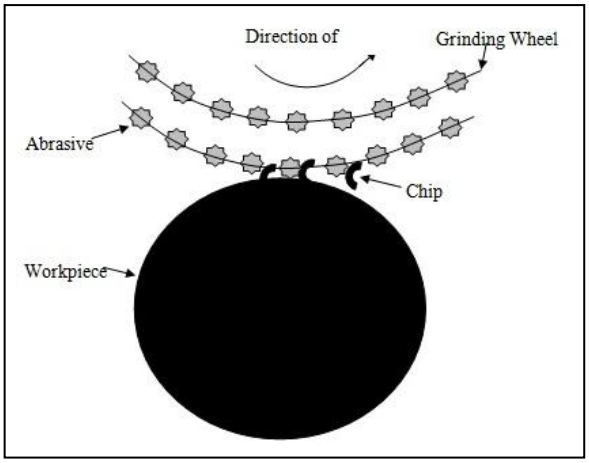

Figure 1.1: Mechanism of grinding process [Jha and Jain, 2005]

A thin layer of workpiece material is removed by the protruding active abrasive grains and the process is capable of producing surface roughness as low as 1µm or lesser in some cases.

1.2.2 Lapping Process

Lapping is the process which works on the principle of three body abrasive wear. The percentage change in roughness value changes directly in relation with the normal force applied. It is one of the low speed, low pressure operation that results in tremendous accuracy, modification of small imperfections in shape, improvement in surface finish and also exceptionally close fitted structure. Flat surface lapping is the most widely used among all the lapping processes [Lynah *et al*., 1989; Owat, 2002]. The abrasive particles are placed between the lap surface and the workpiece and the abrasive action takes place with the relative motion between the three under pressure, Fig. 1.2.

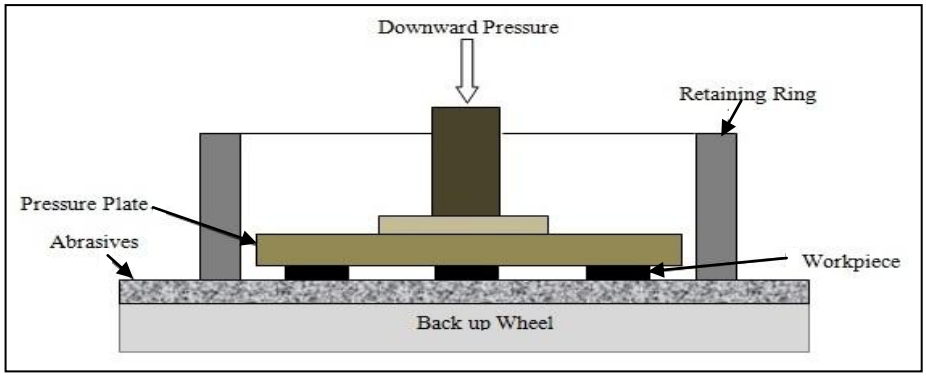

Figure 1.2: Mechanism of lapping process [Khanna and Lal, 2010]

1.2.3 Honing Process

Honing process is particularly used for cylindrical (internal and external) surfaces. It is also used where there is high requirement of geometric and form accuracy in order to produce precise parts [Schnitzler, 2001; Schmitt *et al*., 2011; Todd *et al*., 1994]. With the help of this process dimensional, geometric tolerances and low surface roughness can be attained in a very narrow range. Honing process can be employed just after the drilling or boring operation has been performed [Tolinski, 2008]. The mechanism of honing process for finishing of internal surface of a hallow cylinder is as shown in Fig. 1.3. The lay pattern on the workpiece surface is of cross hatched type. This cross hatched pattern helps in retaining oil on the surface of the workpiece and thus the surface has good oil retaining properties. A larger area is covered in the process of honing, therefore the rise in temperature is less and thus the thermal damage to the workpiece surface is also low.

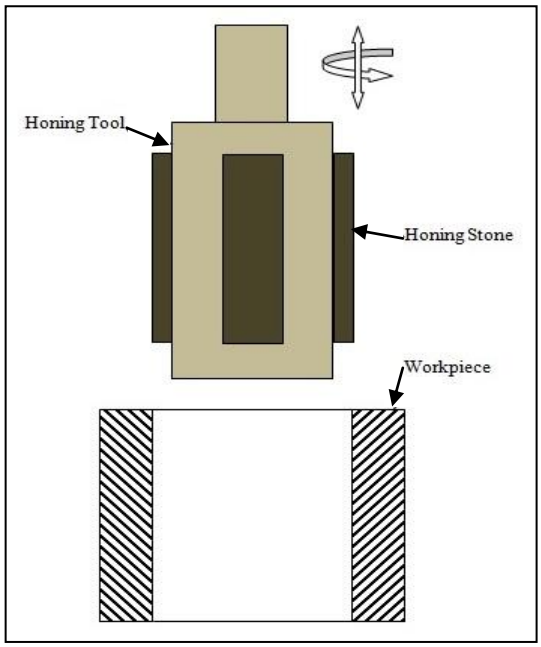

Figure 1.3: Mechanism of honing process [Schmitt and Bahre, 2014]

1.3 Advanced Finishing Process

With the advancement in technology, there is a great demand for highly finished and precise components in every type of industry. Advanced finishing processes have been developed in order to overcome the limitations of the traditional finishing processes. Abrasive flow machining (AFM) [Rao, 2011], chemo mechanical polishing (CMP) [Jain, 2009] etc. are a few of the advanced finishing processes. In recent years, some new

advanced finishing processes have been developed which make the use of magnetic field as a process control parameter. Few of these processes are magnetic abrasive finishing (MAF) [Shinmura *et al.,* 1985], magnetorheological finishing (MRF) [Harris, 2011], magnetorheological abrasive flow finishing (MRAFF) [Jha and Jain, 2004], magnetic float polishing (MFP) [Komanduri, 1996] and ball end magnetorheological finishing (BEMRF) [Singh *et al.*, 2012].

1.3.1 Magnetic Abrasive Finishing

In this process either bonded or non bonded particles can be used. When the tool is rotated at high speed, the abrasive particles in the non bonded powder tend to separate from the iron particles under the influence of centrifugal force. Thus to overcome this problem bonded particles are used. Bonded particles are nothing but sintered ferromagnetic and abrasive particles. This process does not use MR fluid but instead the ferromagnetic abrasive particles are directly applied magnetic field such that they align themselves in the working gap. Figure 1.4 shows the view of magnetic field produced during this process.

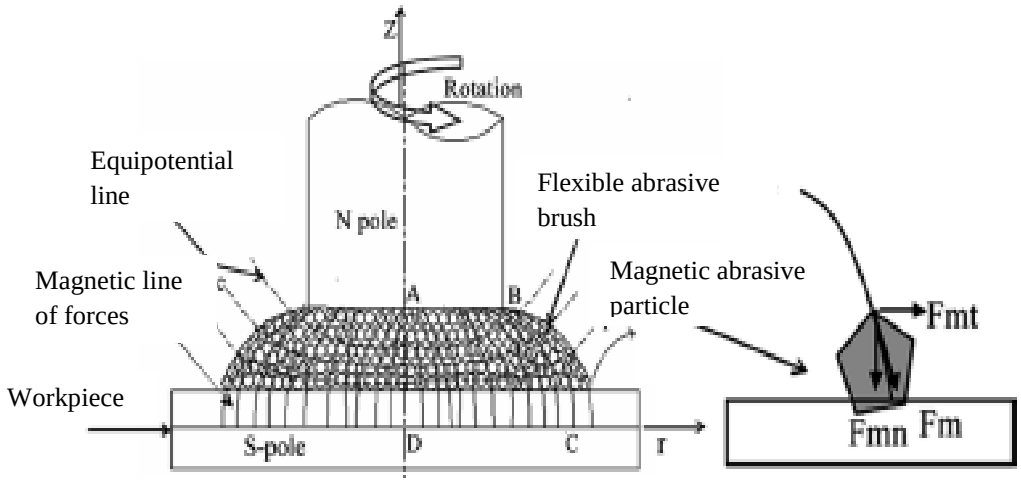

Figure 1.4: Enlarged view of the machining zone, workpiece and electromagnet [Jain, 2008]

The abrasive particles align themselves to the electromagnet holder such that flexible magnetic abrasive brush is formed. Supply can be given in two ways: Pulsating or Static. With lower duty cycles the surface morphology was much better as the scratches were removed from the surface [Jain, 2009].

1.3.2 Magnetorheological Finishing

This process is mainly used for finishing of lenses which are usually made of brittle material and tend to crack during machining [Harris, 2011]. This process also uses magnetorheological fluid which is a suspension of ferromagnetic particles dispersed in a non magnetic carrier medium. The diagram of a setup by Kordonski [1996] is shown in Fig. 1.5. In this process a wheel is rotated and the MR polishing fluid is delivered to it with help of a nozzle and magnetic field is applied across the wheel so that the fluid which comes in the magnetic line of forces gets stiffened and performs finishing. The workpiece or in this case a lens is brought in from the top using a computer controlled arm which hold the workpiece and suspends it on the fluid which is on the rotating wheel. The lens is kept in the area where magnetic field is present. Since columnar structures have formed in the fluid and energy is required to deform them so this force is applied by the workpiece and thus the workpiece is finished. Since the size of the abrasive particles and the normal force applied by these particles is very small thus the material removed is very small and thus a nano level of finishing is obtained.

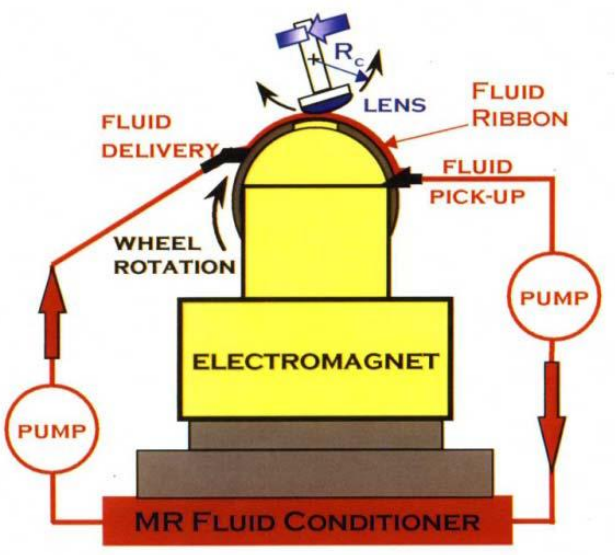

Figure 1.5: Schematic set up of MRF machine [Harris, 2011]

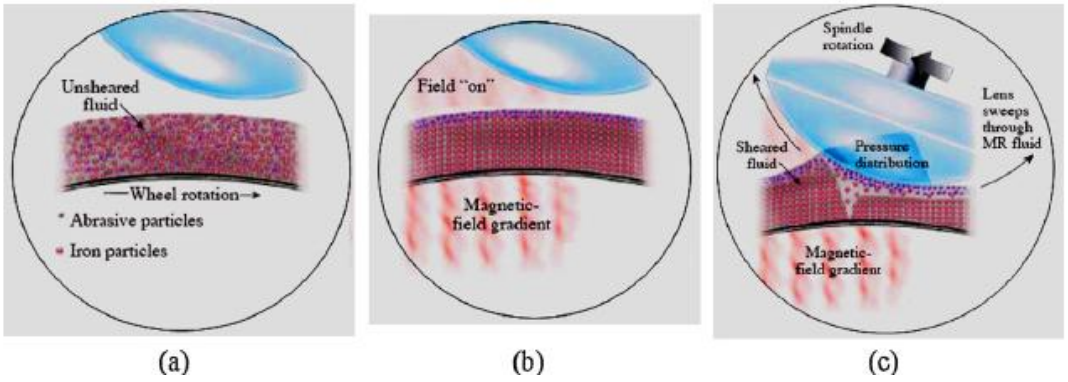

Figure 1.6: Material removal Process, a lens being processed [Mathur *et al.*, 2003]

In Fig. 1.6, (a) is showing the fluid under no magnetic field, (b) shows the fluid when under magnetic field; the particles form chain like structure and (c) shows fluid and workpiece interaction region. A variety of materials can be finished using this process ranging from optical glasses to hard crystals. The process has a limitation of finishing complex 3D surfaces.

1.3.3 Magnetorheological Abrasive Flow Finishing

In this process the finishing fluid i.e. a mixture of abrasives in viscous base medium, acts as self deformable stone and the shape limitation of other processes is overthrown. It is quite similar to abrasive flow machining process in which the fluid medium properties cannot be controlled by external force. In MAFF the carried medium contains carbonyl iron particles and abrasives. This process can also be called as the hybridization of AFM process with MRF as the process can be deterministically controlled by applying magnetic field [Jain and Jha, 2004]. Nano level roughness level can be achieved on internal as well as external surfaces using this process. In this process, for internal geometries, the fluid is pushed in from both sides one by one using hydraulic cylinders such that it replicates a reciprocating motion and the portion of the part where finishing is required, magnetic field is applied across it. Now the portion of the part where magnetic field occurs becomes stiff and because of the relative medium between the fluid and the geometry, the part gets finished. This process can particularly finish geometries where other processes may not because of the uniqueness of adjusting itself to the geometries in the blind area.

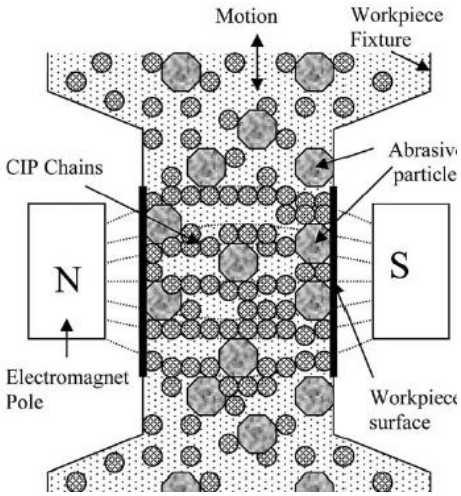

Figure 1.7: Chain like structure formed under the influence of magnetic Field in MRAFF [Jain, 2009]

Figure 1.7 shows that when magnetic field is applied across the geometry the CIP particle in the fluid form column like structure with abrasives entangled between the CIP chains.

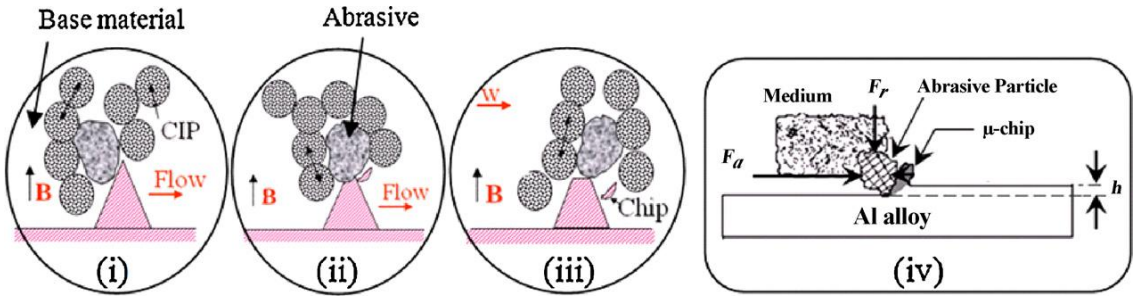

Figure 1.8: (i), (ii), (iii) show the three steps of material removal and (iv) the formation of chip is displayed [Jain, 2009]

1.3.4 Magnetic Float Polishing

Magnetic float polishing process is used for spherical parts e.g. bearing rollers and ceramics balls can be precisely finished with the help of fine abrasive particles. The mechanism of magnetic float polishing process is shown in Fig. 1.9. A levitation force which is generated due to the ferro-hydrodynamic behaviour of the magnetic fluid, acts on the non magnetic particles suspended in it. The magnetic field gradient that is very small and can be controlled is responsible for controlling the levitation force [Komundri, 1996]. In this process a bank of electromagnets is placed under a flat surface. The

ferrofluid is attracted downwards with action of magnetic field and an upward buoyant force acts on the non magnetic material. This buoyant force pushes the non magnetic particles to the area of lower magnetic field. As the abrasive grains and the ceramic balls are of non magnetic material thus they are levitated by the fluid towards the top. The drive shaft is fed downwards so as to press them down to attain a particular force level. Under the influence of levitation force, the balls are finished due to the relative motion between the abrasive particles and the balls.

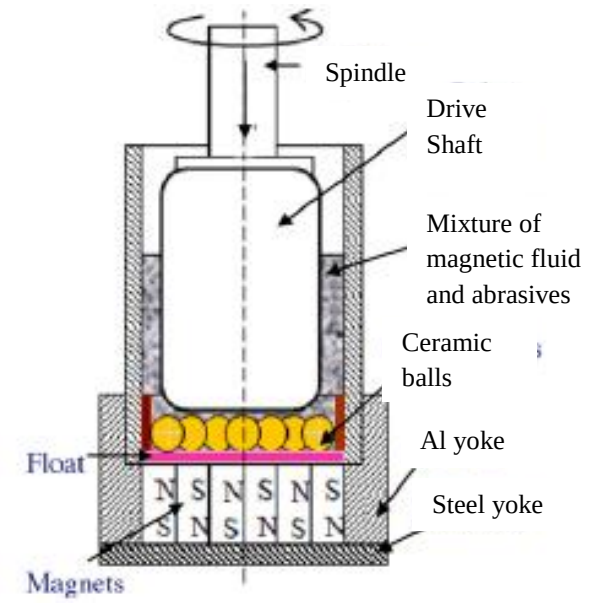

Figure 1.9: Ceramic balls being pressed by the drive shaft to perform finishing [Jain, 2009]

In the Fig. 1.9, shown is a schematic diagram of the setup, it can be seen that the balls are being pressed down against the levitation force because of the magnetic flied applied to the MR fluid.

1.3.5 Magnetorheological Jet Finishing

The magnetorheological jet finishing has been newly developed for finishing of freeform optics, steep concave optics, cavities etc. The setup for magnetorheological jet finishing is as shown in Fig. 1.10. In this type of MR finishing process, a jet of MR fluid is thrown into the internal surface or the geometry of the workpiece and an axial magnetic field is applied to it when the jet is out of the nozzle [Kordonski *et al.*, 2006]. The magnetic abrasive particles finish the internal surface of the work material more precisely. The jet snapshot image of magnetic abrasive jet finishing is shown in Fig. 1.11. The jet of water

loses its coherence when passes through the nozzle. When the magnet is off, the jet of MR fluid passes through nozzle losses its coherence due to its high viscosity. When the magnet is on, the stable jet of MR fluid passes through the nozzle with low viscosity and high velocity jet as shown in Fig. 1.11.

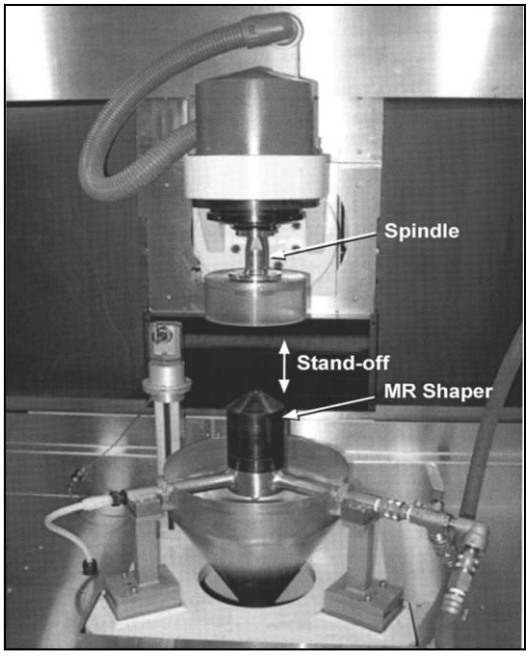

Figure 1.10: Experimental setup of magnetorheological jet finishing [Kordonski *et al.*, 2006]

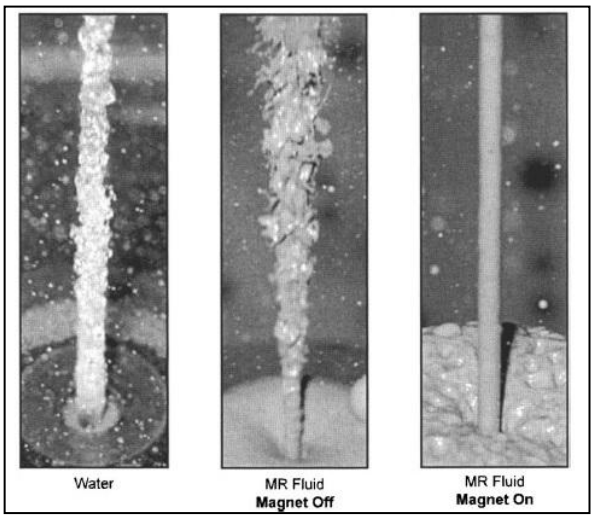

Figure 1.11: Jet snapshot image (velocity- 30 m/s, nozzle diameter- 2 mm) [Kordonski *et al.*, 2006]

1.3.6 Ball End Magnetorheological Finishing

The flexibility to finish 3D intricate surfaces makes this process very unique. Like other MR finishing processes this process has also very good control over forces and thus

produces highly finished surfaces. When MRP fluid is applied at the tip and the magnetic field is switched ON, the rheological properties of the fluid change [Singh *et al.*, 2012]. The abrasives and carbonyl iron particles form chain like structure. The fluid on the surface of the tool tip forms a ball of MR Fluid and hence the name given to the process. The schematic of BEMRF setup has been shown in Fig. 1.12. Due to the higher shear strength, the carbonyl iron particles chains will be able to hold abrasive particles more tightly and robustly when subjected to finishing operation. Due to higher magnetic field the penetration of abrasive particles will increase, Fig. 1.13(a). The MRP fluid rotates on a particular spot on the surface of the workpiece. Due to high shear strength of the MRP fluid, the abrasive particles mixed in it, cut the peaks on the workpiece surface in the form of microchips due to higher shear strength attained by the fluid as shown in Fig. 1.13(b). As continuous feed is provided to the workpiece, finishing action is performed on whole of the workpiece surface leading to overall reduction in surface roughness as shown in Fig. 1.13(c).

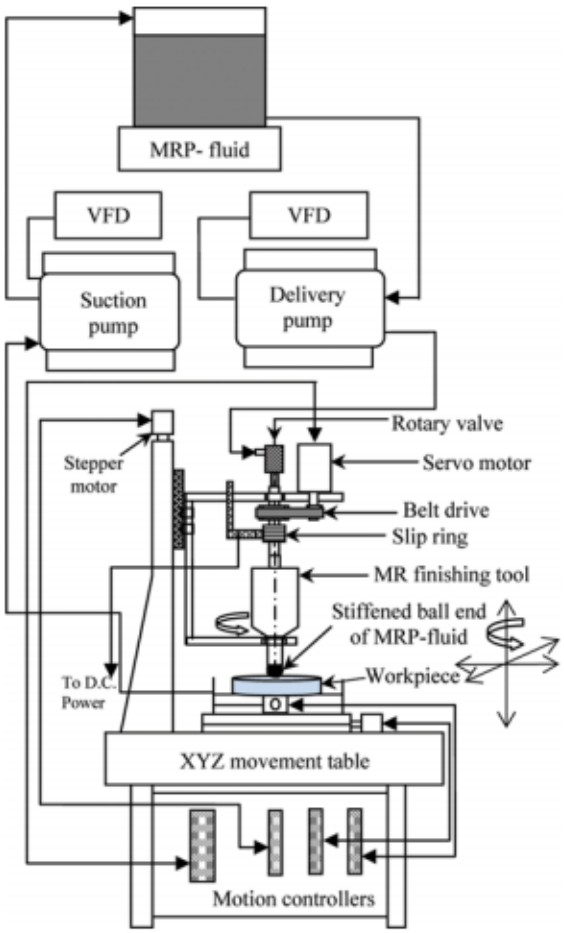

Figure 1.12: Schematic of ball end magnetorheological finishing [Singh *et al.*, 1012]

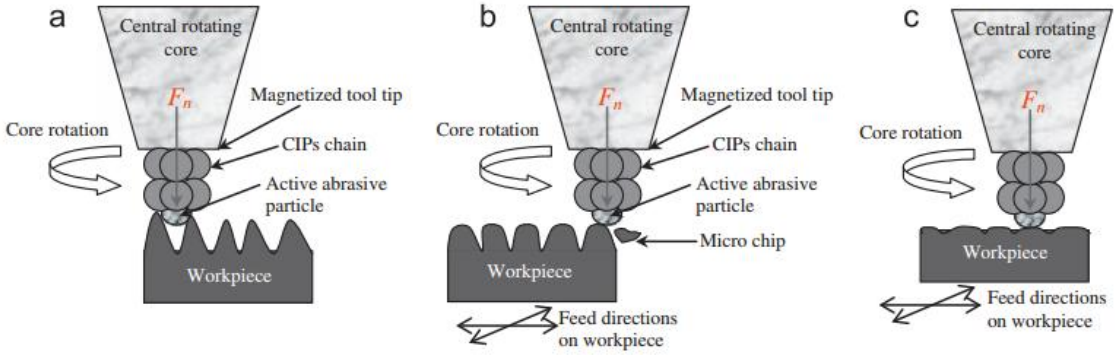

Figure 1.13: Mechanism of material removal in ball end magnetorheological finishing [Singh *et al.*, 2012]

The photograph of BEMRF setup has been shown in Fig. 1.14. The setup uses a low temperature bath to cool off the tool as the heat generated by the electromagnetic coil which may lead to change in rheological properties of the MRP fluid. The current to the electromagnetic coil is provided by the DC regulated supply.

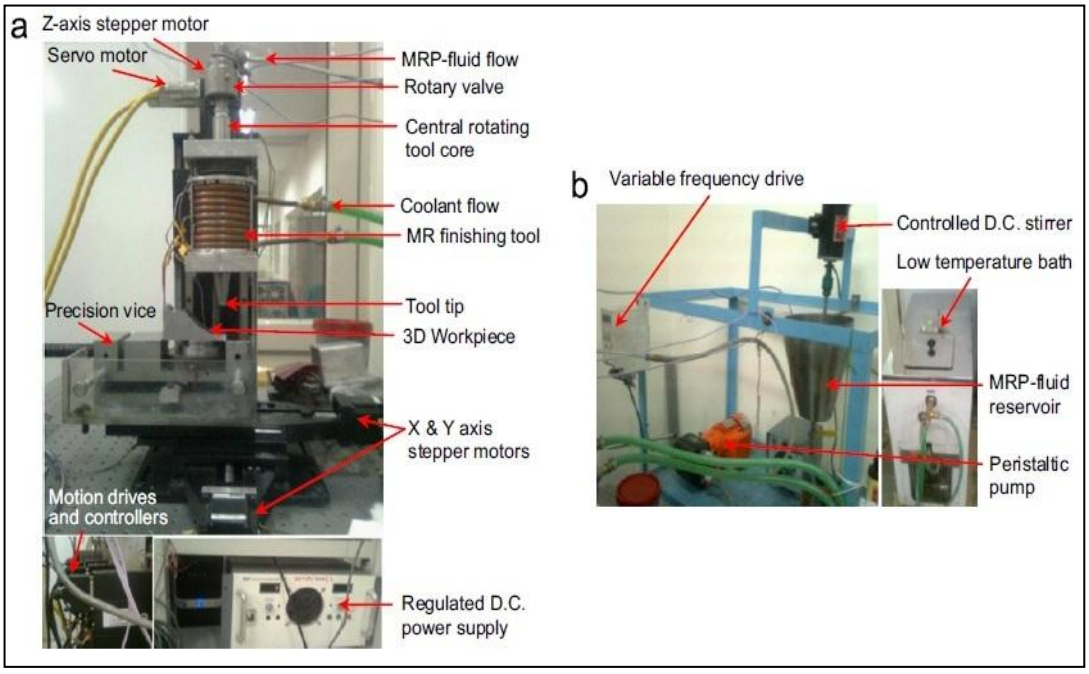

Figure 1.14: Experimental setup of ball-end magnetorheological finishing process and (b) MR polishing (MRP) fluid preparation and delivery system [Singh *et al.*, 2012]

1.4 Permanent Mould and the Need of Nanofinishing

Permanent mould is a container which is used to give particular shape to the product for which it is manufactured. A permanent mould can be made of different number of parts depending on the complexity of the product for which it is being manufactured. Generally, a permanent mould is made of two parts namely cavity block and punch as shown in Fig. 1.15.

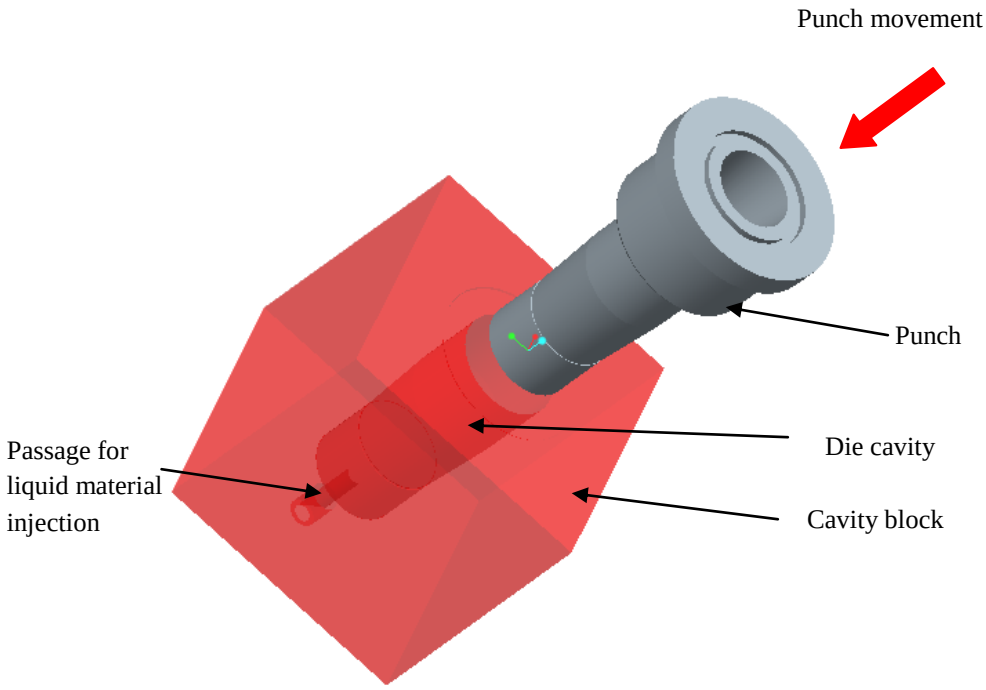

Figure 1.15: A 3D arrangement of permanent mould punch with die cavity

These two parts are mated to achieve the cavity for casting the final plastic cap products. In this manufacturing process, molten plastic is injected into the cavity of the mould through a pre-machined hole and the temperature is kept low around the cavity so that the plastic retains the shape which is imparted to it. The processed plastic cap product is ejected out of the cavity by retracting the punch of permanent mould in use. The surface finish of the mould is of prime importance as it affects the appearance and frictional characteristics of plastic products. For obtaining the smoothness with high quality of plastic products, the moulds used for casting the plastic cap products should have surface roughness in nanometer range. Generally, the process of finishing a permanent mould requires hand held tools, known as die grinders [Monroe, 1996] and thus the process has a prerequisite of very high skill level. Moreover, the materials used

for mould manufacturing are very hard and it makes the process of finishing a tedious task [Mateo, 2011]. The existing finishing processes for mould finishing are traditional in nature. Micro-cracks, micro structural changes, heat affected zone etc. are few of the sub surface defects which are induced during traditional finishing whereas advanced finishing processes have been known for obtaining a high degree of surface finish with almost no surface defects [Jain, 2008].

The need of such high level of finishing and the disadvantages associated with the use of traditional finishing process in case of permanent moulds motivated the author for doing the research in this area. The work involved will help in applying an advanced finishing process in the area of permanent mould finishing with optimised parameters so that the process is not only feasible but also efficient.

Chapter 2

Literature Review

2.1 General

In this chapter, the literature of different processes as per the applications has been discussed. Also, the experimentation done till now to obtain the effects of different parameters on machining rate and surface roughness value have been reported.

2.2 Review of the literature

Mori *et al*. (2003) carried out the work on the effect of electric current on the forces while working on magnetic abrasive polishing apparatus for finishing of SUS-304 stainless steel. The authors found that with the increase in electric current from 0.5-5 Amp, the normal force increases, whereas with the increase in weight of magnetic abrasive, the normal force and tangential force increases simultaneously.

Yamaguchi and Shinmura (2004) performed the experiment on alumina ceramic tube using magnetic assisted finishing process. The experimentation was performed by using different iron particle (150, 330 and 510 µm), diamond abrasive (0-1, 2-4, 4-8 and 8-12 µm) and lubricant (0.1, 0.2, 0.25, 0.3 and 0.35 ml). The results concluded that with the use of iron particle (330 µm), diamond abrasive (0-1 µm) and lubricant (30 ml), the surface roughness reduced to 0.02 µm.

Yin and Shinmura (2004) worked on vibration assisted magnetic finishing process. They compared the output on three different substrates. The finishing was carried out with processed iron particles, magnetic alumina and straight oil type grinding fluid on magnesium alloy (AZ31B), stainless steel (SU304) and brass (C2680). It was found that the outputs – surface roughness and deburring were better in case of magnesium alloy (AZ31B) as compared to other 2 materials.

Jha and Jain (2004) worked on magnetorheological abrasive flow finishing process. They reported the effect of magnetic field strength at different levels on the surface finish of stainless steel. MRP fluid (consisting of 20% CIPs, 20% SiC abrasive powder and 60% viscous base medium) was used as a medium to finish the workpiece surface. It

was observed that with increase in magnetic field strength, the value of average surface roughness decreased as illustrated in Fig. 2.1.

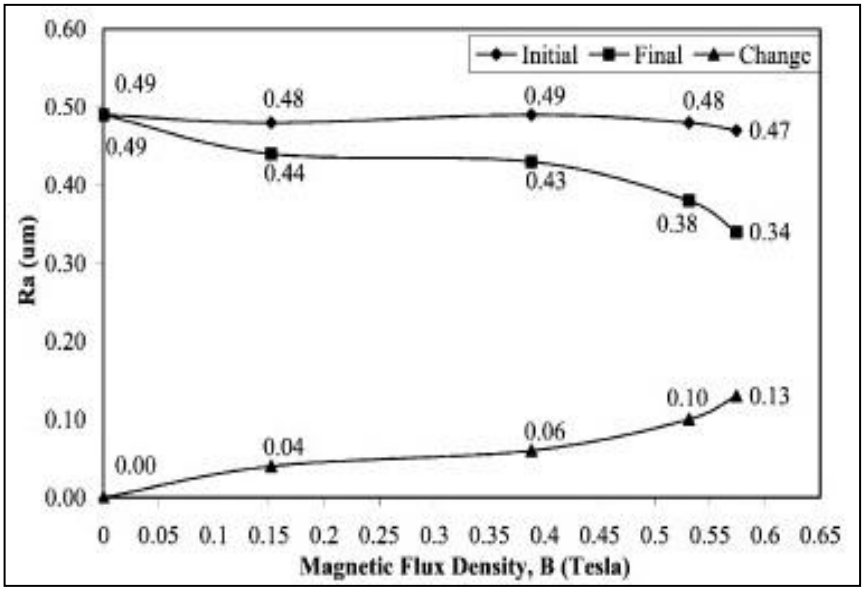

Figure 2.1: Effect of magnetic field strength on Ra value [Jha and Jain, 2004]

Wang and Hu (2005) compared the performance of surface roughness and MRR with finishing time by using a magnetic assisted finishing process for finishing of Ly12 aluminum alloy, 316L stainless steel and H62 brass. The experimentation was carried out with 4 different types of abrasive particle were Al_2O_3/Fe (20% Al_2O_3), TiC/Fe (20% TiC), TiC/Fe (35% TiC), TiC/Fe (7% TiC) along with a finishing fluid (stearinic acid and transformer oil). The results concluded that the value of MRR increases with increases in finishing time, whereas the surface roughness value decreases with increase in finishing time.

Jha and Jain (2006) analyzed the effect of different grades of CIPs particles (CS and HS) on the surface roughness by using magnetorheological abrasive flow finishing process for finishing of stainless steel. The finishing was done by MRP fluid (consisting of 20% CIPs, 20% SiC abrasive powder and 60% viscous base medium). It was observed that higher improvement in surface roughness between 0.32-0.09 µm was made by using CIPs (CS) with SiC-800 mesh size as illustrated in Table 2.1.

Table 2.1: Surface roughness results [Jha and Jain, 2006]

Expt. No.	CIP dia. (D_{CIP}) (µm)	SiC dia. (D_{SiC}) (µm)	D_{CIP}/ D_{SiC}	Initial Ra (µm)	Final Ra (µm)	ΔRa^a (µm)	%ΔRa
1.	18.0 (CS)	19.00	0.95	0.32	0.09	-0.23	-17.87
2.	18.0 (CS)	12.67	1.42	0.28	0.17	-0.11	-39.28
3.	18.0 (CS)	7.50	2.40	0.31	0.23	-0.08	-25.80
4.	3.5 (HS)	19.00	0.18	0.26	0.23	-0.03	-11.54
5.	3.5 (HS)	12.67	0.28	0.28	0.24	-0.04	-14.28
6.	3.5 (HS)	7.50	0.47	0.25	0.24	-0.01	-4.00

Jain (2008) studied the performance of different abrasive flow finishing processes for making a precise finishing in the level of nanometer without producing any damage to the work material. The author reviewed that the different advanced finishing processes can be used for finishing different shapes of work material such as spherical, complex, flat and cylindrical depending upon the type of finishing required.

Cheng *et al.* (2008) worked on the finishing of K9 glass mirror. The authors used wheel shaped polishing tool for finishing the workpiece and used MRP fluid (consisting 33.84% carbonyl iron powder, 57.34% silicon oil, 2.82% stabilizing agent and 6% cerium agent). The experimental study was conducted with abrasive particles and without abrasive particles. The results concluded that the surface roughness decreases to 0.47 nm (with viscosity- 8.9 Pa, voltage- 2V, time- 20 min)

Jain (2009) reviewed the different types of finishing processes such as abrasive based advances micro/nano finishing processes and nano finishing processes with external forces. The author summarizes the work done by the various authors with the help of various finishing processes. The different types of finishing processes can be selected depending upon the type of work material and finishing condition.

Sadiq and Shunmugam (2009) studied the effects of various process parameters (magnetic field, initial Ra, workpiece rotation and process duration) on the roughness value of aluminium and austenitic steel workpiece using magnetorheological abrasive honing process. The Magnetorheological abrasive honing process was used by the authors to study the parameters. For analysing the effect of magnetic field aluminium

alloy workpiece were used and for analysing the effect of initial surface roughness on the final roughness value, austenitic stainless steel was used. These experimentations were done at five different levels of magnetic field keeping the speed of rotation and frequency of reciprocation at 450 rpm and 15 cycles/min resp. It was observed that the finishing and material removal rates were increasing till a certain range and then they started decreasing. For analysing the effect of initial roughness value, two sets each of lower roughness value (finish ground) workpiece (0.446-0.467 microns) and higher roughness value (rough ground) workpiece (0.696-0.776 microns) were used. . It was observed that rough ground workpiece showed more improvement in surface finish as compared to the finish ground workpiece. It was observed that the roughness value came down with increase in finishing time and it was also found that for higher rotation speeds the results were yielded quickly. It was also pointed that at 590 rpm and process time greater than 15 min the results were very convincing.

Wang and Lee (2009) worked on magnetic finishing process for precise finishing of cylindrical type (SKD-110 mold steel. The finishing medium included silicone gel, steel grid (SG) and silicon carbide. The results concluded that the surface roughness with magnetic field showed better results. With the increase in the quantity of SiC particles, the surface roughness decreased, whereas MRR increased.

Jung *et al*. (2009) worked on wheel type MR finishing apparatus. The authors reported the effect of MRR on the surface finish Al_2O_3-TiC. The finishing was done by MR fluid (composed of water based suspension of CI particles). It was observed that further improvement could be made by rectilinear motion and sintered I-CNT abrasive particles.

Sidiq and Shunmugam (2010) investigated the effect of magnetic field on magnetic and non magnetic material using magnetic abrasive honing process. Two sets of specimens used were of material mild steel and stainless steel. Cycle time of 10min with 4 different levels of magnetic flux keeping rotation at 310 rpm and reciprocation at 15cycles/min constant was used. For ferromagnetic material (initial roughness 0.165-0.18 microns), with no magnetic field applied, the average percentage change in surface roughness improvement is only 6%. For non-ferromagnetic material (initial roughness 0.14-0.155 microns), with magnetic flux of 0.25T, an improvement of 2.4% is seen. However with 0.65T flux and cycle time of 10 min the change in improvement seen is 6.7% and with cycle time of 20 min the change seen is 24.2%. With further increase in flux density no

appreciable change was seen however it was remarked that it happens because of greater flux density being away from the specimen holder, the CIPs gather away from the holder which is held in the centre. A new method was suggested in which two ferromagnetic specimens were used simultaneously with non ferromagnetic specimens. With 0.25T magnetic flux a considerable amount of change is seen however with higher magnetic fields this change is very low because the fluid gets magnetically saturated. Now experimentation is done by varying the cycle time and keeping the flux at 0.65T and speed at 320 rpm. It was found that with increase in cycle time the roughness value decreased and this change was observed to be nearly 40% with cycle time of 20min relative to cycle time of 5min.

Das *et al.* (2010) developed a new polishing method for internal finishing of pipes called rotational magnetorheological abrasive flow finishing (R-MRAFF). In this process two main motions were given to the fluid rotational as well as reciprocating. For best results the experiments were designed with the help of design of experiments and to see the effect of each parameter response surface regression analysis was used. The magnetic flux density and forces analysis was done with the help of Maxwell ansoft software. The fluid was prepared with 26.6 vol.% of electrolytic Fe powder and 13.4 vol.% SiC abrasive with the 60% base medium (paraffin oil (48 vol.%) and AP3 grease (12 vol.%)).The most significant factor for finishing was rotating speed and second was extrusion pressure. The minimum surface roughness achieved was 16 nm at magnet rotational speed of 149 rpm and extrusion pressure at 40 bar.

Shankar *et al*. (2010) performed theoretical and experiment investigation on R-AFF process for comparing the performance of ΔRa and MR at different rotational on three types of work material namely Al alloy, Al alloy/SiC MMC with 10% SiC and Al alloy/SiC MMC with 15% SiC. The results concluded that the rotational abrasive flow finishing yields better hardness and higher MRR as compared to the abrasive flow finishing in case of Al alloy/SiC (10%) MMC as illustrated in Fig. 2.2.

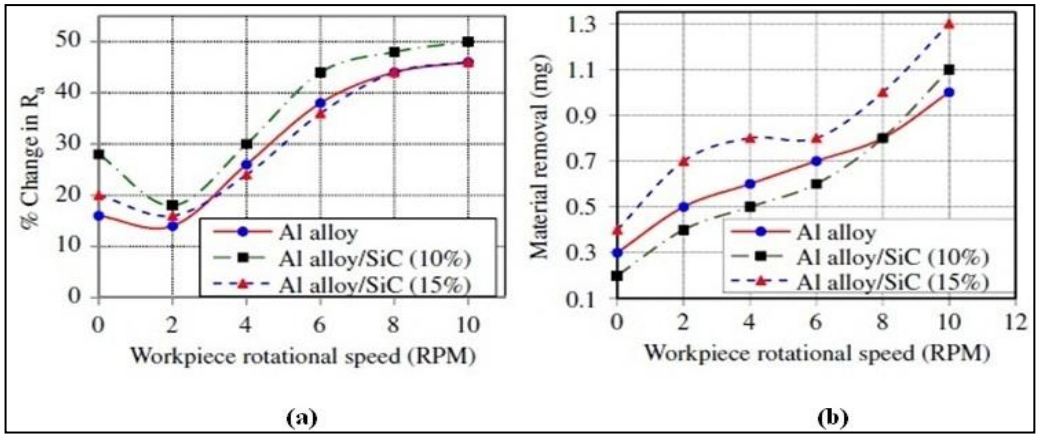

Figure 2.2: Effect of workpiece on rotational speed on (a) Ra (b) MR for the three workspaces (speed-550 RPM, pressure- 6.25 MPa, M-10%) in AFF (RPM- 0) and in R-AFF [Shankar *et al*., 2010]

Singh *et al.* (2011) developed a new MR finishing process for 3D intricate shaped surfaces. Two different workpiece materials: ferromagnetic and non-ferromagnetic were used. Working gap of 5mm to 1mm was studied. It was found that finishing forces and finishing area were greater at 1 mm working gap relative to 5mm gap. It was also found that with 100 rpm of tool and 100 min of finishing time on ferromagnetic material the surface roughness decreased from 414.1 nm to 70 nm. With 600 rpm, 0.2 T magnetic flux and finishing time of 60 min on non-ferromagnetic material surface roughness decreased from 336.8 nm to 102 nm. It was also found that when lower magnetic flux densities than 0.2T were used with tool rpm of 600, the ball shape of tool tip was not stable because of the radially outward centrifugal force acting on the CIPs.

Singh *et al.* (2012) studied the effect of finishing time on the surface roughness of fused silica glass using ball end magnetorheological finishing tool. For this experimentation CIPs of CS grade, abrasive powder as cerium oxide and carrier fluid deionised water are used in 30%, 10%, 60% volume concentration respectively. Finishing cycle time of 30 min was taken, rotation speed at 400 rpm, working gap distance at 1.5 mm, feed rate for two end fro motion of workpiece and current supply at 4A and 2.4A was taken into consideration. Observation of roughness value, RMS value and max roughness value as obtained from the experiments performed are given in Table 2.2.

Table 2.2: Results obtained after experimentation [Singh *et al.*, 2012]

Effect of finishing cycle time on final surface roughness.

Finishing time (min)	Ra (nm)	RMS (nm)	Rmax (nm)
0	0.74	1.03	5.13
30	0.44	0.73	2.27
60	0.39	0.59	2.19
90	0.33	0.41	1.64
120	0.27	0.39	1.35
150	0.14	0.26	0.94

After finishing at 4A current when the specimen was taken under atomic force microscope it was found that some deep scratches were formed on the surface. It was remarked that it could be possible because at such high current the finishing spot got much stiffer than required.

Sidpara and Jain (2012) analyzed the effect of CIP and abrasive concentration, wheel rotation speed, and initial surface roughness on the finishing of single crystal silicon blank using MR finishing process. Cerium oxide abrasives were used and de-ionized water was used as liquid medium for finishing silicon along with grysrol for providing stability to the MR fluid. 3 cycles with each cycle time of 70 min is considered With the increase in concentration of CIPs it was found that the MRR increases and the surface roughness value decreases because of stronger chains formed. With the increase in concentration of abrasive particles it was found that the MRR decreases with increase in surface roughness value. On further study it was found that 5% concentration of the abrasive particle is the optimum value for high MRR and low roughness value.

Kyung-In Jang *et al.* (2012) proposed new process for deburring using magnetorheological fluid. The authors were successful in applying this process for removal of metal burrs with a height of 200 µm and thickness of 1 µm in micro-moulds with extensive yielding and abrasive wear. The average Ra of brass decreased from 192nm to 34nm after 4 min of processing. For stainless steel, the average Ra decreased from 379.8nm to 147.1nm.

Hong *et al.*, (2012) performed the experiments to finish the alumina reinforced zircon ceramics (used in dental application 3YTZP/Al_2O_3 -20%) with the help of MR finishing process. MR fluid is prepared with 50% CIP's, 48% abrasive slurry with diamond abrasives and glycerin is used as a stabilizer. The process parameters are (speed-200 and

300 rpm, magnetic field- 3.8,4.7,5.5 and 6.1 KA/m, Time- 20,30,40 &60 min). The surface roughness decreases from 0.272 µm to 1.96 nm on 300rpm, magnetic field-3.8 KA/m & 60 min.

Jiao *et al.* (2013) investigated the new modified magnetic compound fluid (MCF) wheel which was used for finishing the fused silica glass. The author developed the setup with permanent ring shaped magnet which was used for generating the magnetic field. The author compared the new modified MCF wheel with unmodified MCF wheel and saw the results by comparing the material removal and surface roughness. The MCF slurry composition was taken as 58% CIP's, abrasive (cerium oxide) as 12% and magnetic fluid as 30%. The author also studied the effect of rotational speed and clearance between workpiece and wheel on material removal and surface roughness of workpiece. The final surface roughness that was achieved by modified and unmodified wheel were Ra=5.624 and 14.67 from initial roughness of 200nm and material removal was 0.04 mm^3 and 0.0088 mm^3 respectively at rotation speed 500 rpm and clearance 0.5mm.

Pandey *et al*. (2013) conducted a study to see the effect of process parameters of BEMRF to finishing the EN31. The authors selected 3 parameters magnetizing current, working gap and nozzle speed. 3 level design was prepared and L-9 orthogonal array was used. ANOVA was applied to analyze experimental data to find the contribution of each parameter to achieve final roughness. The MR fluid was prepared with 20% CIP's particle, 20% of Sic abrasives (800 mesh size) and 60% base fluid. The optimized parameters for finishing the EN31 on BEMRF were 1.4A current, 0.75mm working gap and 300 rpm nozzle rotation speed. The final roughness was achieved 44 nm from 246 nm.

Singh *et al*. (2013) mathematically explained the mechanism of material removal in ball end magnetorheological finishing process. The authors prepared a mathematical model for the normal forces generated during the process of finishing. The model was then validated experimentally by varying the working gap. The authors also explained that with increase in normal force the mechanism changed from three body wear mechanism to two body wear mechanism as the constraint contact of abrasive particles with the workpiece surface was more in case of higher normal force.

Singh *et al*. (2013) synthesized MR polishing fluid indigenously and characterized the rheological properties of MRP fluid using plate type magnetorheometer. MR polishing fluid was prepared using 20% CIP of CS grade, 20% silicon carbide abrasives and 60% of visco-elastic fluid. It was found that the Mr polishing fluid exhibited a very good stability against gradually increasing shearing rate. The MRP fluid was utilized for finishing of ferromagnetic workpiece.

Pattanaik and Agarwal (2014) designed a new setup to finish the free form surfaces with the help of magnetorheological fluid. Authors modified the pillar type drilling machine and used it to finish the freeform surfaces. The study was conducted on copper alloy. Flat and cylindrical surfaces were taken as workpiece geometries. The magnetic field was developed with the help of permanent magnet (Nd-Fe-B, N35 grade). The experiments were conducted with different type of conditions in which composition of MR fluid, abrasive sizes and rotation speed of workpiece and vessel containing MR fluid were varied. It was concluded that finishing was done in less time when the rotation speed was given to both workpiece and vessel containing MR fluid rather the only to the workpiece. The decrease in surface roughness of flat portion of job was more as compared to the cylindrical surface.

Niranjan *et al.* (2014) studied on the workpiece surface roughness by changing the MR fluid with new composition of fluid called bidisperse MR fluid. MRP fluid was prepared with different compositions and compared with each other for best results. They uses two different grades of CIP's (CS & HS grade). The average particle size of CIP's of CS & HS are 6–7 µm and 1.8–2.3 µm, respectively and SiC abrasive particles size 19 µm. The best results are obtained with this composition CIP 16 vol. % CS grade, 4 vol. % HS grade, 25 vol.% SiC abrasive

Niranjan and Jha (2014) worked on BEMRF for finishing of mild steel. The authors made use of bidisperse MRP fluid. The results concluded that the surface roughness value decreases to Ra- 0.1406 µm, Rq- 0.1967 µm and Rz- 1.1403 µm as illustrated in Fig. 2.3.

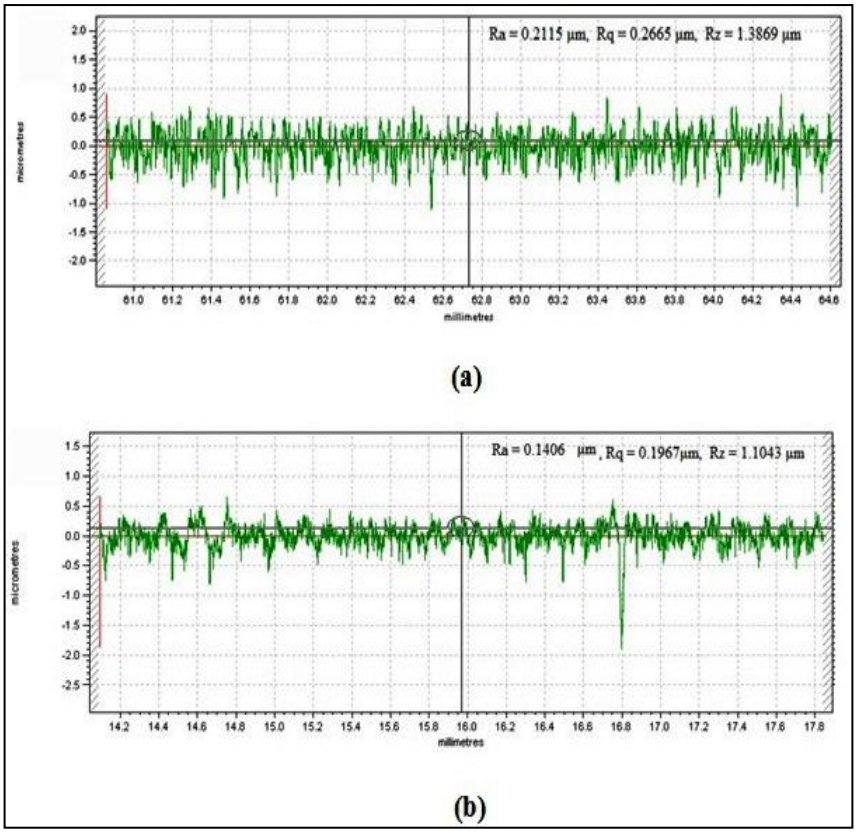

Figure 2.3: (a) Surface roughness profile before finish (b) Surface roughness profile after finish using bidisperse MR fluid (sample 3) [Niranjan and Jha, 2014]

Niranjan *et al*. (2014) compared the performance of different MRP fluid (bidisperse and monodisperse) by using BEMRF for finishing of mild steel. It was observed that the surface finish produced by bidisperse was better as compared to monodisperse MRP fluid as illustrated in Fig. 2.4.

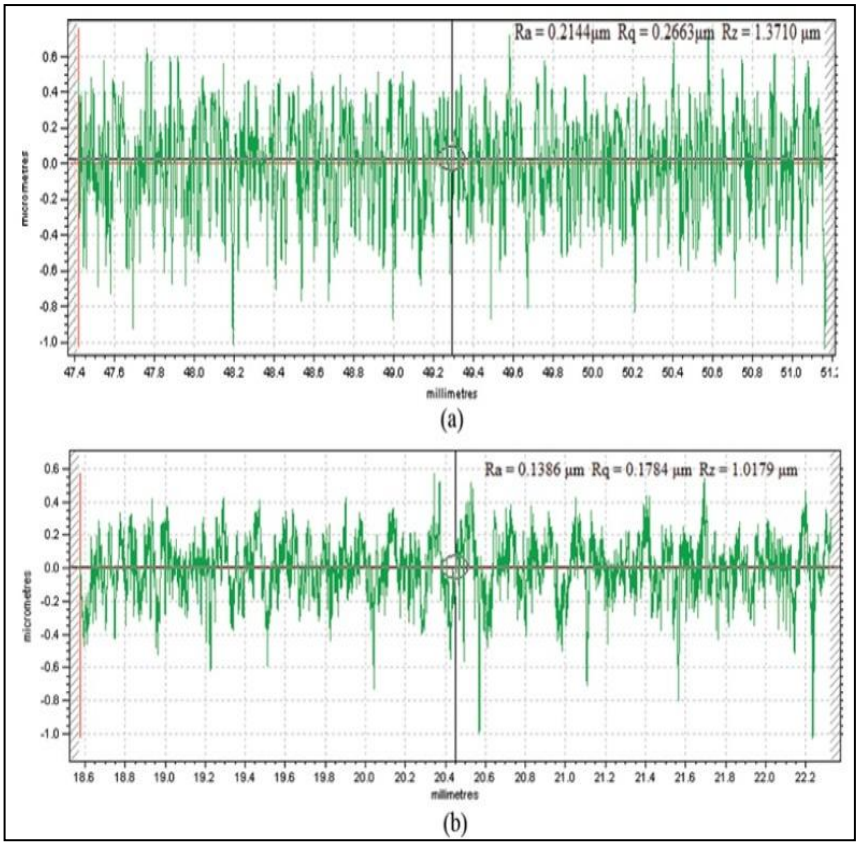

Figure 2.4: (a) Surface roughness profile before finish (b) Surface roughness profile after finish using monodisperse MR fluid (sample 3) [Niranjan *et al*., 2014]

Gheisari *et al.* (2014) developed a magnetorheological finishing process for an ultra precision finishing of aluminum work material (cylindrical type). The water based suspension of micron sized diamond particles are used for MR fluid. The optimum parameters were (current- 9A and working gap- 5mm). The initial surface roughness of the work material was 170 nm. The experimentation was conducted in three stages. In first stage, the work material was speed varies from 250-1000. In second stage, the process time varies from 20-100 min. In third stage, the effect of a fast ram on the surface roughness was considered. The results concluded that the surface roughness value improves by 40 nm with the increase in rotational speed (1000 rpm). The surface roughness value decrease to 42 nm whereas through the raise in finishing time (90 min), the surface irregularity value improves by 78 nm when the fast ram (with 0.5 m/sec) was applied.

Huiru guo *et al.* (2014) worked on the finishing of electroless nickel-phosphorus plated mold used for hot press of optical glasses using magnetic compound fluid slurry. The work involved of two different types of slurries for removing the turning marks produced by single crystal diamond turning on the mold surface. One of the slurries used high quality CIPs with Al2O3 as abrasives while the other slurry used CIPs coated with zerconia abrasives. Both the slurry seemed to work satisfactorily in removing the marks produced by the turning tool but the slurry with Al2O3 as abrasive left scratches on the work surface. The second slurry with zerconia abrasives showed promising results. There were no scratches observed and it also increased the flatness of the workpiece from 0.2μm to 0.1 μm.

Y.Q. Wang *et al.* (2015) developed a new setup for ultra-finishing the flat work pieces and saw the effects of trough speed, work and excitation gap width, particle concentration on MRR for K9 glass. A permanent magnetic yoke with straight air gap was used for generating the magnetic field. The polishing setup demonstrated that the glass surface improved to a roughness value of 1 nm in Ra after 60 min of polishing, from the initial average roughness of 127 nm.

Mingjun Chen *et al.* (2015) developed a novel precision MRF process using small ball end permanent magnet polishing head with 4mm diameter. The process was developed to finish the small curvature radius of concave type shapes. Ansoft software was used to check the distribution of magnetic flux density at polishing head which was 93.3%.The fluid was prepared with volume concentration of 36% CIP, water based fluid medium at 57%, cerium oxide abrasives as 6% and stabilizing agent as 1%. A device is attached to supply the water in the MR fluid to stable the fluid concentration because the water will evaporate. A flat piece with size 20*10*5 mm of plane glass of fused silica was used to check the feasibility for non-metallic material. The final roughness was achieved as 0.517nm from initial 214nm at C-axis angular position 65^0, spindle speed 5000rpm, feed 1.8mm/min and 100min. To check the feasibility of process for metallic workpiece a curve stainless steel workpiece of 6*6*0.8 mm with 4mm radius curvature was used. The final roughness achieved was Ra 0.005nm from Ra 230nm initial with parameter C-axis angular position 70^0, spindle speed 5000rpm, feed 4.8mm/min and 300min. Aluminum oxide abrasive was used for the metallic workpiece because cerium oxide abrasive is not suitable for the stainless steel.

K. Saraswathamma *et al.* (2015) studied the effect of input parameters (fluid composition parameters and machine process parameters) using BEMRF process on the silicon wafer. The authors used cerium oxide as abrasives and deionized water as carrier medium. Experimental plan was prepared using statistical design of experiments. Core rotational speed, working gap, and magnetizing current were used as process parameters in the design and percentage reduction in surface roughness was considered as response. Using ANOVA, effect of each parameter was analyzed. It was observed that maximum contribution was made by the working gap followed by magnetizing current and core rotational speed. The average Ra of silicon wafer decreased from 457nm to 89.8nm.

Jin Wang (2015) proposed a new method to finish pierced die manufactured with wire electric discharge machining. The pierced die can be polished by this new method to improve the surface quality of the die. The polished die was made from tool-steel Cr12. Diameter of wire used to cut the die was 0.1mm. A core with permanent magnets was made to finish the pierced die. The MR fluid contains CIP, SiC (3000), water and polyethylene glycol. The working gap was 0.5mm. The finishing was done with the permanent magnet and core by giving reciprocating motion. The final roughness was achieved as 0.132 µm at flat surface and 0.278 µm at corner from initial Ra 0.303 µm with 12000 reciprocating motion in 290 min. The experiments were conducted by changing the diameter of wire from which was concluded that to decrease the surface roughness the increase the diameter of wire.

Payam Saraeian (2016) optimized the MAF process parameters working gap, abrasive size and rotation speed for finishing of AISI321 steel by applying full factorial method at three level. The MAF fluid was prepared with CIPs, Sic abrasive and SAE40 oil. The finishing was done on workpiece 50 mm lengths for 20 min. The three level for rotation speed (355, 500, 1000 rpm), working gap (0.5, 1, 2mm) and abrasive size (100, 200, 300 mesh) was used. The best result was achieved at 1mm gap, 500 rpm and with abrasive size 100 mesh. Working gap is the most effective parameter for finishing followed by rotation speed.

2.3 Research Gap:

From the literature review it is clear that very little work has been done on the finishing of permanent mould material EN31 using magnetorheological fluid based nanofinishing processes. Moreover, the little work that has been done till now uses ball end magnetorheological finishing tool with a central hole. The research gap observed is as follows:

- Till now work involved in nano finishing of EN31 using BEMRF has been done using a hollow tool core.
- Work done on EN31 using ball end magnetorheological finishing process has been done without giving any heat treatment to the material i.e. hardness has not been achieved matching the industrial standards. So the hardness of the material while performing the finishing operation remained nearly 10 HRC, which is comparatively very low to the actual hardness of the material when subjected to finishing process in industry for die and mould applications.
- The statistical analysis has not been made for hardened EN31 steel using parameter such as feed rate, abrasive concentration and CIP concentration.

2.4 Objectives of the Present Work

Based on the literature survey and to nano-finish the hardened EN31 steel used in die and mould applications in industries. The following objectives were framed to accomplish the goal of present work.

- To demonstrate the capability of ball end solid rotating core magnetorheological finishing process in finishing of hard material such as EN31 used in actual applications in industries for die and mould manufacturing.
- To optimize the process parameters for finishing of high hardness EN31 permanent mould material using ball end solid rotating core magnetorheological finishing process.
- To demonstrate the feasibility of ball end solid rotating core magnetorheological finishing process in practical application of finishing permanent mould in industries.

Chapter 3

Material and Methodology

3.1 Introduction

The permanent moulds can be of various shapes and sizes. Their shape and size is dependent on the geometry of the product for which they are being manufactured. For most of the plastic products, the shape of the permanent mould is very complex 3D surface.

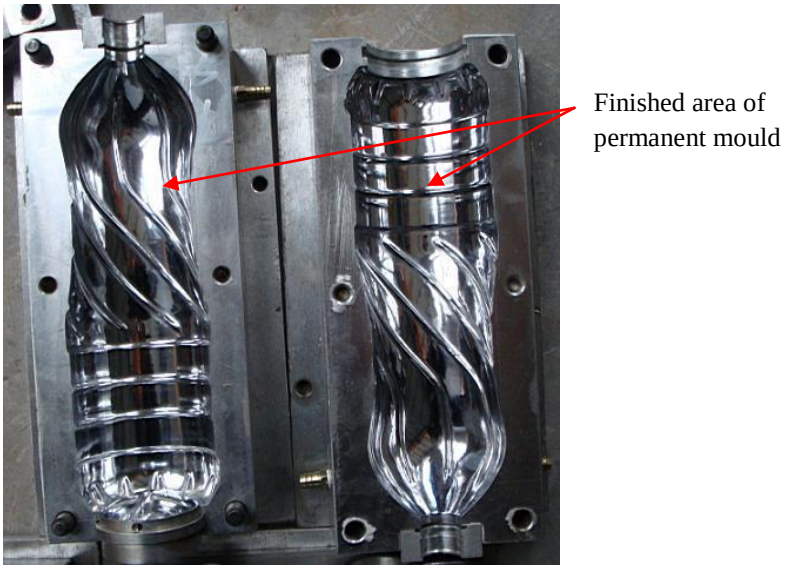

Figure 3.1: A finished permanent mould for a water bottle

[http://img.diytrade.com/cdimg/502513/3198071/-1/1246240751/Abaram_Plastic_Mould_Manufacturing_Co_Ltd.jpg]

From the literature review it can be justified that ball end magnetorheological finishing process is the most suitable magnetic abrasive based finishing process that can be used for finishing of permanent moulds [Singh *et al*,; 2011, Bedi & Singh, 2015]

It is also clear from the literature that the process parameters are dependent on the type of material (ferrous or non-ferrous) and the material hardness. So, in order to perform experiments to find the optimum combination, preliminary experiments were conducted. Based on these preliminary experiments, design of experiment was prepared and the optimum combination of these parameters was concluded.

3.2 Ball End Solid Rotating Core Magnetorheological Finishing Tool

The tool is formed using a solid iron core with electromagnetic coil wrapped around it. The core is held inside the mounting bracket using bearings and the top end of the tool is connected to the motor via a belt pulley arrangement as shown in Fig. 3.2.

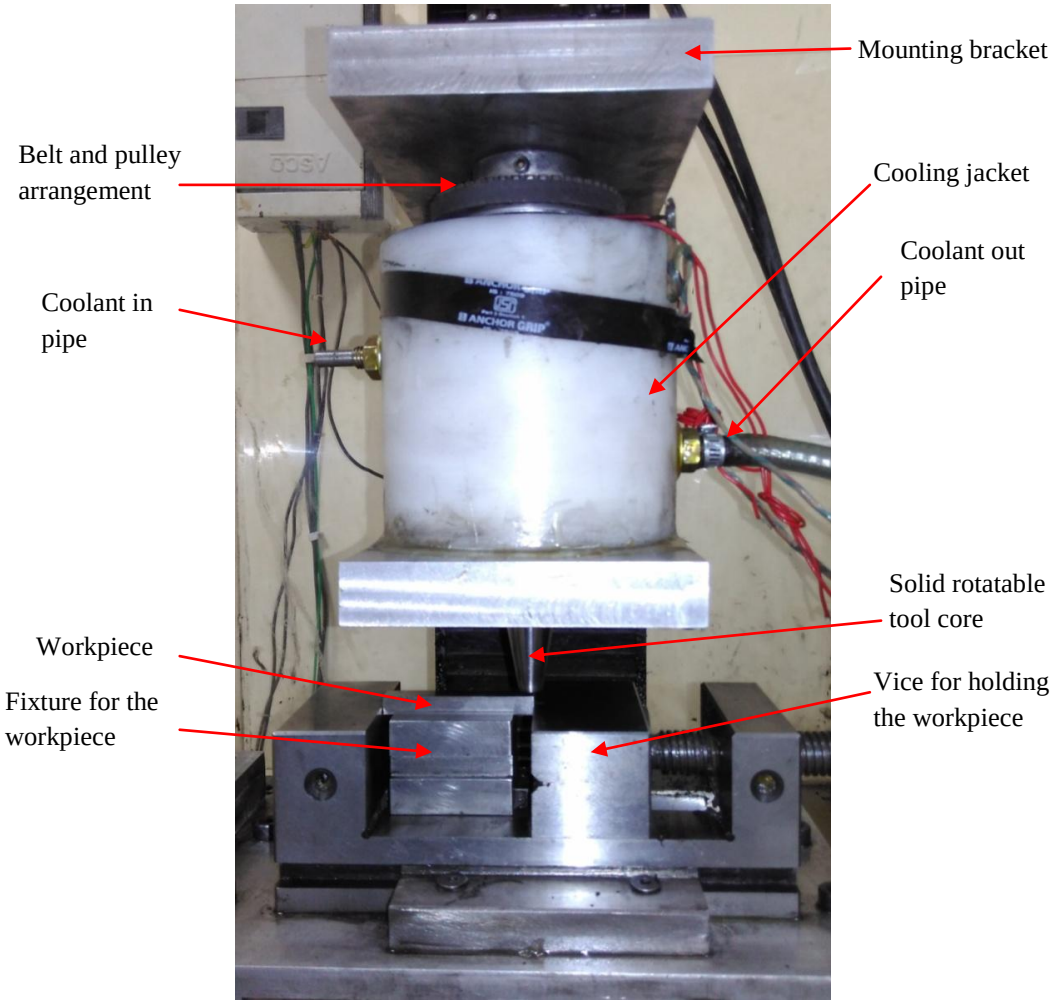

Figure 3.2: Tool being held using the mounting bracket and the workpiece clamped in the vice

Some recent developments have been made in the design of ball end magnetorheological finishing tool. The previous ball end magnetorheological finishing (BEMRF) tool has a central hole for the passage of MR polishing fluid through it. But because of this central hole the magnetic flux distribution at the tip of tool was not uniform [Singh *et al.*, 2012]. For eliminating this drawback, a new modified ball end magnetorheological finishing tool was developed. The new modified BEMRF tool uses a

solid core i.e. without any central hole. Analysis of magnetic flux distribution at the tip of tool was done using Maxwell ansoft v13 (student version) (Fig. 3.3). Relative permeability of tool core was taken as 4000 and that of the workpiece was taken as 380. Excitation current of 3A was provided to the electromagnetic coil and gap of 0.6 mm was maintained for the analysis. It was found that the magnetic flux distribution was uniform at the tip of the tool.

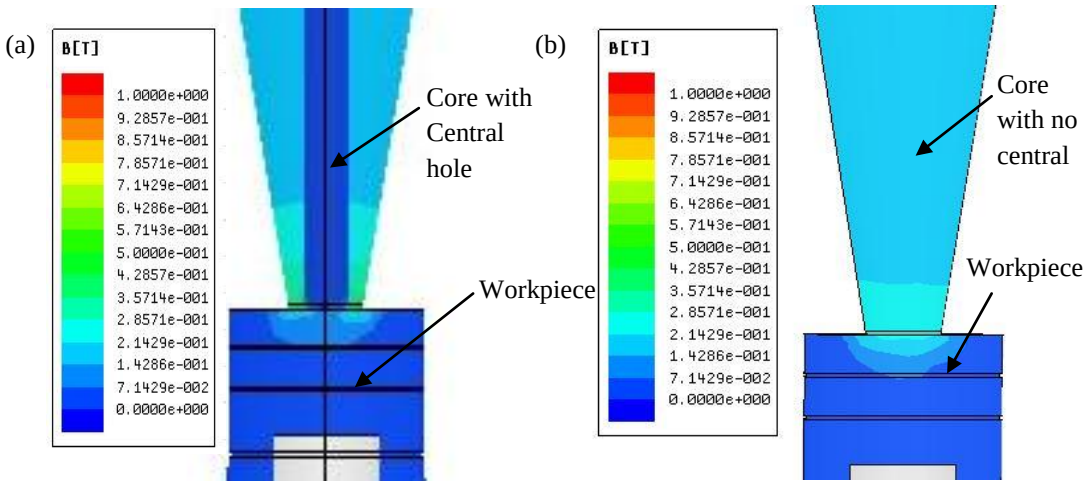

Figure 3.3: Analysis of two different tool cores and workpiece with MR polishing fluid between them, (a) tool core with central hole and (b) tool core without central hole

The electromagnetic coil of the tool has 2100 turns of copper wire and gauge size is 20. Dimensions of the tool have been given in the Fig. 3.4.

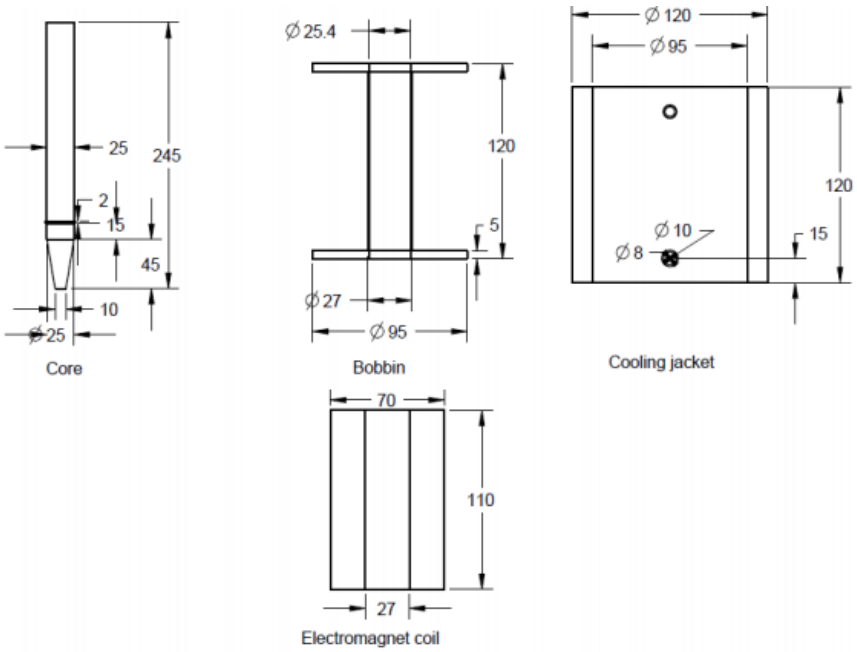

Figure 3.4: Drawing of the tool showing different parts and their dimensions

In the previous BEMRF tool, the MR polishing fluid was pumped the central hole of the tool whereas in the new modified BEMRF tool with solid rotating core, the MR polishing fluid is applied manually.

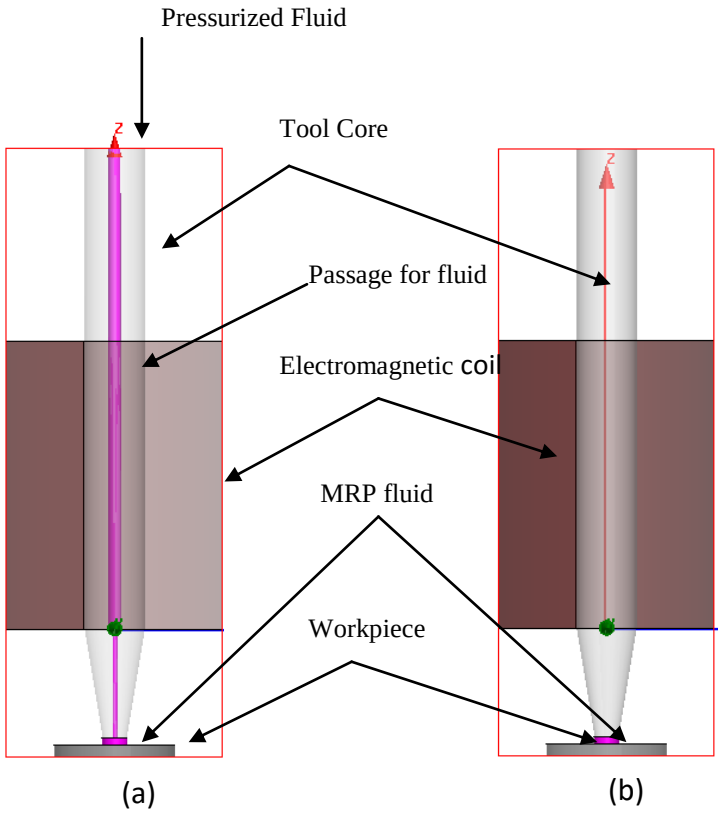

Figure 3.5: Model of BEMRF tool (a) with central hole (b) without central hole

3.3 Experimental Setup

The new modified BEMRF tool with solid rotating core (without central hole) was mounted on a PLC controlled 3-axis machine. Tool is mounted on the Z axis while the workpiece moments are governed by the movement of X-Y slide. The machine can be operated using a human machine interface as shown in Fig. 3.6.

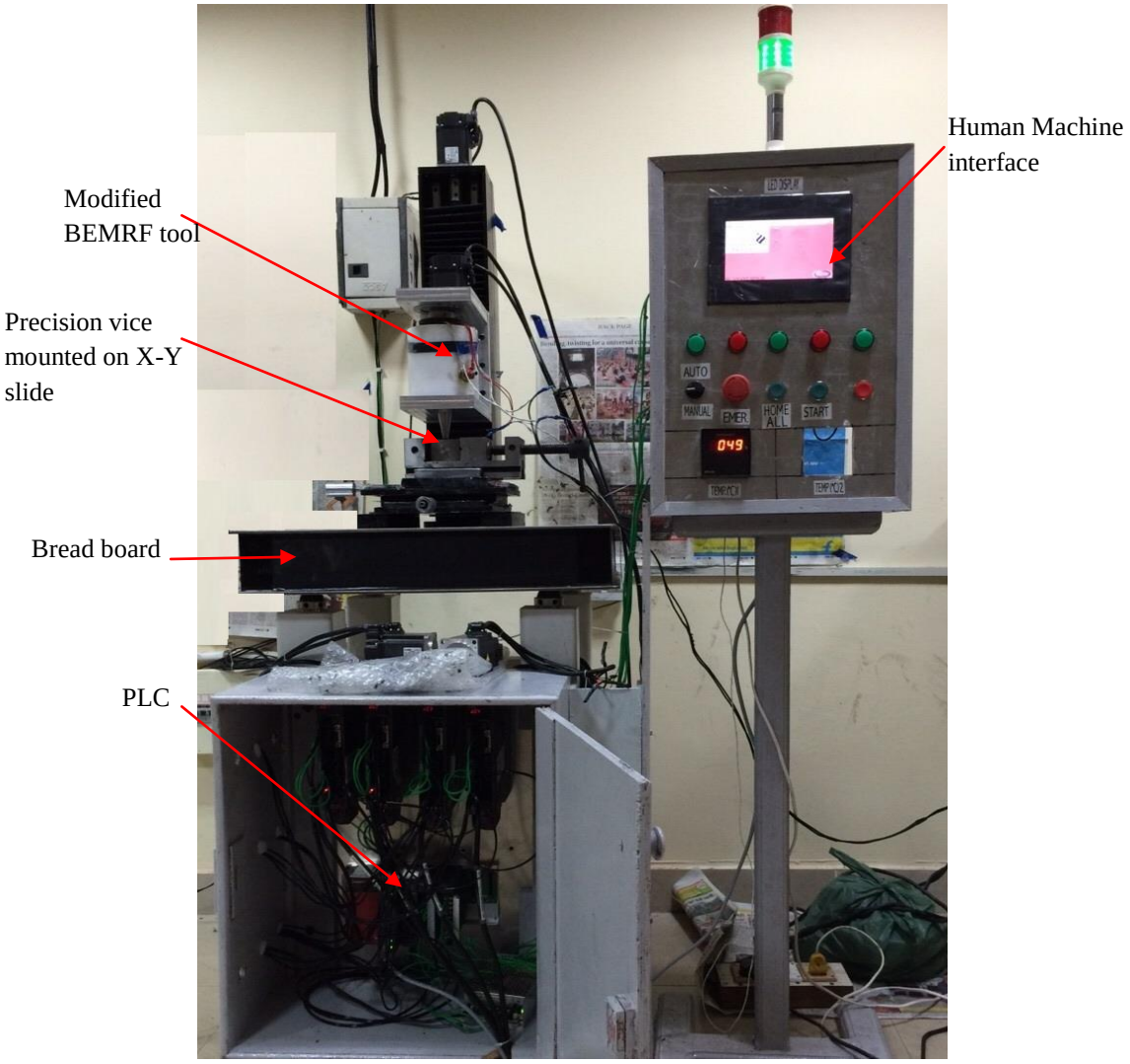

Figure 3.6: Photograph of the modified MR finishing setup

The workpiece is mounted on a precision vice, which is coupled to the bed of X-Y axis slide. A fixture is used to hold the workpiece in the vice as shown in Fig. 3.7.

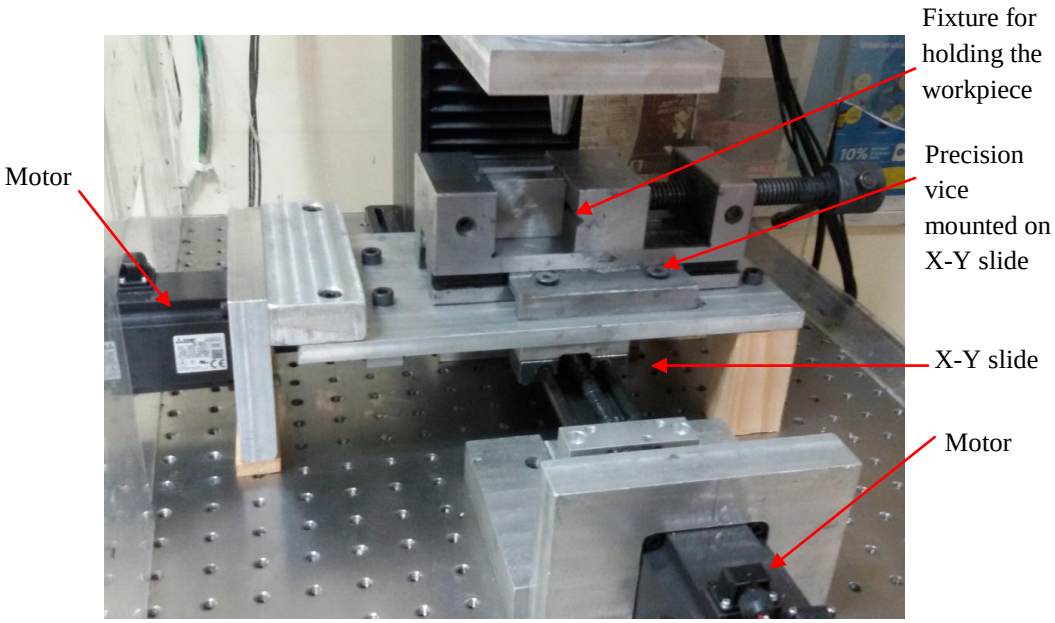

Figure 3.7: Arrangement for holding and moving the workpiece in X and Y axis

The tool uses an electromagnet which gets heated up due to the resistance produced by the wire material and this heat if transferred to the tool tip will lead to change in the rheological properties of the MR polishing fluid. So in order to keep the temperature near the ambient temperature range, a low temperature bath is used as shown in Fig. 3.8. Transformer oil is used as a coolant because of two main reasons:

1) It creates a considerable level of insulation around the conductors and coils
2) It has a good heat extraction property

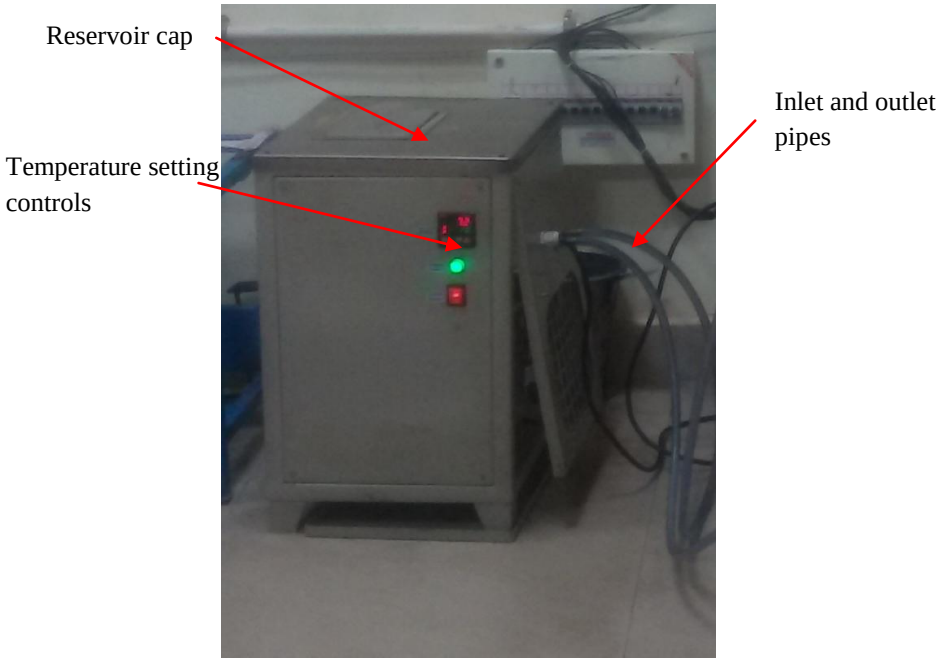

Figure 3.8: Low temperature bath

3.4 Material Selection

The material used for manufacturing of permanent moulds is very hard and tough. More the material is hard more will be its working life. According to society of plastic industries, permanent moulds should have minimum hardness of 35 HRC. A typical permanent mould produces around 100000 products in its life cycle [Mateo *et al.*, 2011]. It can then be re ground so as to increase its life. But this re grinding will lead to change in dimensions of the final product. From the literature survey it was found that P20 tool steel and EN31 grade tool steel (BRITISH BS 970:1955) are the most widely used material for manufacturing of permanent moulds for plastic products. Both materials can achieve high harness after heat treatment. On further literature survey it was found that EN31 is the most widely used material among all the materials used for mould manufacturing. EN31 is used for ball and roller bearing, spinning tools, beading rolls, punches ad dies. This steel has high resisting nature against wear ad can be subjected to components which are subjected to severe abrasion, wear or high surface loading. The hardness that can be achieved on EN31 steel is 60-62 HRC. [Guo and Liu, 2002]. Table 3.1 provides the information regarding the standard percentage composition range of different elements of the EN31 steel [Guo and Liu, 2002] and the composition of EN31 workpiece as obtained after spectroscopy.

Table 3.1: Comparison of standard and actual composition of workpiece

Element	Standard composition (%)	Workpiece composition (%)
Fe	96.5-97.5	96.6
C	0.95-1.10	0.966
Si	0.35 max	0.24
Mn	0.2-0.5	0.485
P	0.025 max	0.021
S	0.025 max	0.024
Cr	1.3-1.6	1.4

Other properties of EN31 are given in Table 3.2.

Table 3.2 Properties of EN31

Property	Values
Density	0.282 lb/in^3
Hardness	~62 HRC
Ferromagnetic	Yes
Relative Permeability	>300
Melting point	2595 F

3.5 Workpiece Preparation

As the work involved is finding the optimum parameters for finishing of permanent moulds, it is not necessary to apply the process and experimentation on an industrial product. Therefore, for better analysis and easy measurement the workpiece size of 10 mm × 50 mm × 5 mm was prepared from a raw ingot and roughly ground using surface grinder as shown in Fig. 3.9.

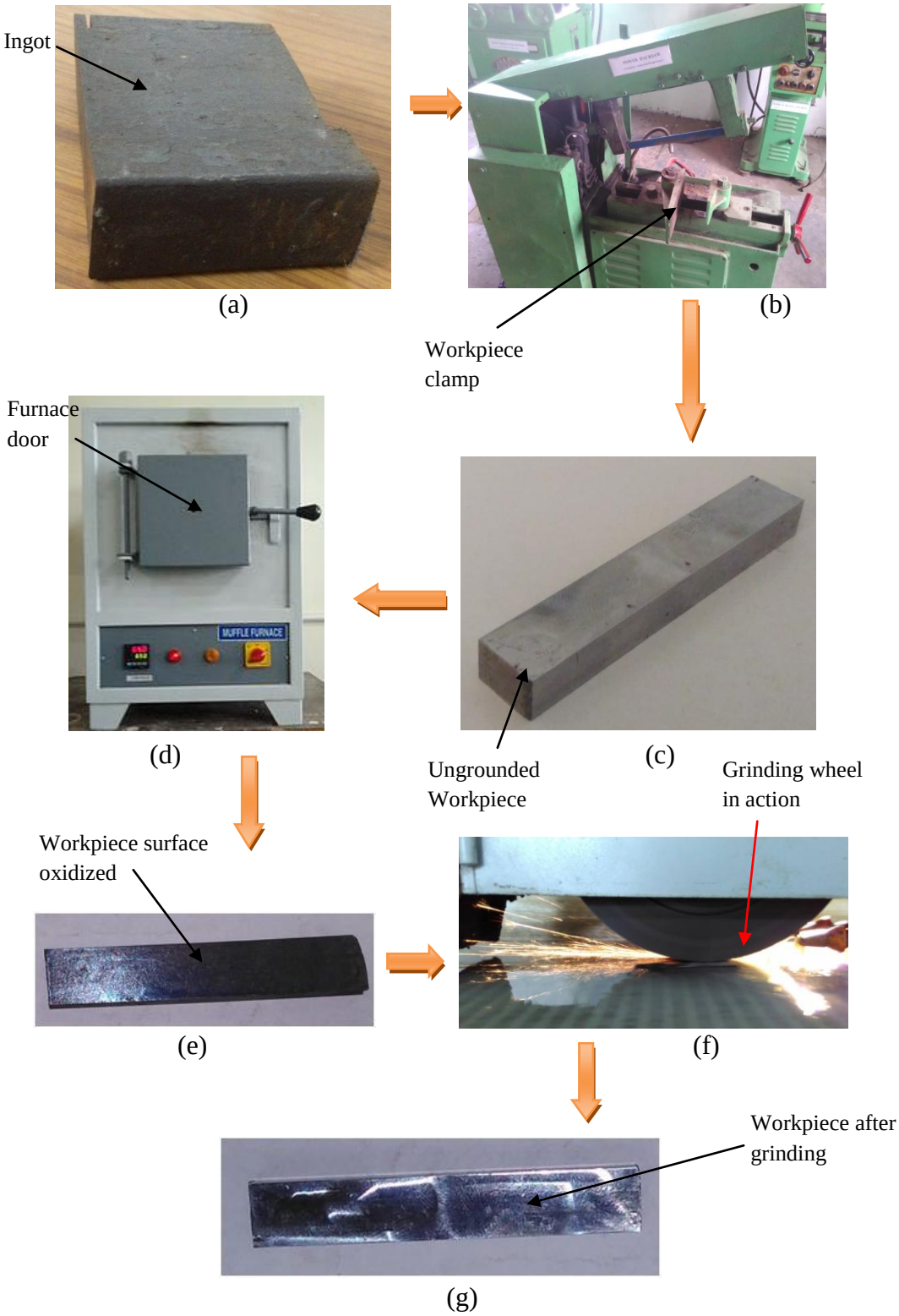

Figure 3.9: Pictorial flow diagram for the steps followed while workpiece preparation (a) raw ingot of EN31, (b) power hacksaw used for cutting the workpiece, (c) workpiece machined from ingot, (d) muffle furnace used for heat treatment, (e) workpiece after heat treatment, (f) grinding operation on heat treated workpiece and (g) workpiece after grinding

Allowance of 1.5 mm was provided by keeping in mind the oxidation of surfaces and regrinding of the workpiece after heat treatment. Therefore the dimensions before heat treatment were 11.5mm × 51.5mm × 6.5mm. Figure 3.10 shows the workpiece after heat treatment and after grinding.

(a) 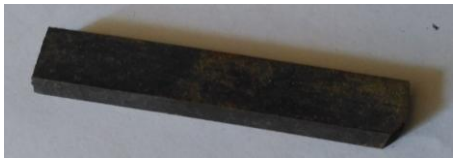 (b) 

Figure 3.10: Photographs of the workpiece after (a) heat treatment and (b) grinding

Another observation was made after the final grinding of the workpiece was the formation of surface cracks. On literature survey regarding the same it was found that these cracks are formed due to tradition finishing process applied to hard materials such as EN31 [Helieby and Rowe, 1981]. The surface of the workpiece was observed under SEM and it was observed that the width of the cracks formed is around 2-3 μm as shown in Fig. 3.11.

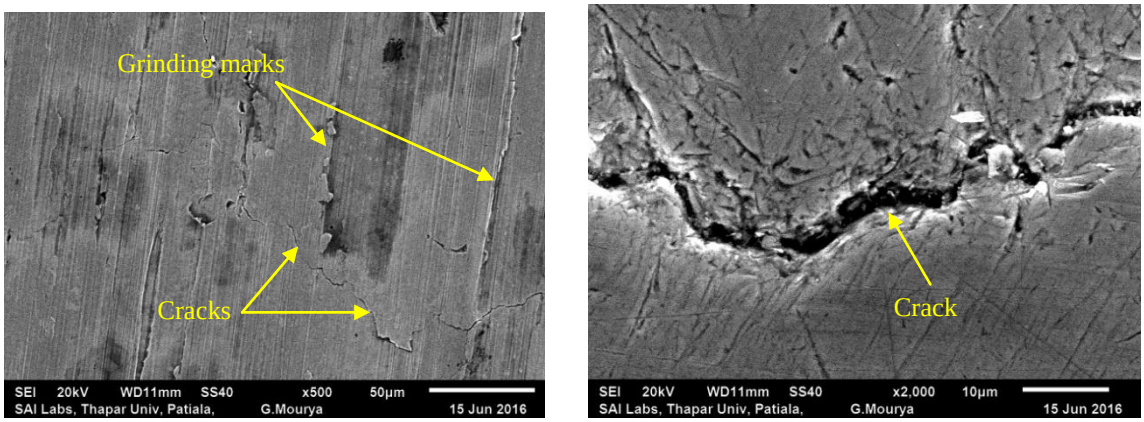

Figure 3.11: Workpiece after grinding examined under SEM (a) at 500X magnification with grinding marks along with cracks and (b) at 2000X magnification with a closer view of the crack

3.6 Heat Treatment of Workpiece

As from the literature review it is clear that the finishing operation is performed on the permanent mould after it is hardened. As discussed, the material being used is EN31 and

the achievable hardness is around 62 HRC. The workpiece with manufacturing allowances were heat treated using muffle furnace.

3.6.1 Hardening

Hardening is a type of heat treatment process used to increase the hardness of a material. In this process the material is taken to its austenitic temperature and is held there for some soaking time which is dependent on the thickness of the material being hardened. The material is then quickly drawn from the furnace and dipped in oil or water at room temperatures. This results in increase in hardness of the material. The workpiece were quenched in oil which was kept at around 70°c so as to avoid crack formation on the workpiece surface. The workpiece were then taken out of the oil and kept in air so as to achieve the room temperature. The hardness of workpiece was found to be 60 ± 3 HRC. The parameters used are given in table 3.3.

Table 3.3: Parameters used for heat treatment (hardening) of workpiece material

S.No.	Parameter	Level
1	Hardening Temprature	850°c
2	Soaking time	20 min
3	Heating rate	600°c/hour

3.6.2 Tempering

Tempering is the process of improving the toughness of material by decreasing its hardness. As a material is hardened the mechanical properties like brittleness, hardness etc change. In order to reduce the harness and make the material more tough, the process of tempering is applied. The workpiece was then tempered to induce toughness in the material. The parameters used for tempering are given in table 3.4:

Table 3.4: Parameters used for heat treatment (tempering) of workpiece material

S.No.	Parameter	Level
1	Tempering Temperature	280°c
2	Soaking time	1 hour
3	Heating rate	600°c

After one hour the furnace doors were partially opened and the workpiece were allowed to cool till they achieved room temperature. The hardness of tempered

workpiece was found as 50 ± 3 HRC. The workpiece were then ground using surface grinder to the required dimensions.

3.7 Methodology

The major objective of this work is to optimize the parameters and demonstrate the feasibility of the present process in finishing of hardened EN31 steel used for permanent mould manufacturing in industries. The step by step procedures have been followed for accomplishing the foresaid objectives. Figure 3.12 shows the methodology in the form of a flow chart.

1) Proper literature survey for determining the need of finishing, present methods being applied for finishing in industry, the need for new advanced methods, feasibility of application of new advanced finishing methods and other data available on the application of new advanced finishing methods.
2) Study various advanced finishing processes and selection of one of them on the basis of feasibility.
3) Selection of material on the basis of industrial application.
4) Selection of parameters on the basis of literature survey.
5) Designing the experiment
6) Preparation of workpiece
7) Performing the experiments
8) Concluding the results
9) Optimization of parameters

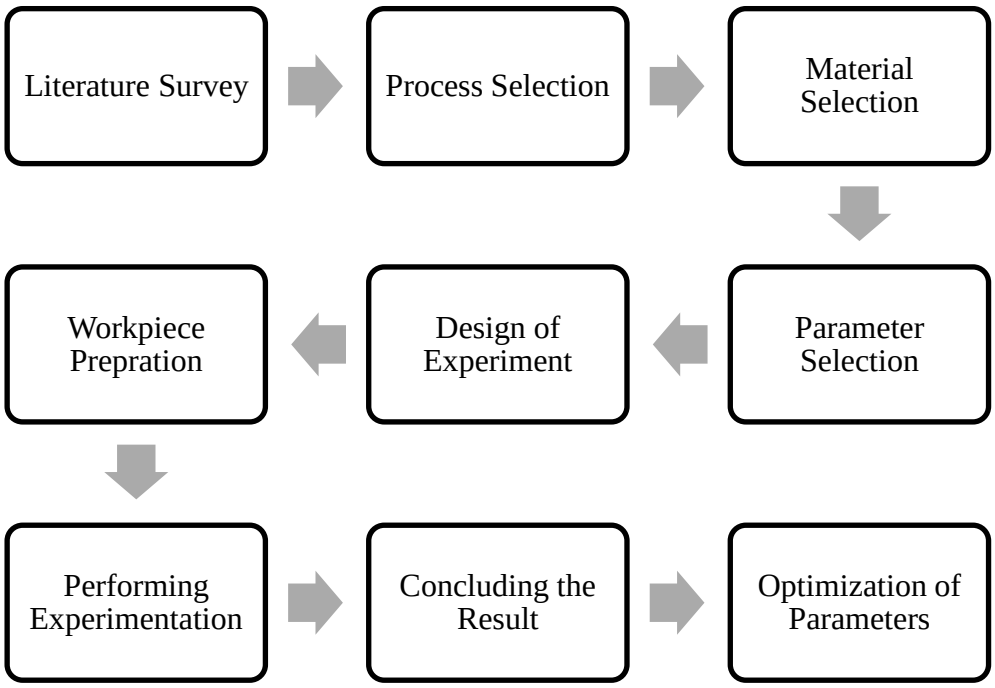

Figure 3.12: Flow chart of the methodology being followed

Chapter 4

Synthesis of MR Polishing Fluid and Preliminary Experimentation

4.1 Introduction

In all the magnetic based nano finishing processes, the finishing action is performed using the MR polishing fluid. MR polishing fluid is viscous fluid which is applied at the tip surface of the tool and it fills the gap between the gap between the tool tip and the workpiece surface. The MR polishing fluid can be prepared in different composition as per requirement. For different materials, the optimum composition of MR polishing can be different for obtaining best surface finish. Hence to optimise the composition of MR polishing fluid, various set of experiments were performed that had different composition as per the design level. This chapter discusses the method of preparation of MR polishing fluid, calculations involved for calculating the weight of different volume concentrations, the apparatus used and the preliminary experimentation conducted for deciding the parameters.

4.2 Synthesis of MR Polishing Fluid

The working of any magnetic abrasive based finishing method is based on the application of MR polishing fluid between the tool and the workpiece. It is also evident from the literature survey that the concentration of MR polishing fluid plays a very effective roll in the finishing process [Sidpara and Jain, 2011]. Thus it is considered as a design parameter and to obtain precise results the concentration of elements of MR polishing fluid need to be exact. The MR polishing fluid consists of three vital elements- carbonyl iron particles (CIPs), abrasives and base fluid and their concentration is taken by percentage volume [Jain, 2009]. The base fluid further consists of heavy paraffin and AP3 grease (by weight). The CIP mesh size is taken as 400 and that of abrasive is taken as 800. As per the plan of experiment, the composition of different sets of experiments is different; hence the composition is varied as per design requirement. Calculations based on chapter 4.2.1 will help in obtaining the weights required for different volume percentage concentrations.

4.2.1 Calculations Involved

Density of CIP – 7.8 g/cm^3

Density of abrasive- 3.22 g/cm^3

Density of base fluid- 0.76 g/cm^3

Let CIP required = C %

Let Abrasive required = A %

Then, Base fluid = 100-(C + A) %

= B % (say)

Therefore, for synthesising 1000 cm^3 of MR polishing fluid

Weight of CIP = (((C/100) × 1000) × 7.8) grams

Weight of Abrasive = (((A/100) × 1000) × 3.22) grams

Weight of Base Fluid = (((B/100) × 1000) × 0.76) grams

If the MR polishing fluid is to be prepared in a lesser quantity, the percentage of weight required to the total weight of individual element can be calculated [Singh *et al,*. 2011].

4.2.2 Fabrication of Stirring Machine

For the proper stirring of MR polishing fluid composition, a stirring machine is required. The viscosity of the MR Fluid is very high and hence a very powerful and rugged machine is required. The mixing time for MR polishing fluid may go up to 1 hour. For this purpose, a stirring machine was fabricated. Initially CAD model was prepared and later drawings were generated as shown in Fig. 4.1. Based on the drawing generated and using various manufacturing processes the setup of stirring machine for synthesising the MR polishing fluid was fabricated. The actual machine after fabrication is shown in Fig. 4.2.

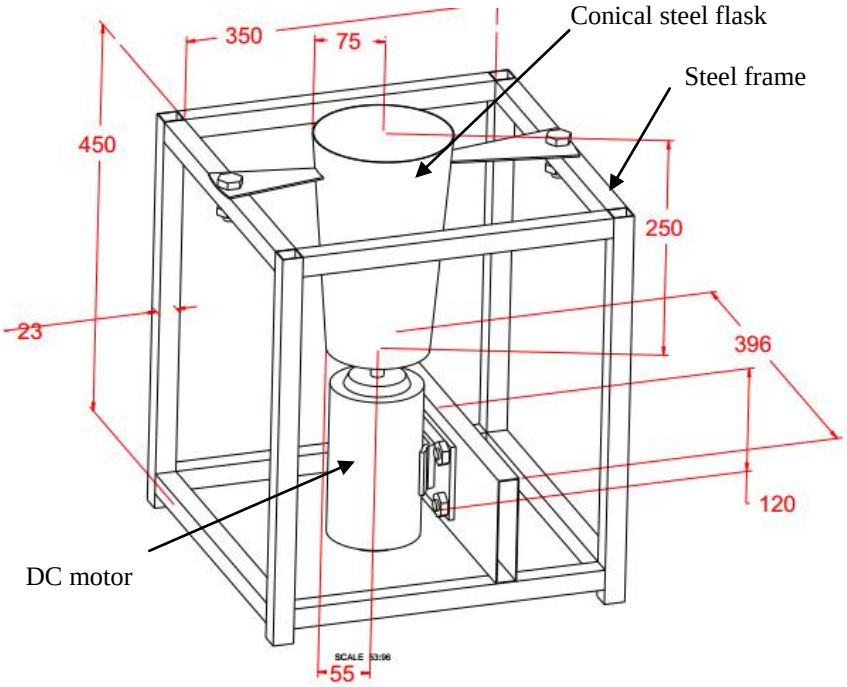

Figure 4.1: Drawing of the stirring machine with dimensions

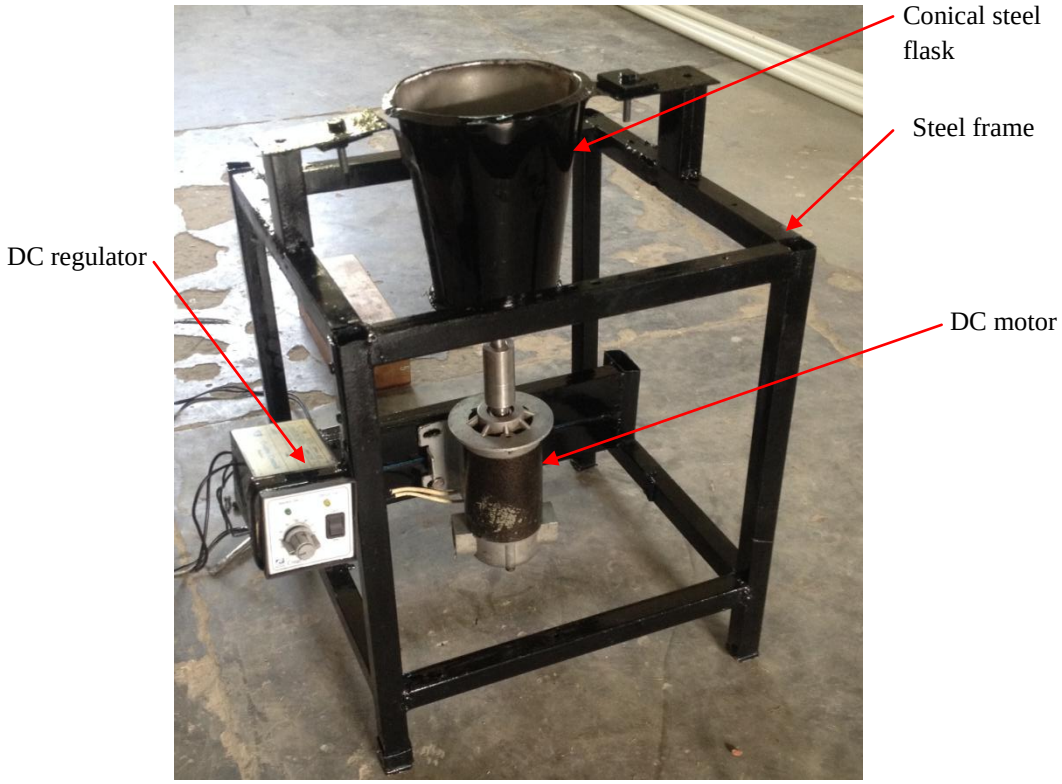

Figure 4.2: Photograph of stirring machine after fabrication

4.3 Preliminary Experimentation

Initially, a permanent mould punch made of P20 steel was used for conducting preliminary experimentation. The material is ferromagnetic in nature and its hardness is found as 431 VHN. . The composition if the material was verified using spectrometer. The composition of the material was found as Fe-93.9%, C-0.5%, Si-0.8%, Mn-0.9%, P-0.03%, S-0.03%, Cr-2.3%, Mo-0.5%, Ni-0.098%, Al-0.001%, Co-0.0201%, Cu-0.3%, Nb-0.0289%, Ti-0.018%, V-0.469%, W-0.105%. The preliminary experimentation was applied on the flat surface of the workpiece for 30 minutes. Initial surface roughness was measured using Mitutoyo SJ 400 contact type surface profile meter. The magnetorheological polishing fluid for this work composes of 20% carbonyl iron particles of 400 mesh size, 20% silicon carbide (SiC) with 800 mesh size used as abrasives and base fluid as 60 % (80% paraffin oil and 20% AP3 grease), by volume. The mixture was thoroughly mixed using the self developed stirring machine. Figure 4.3 shows the photograph taken when the ball end solid rotating core tool was performing the finishing operation.

Figure 4.3: Ball end solid rotating core tool while performing the finishing operation

Preliminary experimentation was conducted at 30 mm/min feed and 0.6 mm gap. Details of other variable process parameters for preliminary experimentation conducted are given in Table 4.1.

Table 4.1: Parameters and response while conducting the preliminary experimentation

S.No.	Parameters		Initial Average	Final Average
	Current (A)	Tool rotation (rpm)	Roughness (nm)	Roughness (nm)
1	1	300	1080	900
2	2	500	1080	880
3	3	1000	1080	670
4	3	1500	1080	490
5	4	1500	1080	710

After examining the response obtained from preliminary experimentation, the flat surface of the punch which acts as one of the face of the cavity formation in the cavity block was finished using the same process. The process parameters were 3A current, 1500 rpm tool rotation, 30 mm/min feed and 0.6 mm gap. After 120 minutes of finishing, the surface roughness value reduced from 1080 nm to 30 nm. The surface morphology was also examined using metallurgical microscope (laica) and mirror image test. Figure 4.4 shows the images for flat surface under the metallurgical microscope and mirror image test.

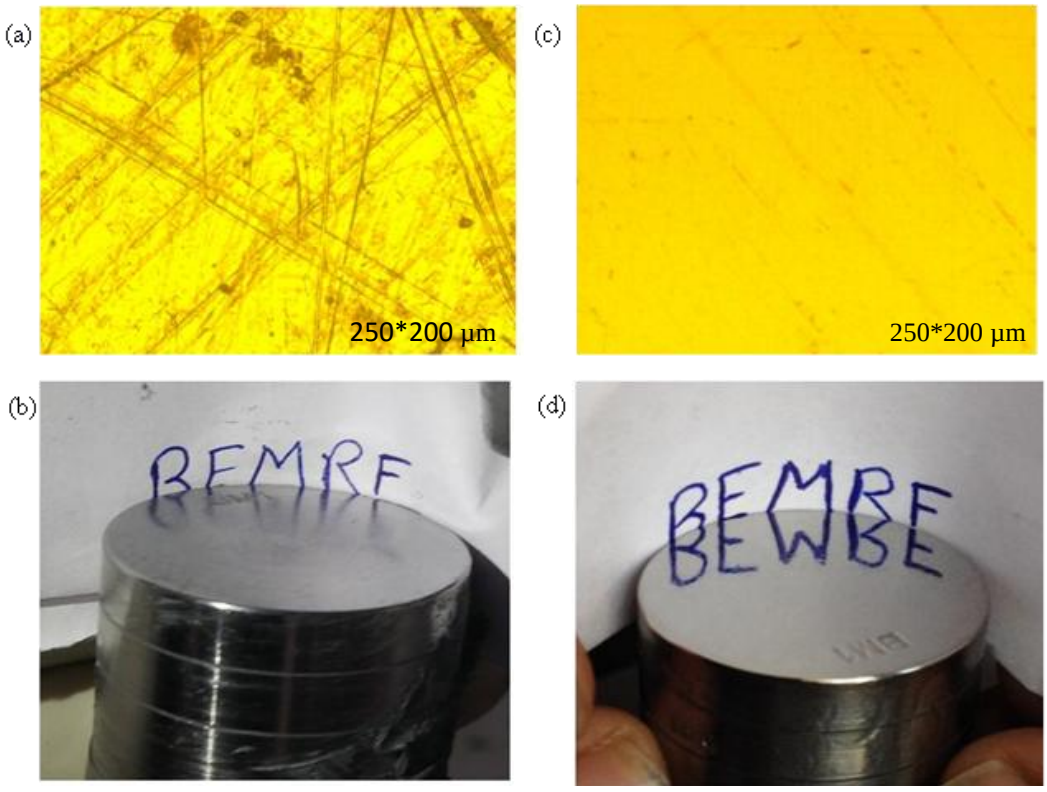

Figure 4.4: Metallurgical (Laica) microscopic images of flat surface before finish (a) of flat surface of present workpiece before and (c) after 120 minutes of finishing at 200x as well as mirror images (b) before and (d) after 120 minutes of finishing

Now, the experimentation was conducted on EN31 workpiece which has a hardness of 50 ±3 HRC. In order to correctly determine the levels of parameters for designing the experiment, preliminary experimentation was carried out. Initial experiments were carried out with MR polishing fluid having carbonyl iron particles (CIPs) as 20% by volume, SiC abrasives as 20% by volume and base fluid 20% by volume. Current levels were varied from 1 A to 5 A, tool Rotation was varied from 200 rpm to 2300 rpm as shown in Table 4.2.

Following are the details of preliminary experimentation conducted:

Constant parameters are as follows:

1) Feed – 30mm/min
2) Abrasive material – Silicon carbide (SiC)
3) Abrasive mesh size – 800
4) CIP mesh size – 400
5) Abrasive concentration – 20% by volume

6) CIP concentration – 20% by volume

Table 4.2: Variable Parameters for preliminary experimentation and the results obtained

Experiment No.	Current (A)	Tool Rotation (rpm)	Initial Ra (nm)	Final Ra (nm)
1	2	300	230	200
2	3	700	250	190
3	5	700	200	120
4	5	1700	270	200
5	3	2300	260	80

By conducting these preliminary experimentations it was clear that there was a considerable difference between the results for different levels of above said parameters.

4.4 Conclusion

- As the MRP fluid is a viscous fluid therefore a stirring machine was prepared for proper stirring of the MRP fluid constituents.
- The stirring machine helped in frequent preparing of MRP fluid with different compositions as required in the plan of experiments.
- From the literature survey and preliminary experiments conducted on P20 steel and EN31 steel it was observed that the process parameters are greatly dependent on the hardness of material.
- In case of preliminary experimentation on EN31 steel, significant variation in the surface roughness was seen with current up to 5A and tool rotation ranging from 700 to 2300.

Chapter 5

Plan of Experiments

5.1 Introduction

The ball end solid rotating core magnetorheological finishing process was used for the detailed study of finishing process using different parameters on permanent mould material EN31 (ferromagnetic). The study was conducted using statistical design of experiments. The planning and investigation of the effects of the magnetizing current, tool rotation speed, feed rate, abrasive concentration and CIP concentration on the percentage change in roughness was done using response surface methodology (RSM). The effects of these parameters individually and in combination have been discussed in detail and the best possible combination of all the parameters has been indentified within the experimental range of parameters. After analysis of the experimental results it was observed that the percentage change in roughness was affected mainly by CIP concentration followed by tool rotation, abrasive concentration, feed and current. The optimal process parameters were identified from the levels of the experimental design. Scanning electron microscopy was conducted to study the surface morphology. The performance of the present ball end solid rotating core magnetorheological finishing process has been evaluated with identified more significant process parameters.

5.2 Process Parameters

Based on the literature survey of BEMRF it was found that the parameters as given in Table 5.1 had a significant effect on the finishing of various materials. Out of the listed parameters, five of them were selected for the parametric study as discussed in the following sections:

Table 5.1 Parameters selection for experimentation

Parameters	Selected
Tool rotation	Yes
Current	Yes
Working gap	No
Feed	Yes
Abrasive size	No
Abrasive concentration	Yes
CIP concentration	Yes

5.2.1 Tool Rotation (N)

Rotation of tool core has a significant effect in the finishing of workpiece as the indentation force i.e. provided by the magnetizing current along with this shearing force as provided by the rotation of the tool core form a resultant force on the active abrasive particles which helps in removal of material from the surface of the workpiece in the form of micro chips. Experimental range for tool rotation was selected as 700 rpm to 2300 rpm. The levels of tool rotation were selected on the basis of "α" value for statistical design. The range of these values was chosen on the basis of preliminary experimentation which has been discussed in the Table 4.2.

5.2.2 Current (I)

The current is provided to the electromagnetic coil using a DC regulated power supply. Due this current, magnetic field is generated whose direction is given by Ampere's right hand thumb rule. The strength of magnetic flux density which is generated due to the magnetizing current applied to the electromagnetic coil, has huge influence on the rheological properties of the MRP fluid that is applied at the tip surface of the tool core. By varying the magnitude of magnetizing current, the stiffness of the MRP fluid can be controlled. It is also a major parameter in the MR finishing process as the indentation force is dependent on the magnetizing current. Experiments were conducted by varying the magnetizing current from 1A to 5 A. These values of current were selected in the range on the basis of preliminary experimentation and the prescribed design of the electromagnet. Lower and upper value of current is limited by gauge of wire in electromagnet coil.

5.2.3 Feed Rate (F)

The speed with which the tool moves along a certain path on the surface of workpiece is called its feed. Too high or too low feed could result in significant increase of finishing time of the workpiece. Moreover it might also result in variation of roughness obtained on the surface of the workpiece. Experiments were conducted with feed varying from 10 mm/min to 50 mm/min, as per the levels defined in the design. The range was chosen on the basis of capability of machine.

5.2.4 Abrasive Concentration (A)

Abrasive particles are added in the MR fluid in order to remove the material in the form of micro chips. The chipping off action is performed by the active abrasive particles at the surface of the tool tip. These abrasive particles are gripped between the CIP chains. The amount of abrasive particles will have considerable effect on the cutting action performed by the tool. Experiments were conducted with the concentration in percentage volume varying from 10% to 30%, as per the design levels. The range was selected on previous literature available.

5.2.5 Carbonyl Iron Powder Concentration

CIPs are important element of MR polishing fluid. They are responsible for gripping the abrasive particles in the chain like structures formed by them when magnetic field is applied across them. The strength of the chains is defined by the magnetizing current while the density of the chains is completely dependent on the number of CIPs added. For a particular level of abrasives, if the CIPs are too low, they might not be able to grip enough abrasive particles and if the CIPs are too high it may result in lower abrasive concentration thus leading to reduced cutting action. Experiments were conducted with concentration in percentage change varying from 10% to 30%, as per the design level. The range was selected on the basis of previous literature.

5.3 Design of Experiment

Systematic investigation of the effect of process variables on the percentage change in surface roughness value was done using the designed experiments. The set up shown in Fig. 3.5 was used for performing the designed experimentation. For easy observations and analysis under a scanning electron microscopy (SEM), the experiments were

performed on flat ferromagnetic workpiece of EN31 material with dimension 10 mm × 50 mm × 5 mm, which were obtained after various processes as discussed in chapter 3.5. The initial surface roughness (Ra_i) was in the range of 200 nm to 350nm. As the initial surface roughness values of ground workpiece cannot be equal for all the workpiece. Therefore, considering this variation in the initial roughness values, the ratio of change in surface roughness to the initial roughness was taken as response and it is given by Eq. 5.1.

As the tool tip diameter and width of the workpiece (as seen from the top) were not same, so raster scanning method was followed using the X-Y-axis servo motor, as shown in Fig. 5.1.

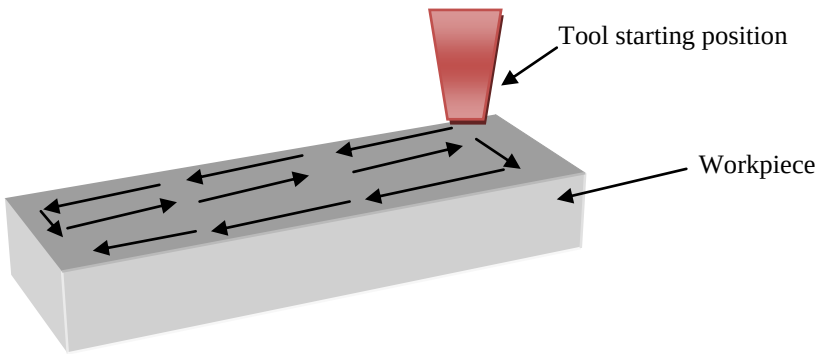

Figure 5.1: Schematic diagram of tool following the raster scanning path for finishing the workpiece surface

The current is immediately provided to the electromagnetic coil after the application of MR polishing fluid at the tip surface area of the tool. A semi solid structure of MR polishing fluid which is physically shaped like a ball is formed at the tip surface of the tool core as shown in Fig. 5.2.

(a) (b)

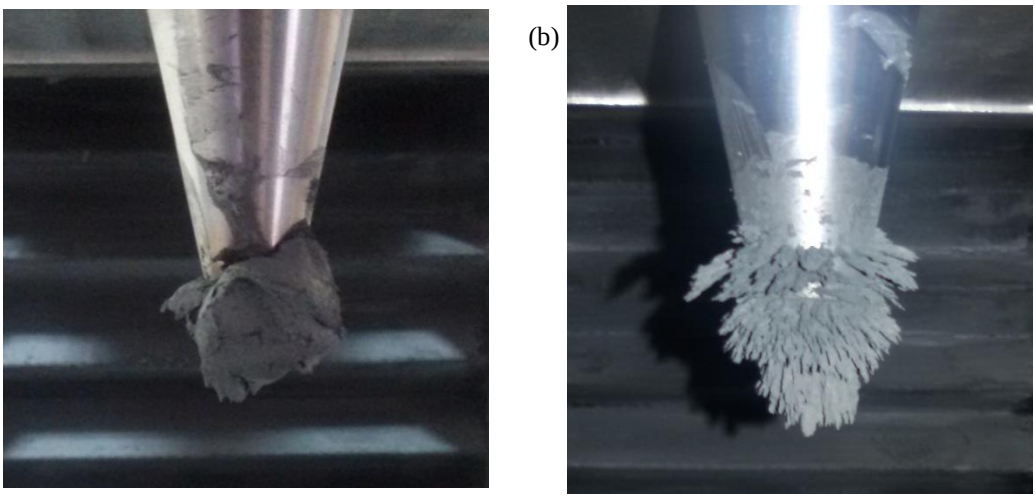

Figure 5.2: MRP fluid when (a) magnetic field is off (b) magnetic field is on

Response surface methodology (RSM) consists of a group of statistical and mathematical techniques used in the development of a suitable functional relationship between the inputs and the output. In full factorial experiments, all combinations of the factor levels are used for measuring the responses. The experimental conditions decide the combination of factor levels in the design. Five levels, central composite design with six central runs was used to conduct the experiments. 'F' test via analysis of variance (ANOVA) was conducted in order to understand the significance of regression equation in explaining the relationship between the response output and the control variables. RSM was used to investigate the effects of five process variables on percentage change in surface roughness (% ΔRa). Material removal rate was not considered as a response as the material removed from this super finishing process is too low (micrograms) to measure by the normal precision measuring balance.

Table 5.2 lists the actual values of different parameters used in conducting the experimentation. The other experimental conditions are listed in Table 5.3. MRP- fluid as per the required percentage volume concentrations can be prepared using the calculations given in chapter 4.2.1. Experiments were divided and conducted in groups based on same composition of MRP fluid, as per the plan of experiments given in Table 5.4.

Table 5.2 Coded levels and corresponding actual values of process parameters

S.No.	Parameter	Unit	Levels				
			-2	-1	0	1	2
1	Current (I)	A	1	2	3	4	5
2	Tool Rotation (N)	rpm	700	1100	1500	1900	2300
3	Feed (F)	mm/min	10	20	30	40	50
4	Abrasive (A)	%	10	15	20	25	30
5	CIP (C)	%	10	15	20	25	30

Table 5.3: Experimental parameters and conditions

Parameters	Conditions
Finishing cycle time	60 minutes
Silicon carbide abrasive powder	800 mesh size
CIP powder	400 mesh size
Workpiece material EN31 (hardness 50 ±3 HRC)	Ferromagnetic

Table 5.4: Plan of experiments

Std order	Run order	Actual Values				
		Current I	Tool Rotation N	Feed F	Abrasive (%) A	CIP (%) C
1	23	2	1100	20	15	15
2	32	4	1100	20	15	15
3	34	2	1900	20	15	15
4	40	4	1900	20	15	15
5	10	2	1100	40	15	15
6	24	4	1100	40	15	15
7	30	2	1900	40	15	15
8	2	4	1900	40	15	15
9	22	2	1100	20	25	15
10	7	4	1100	20	25	15
11	1	2	1900	20	25	15
12	39	4	1900	20	25	15
13	29	2	1100	40	25	15
14	50	4	1100	40	25	15
15	3	2	1900	40	25	15
16	14	4	1900	40	25	15
17	46	2	1100	20	15	25
18	11	4	1100	20	15	25
19	42	2	1900	20	15	25
20	19	4	1900	20	15	25
21	9	2	1100	40	15	25

22	47	4	1100	40	15	25
23	48	2	1900	40	15	25
24	43	4	1900	40	15	25
25	37	2	1100	20	25	25
26	26	4	1100	20	25	25
27	18	2	1900	20	25	25
28	49	4	1900	20	25	25
29	12	2	1100	40	25	25
30	33	4	1100	40	25	25
31	21	2	1900	40	25	25
32	36	4	1900	40	25	25
33	15	1	1500	30	20	20
34	20	5	1500	30	20	20
35	6	3	700	30	20	20
36	16	3	2300	30	20	20
37	13	3	1500	10	20	20
38	35	3	1500	50	20	20
39	44	3	1500	30	10	20
40	45	3	1500	30	30	20
41	28	3	1500	30	20	10
42	41	3	1500	30	20	30
43	5	3	1500	30	20	20
44	31	3	1500	30	20	20
45	27	3	1500	30	20	20
46	38	3	1500	30	20	20
47	8	3	1500	30	20	20
48	17	3	1500	30	20	20
49	4	3	1500	30	20	20
50	25	3	1500	30	20	20

Table 5.5: Summary of responses

Std. order	Factors					Initial roughness values	Final roughness values	% change in roughness value
	I	N	F	A	C	Ra_i	Ra_f	% ΔRa
1	2	1100	20	15	15	300	171.00	43.00
2	4	1100	20	15	15	280	168.00	40.00
3	2	1900	20	15	15	290	44.19	84.76
4	4	1900	20	15	15	320	149.33	53.33
5	2	1100	40	15	15	330	245.14	25.71
6	4	1100	40	15	15	350	185.00	47.14
7	2	1900	40	15	15	290	122.63	57.71

8	4	1900	40	15	15	280	148.00	47.14
9	2	1100	20	25	15	290	140.86	51.43
10	4	1100	20	25	15	320	126.48	60.48
11	2	1900	20	25	15	330	141.90	57.00
12	4	1900	20	25	15	320	233.60	27.00
13	2	1100	40	25	15	330	304.86	7.62
14	4	1100	40	25	15	350	265.00	24.29
15	2	1900	40	25	15	290	226.48	21.90
16	4	1900	40	25	15	320	272.76	14.76
17	2	1100	20	15	25	330	221.57	32.86
18	4	1100	20	15	25	320	187.43	41.43
19	2	1900	20	15	25	330	33.00	90.00
20	4	1900	20	15	25	350	180.00	48.57
21	2	1100	40	15	25	360	159.43	55.71
22	4	1100	40	15	25	320	128.00	60.00
23	2	1900	40	15	25	330	30.30	90.81
24	4	1900	40	15	25	240	48.00	80.00
25	2	1100	20	25	25	240	99.43	58.57
26	4	1100	20	25	25	250	137.50	45.00
27	2	1900	20	25	25	260	30.95	88.10
28	4	1900	20	25	25	290	125.94	56.57
29	2	1100	40	25	25	280	110.40	60.57
30	4	1100	40	25	25	240	52.80	78.00
31	2	1900	40	25	25	210	30.00	85.00
32	4	1900	40	25	25	270	51.43	80.95
33	1	1500	30	20	20	280	148.00	47.14
34	5	1500	30	20	20	290	160.19	44.76
35	3	700	30	20	20	360	202.63	43.71
36	3	2300	30	20	20	320	54.40	83.00
37	3	1500	10	20	20	330	136.71	58.57
38	3	1500	50	20	20	250	121.43	51.43
39	3	1500	30	10	20	260	146.34	43.71
40	3	1500	30	30	20	250	212.50	15.00
41	3	1500	30	20	10	260	125.05	51.90
42	3	1500	30	20	30	290	58.00	80.00
43	3	1500	30	20	20	280	138.67	50.48
44	3	1500	30	20	20	240	116.57	51.43
45	3	1500	30	20	20	290	145.00	50.00
46	3	1500	30	20	20	270	115.71	57.14
47	3	1500	30	20	20	280	138.67	50.48
48	3	1500	30	20	20	290	146.38	49.52
49	3	1500	30	20	20	360	205.71	42.86
50	3	1500	30	20	20	320	170.67	46.67

5.4 Response Surface Regression Analysis

The responses for the experimentation conducted are presented in Table 5.5. Response surface for percentage change in Ra value is analyzed.

$$\% \Delta Ra = [(Ra_i - Ra_f) / Rai] \times 100 \quad (5.1)$$

Where ΔRa = Change in average roughness

Ra_i = Initial average roughness

Ra_f = Final average roughness

From the model which is not aliased, highest order polynomial was selected on the basis of sequential model sum of squares calculations. Contribution of terms of increasing complexity to the total model is shown in Table 5.6 of sequential model sum of squares. Because of high F- value and least P- value, significance of adding quadratic terms to two factor interaction and linear term is highest, and thus it suggests its suitability. Calculated lack of fit for all possible models is shown in Table 5.7. Lack of fit is insignificant for the selected quadratic model.

Quadratic model was selected on the basis of Tables 5.6 and 5.7. All the terms such as I, N, F, A, C, IN, IF, IA, IC, NF, NA, NC, FA, FC, AC, I^2, N^2, F^2, A^2 and C^2 were included in the response surface model in the first phase. The model F-value of 22.65 implies the model is significant. There is only a 0.01% chance that an F-value this large could occur due to noise. Values of "Prob. > F" less than 0.05 indicate model terms are significant. For a hypothesis test, a value for which a *p –value* less than or equal to α is considered statistically significant is called its significant level (0.05). 0.1, 0.05 and 0.01 are the typical values for α. These values correspond to the probability of observing such an extreme value by chance. The "Lack of Fit F-value" of 3.12 implies there is a 6.35% chance that a "Lack of Fit F- value" this large could occur due to noise. $\alpha = 0.05$ is taken as the significance level for studying the present work.

Table 5.6 Sequential model sum of squares

Source	Sum of Squares	DoF	Mean Square	F Value	p-value Prob > F	
Mean vs. Total	1.401E+005	1	1.401E+005			
Linear vs. Mean	9130.14	5	1826.03	6.91	< 0.0001	
2FI vs. Linear	8501.29	10	850.13	9.25	< 0.0001	
Quadratic vs. 2FI	**1876.58**	**5**	**375.32**	**8.72**	**< 0.0001**	**Suggested**
Cubic vs. Quadratic	784.54	15	52.30	1.58	0.2005	Aliased
Residual	464.36	14	33.17			
Total	1.608E+005	50	3216.57			

Table 5.7 Lack of fit

Source	Sum of Squares	DoF	Mean Square	F Value	p-value Prob > F	
Linear	11511.15	37	311.11	18.84	0.0003	
2FI	3009.86	27	111.48	6.75	0.0071	
Quadratic	**1133.28**	**22**	**51.51**	**3.12**	**0.0635**	**Suggested**
Cubic	348.74	7	49.82	3.02	0.0842	Aliased
Pure Error	115.62	7	16.52			

Table 5.8 ANOVA for percentage change in Ra

Source	Sum of Squares	DoF	Mean Square	F Value	p-value Prob > F	
Model	19508.02	20	975.40	22.65	< 0.0001	significant
I	384.70	1	384.70	8.93	0.0057	
N	2951.03	1	2951.03	68.52	< 0.0001	
F	43.80	1	43.80	1.02	0.3216	
A	501.06	1	501.06	11.63	0.0019	
C	5249.55	1	5249.55	121.90	< 0.0001	
IN	1815.03	1	1815.03	42.15	< 0.0001	
IF	678.79	1	678.79	15.76	0.0004	
IA	16.53	1	16.53	0.38	0.5404	
IC	75.91	1	75.91	1.76	0.1947	
NF	6.378E-004	1	6.378E-004	1.481E-005	0.9970	
NA	843.92	1	843.92	19.60	0.0001	
NC	587.35	1	587.35	13.64	0.0009	
FA	341.41	1	341.41	7.93	0.0087	
FC	3078.32	1	3078.32	71.48	< 0.0001	
AC	1064.03	1	1064.03	24.71	< 0.0001	
I^2	13.66	1	13.66	0.32	0.5777	
N^2	437.59	1	437.59	10.16	0.0034	
F^2	82.81	1	82.81	1.92	0.1761	
A^2	737.92	1	737.92	17.13	0.0003	
C^2	604.61	1	604.61	14.04	0.0008	
Residual	1248.90	29	43.07			
Lack of Fit	1133.28	22	51.51	3.12	0.0635	not significant
Pure Error	115.62	7	16.52			
Cor Total	20756.91	49				

Other ANOVA parameters are given in Table 5.9. Response value is predicted by the 'predicted R^2' which is a measure of how good the model is. The "Pred. R-Squared" of 0.7889 is in reasonable agreement with the "Adj. R-Squared" of 0.8983; i.e. the difference is less than 0.2. "Adequate Precision" measures the signal to noise ratio. The ratio of 21.841 indicates an adequate signal (ratio > 4 is required).

Table 5.9 Other ANOVA parameters

Std. Dev.	6.56	R-Squared	0.9398
Mean	52.93	Adj. R-Squared	0.8983
C.V. %	12.40	Pred. R-Squared	0.7889
PRESS	4382.47	Adeq. Precision	21.841
-2 Log Likelihood	302.79	BIC	384.95
		AICc	377.79

S.D.: standard deviation, C.V.: Coefficient of variation, *Predicted residual sum of squares.

Table 5.10 Factor coefficients (coded form)

	Coefficient		**Standard**	**95% CI**	**95% CI**	
Factor	**Estimate**	**DOF**	**Error**	**Low**	**High**	**VIF**
Intercept	49.57	1	2.27	44.92	54.22	
A-I	-3.10	1	1.04	-5.22	-0.98	1.00
B-N	8.59	1	1.04	6.47	10.71	1.00
C-F	-1.05	1	1.04	-3.17	1.08	1.00
D-A	-3.54	1	1.04	-5.66	-1.42	1.00
E-C	11.46	1	1.04	9.33	13.58	1.00
AB	-7.53	1	1.16	-9.90	-5.16	1.00
AC	4.61	1	1.16	2.23	6.98	1.00
AD	0.72	1	1.16	-1.65	3.09	1.00
AE	-1.54	1	1.16	-3.91	0.83	1.00
BC	-4.464E-003	1	1.16	-2.38	2.37	1.00
BD	-5.14	1	1.16	-7.51	-2.76	1.00
BE	4.28	1	1.16	1.91	6.66	1.00
CD	-3.27	1	1.16	-5.64	-0.89	1.00
CE	9.81	1	1.16	7.44	12.18	1.00
DE	5.77	1	1.16	3.39	8.14	1.00
A^2	-0.65	1	1.16	-3.03	1.72	1.00
B^2	3.70	1	1.16	1.33	6.07	1.00
C^2	1.61	1	1.16	-0.76	3.98	1.00
D^2	-4.80	1	1.16	-7.17	-2.43	1.00
E^2	4.35	1	1.16	1.97	6.72	1.00

DOF: Degrees of freedom, CI: Confidence interval, VIF: Variance inflation factor.

The coefficient estimate for the factor is surrounded by the 95% confidence interval which has 95% high and low confidence interval (CI) values as the upper and

lower bound. The range of values in which the true coefficient should be found in 95% of the time is shown in Table 5.10. Factor has no effect is this range spans 0 (one limit is positive and the other negative). The measure of how much the variance of the model is inflated by the lack of orthogonality in the design is given by variance inflation factor (VIF). The VIF is one when a factor is orthogonal to all other factors. If the value is greater than 10, it indicates that the correlation is very high among the factors. The final equation in terms of coded factors is given on the basis of the coefficients calculated in Table 5.10.

Final equation in terms of coded factors:

% change in roughness, % ΔRa= 49.57 -3.10 A +8.59 B -1.05C -3.54 D +11.46 E -7.53 AB +4.61 AC +0.72 AD -1.54 AE- 4.464e-003 BC -5.14 BD +4.28 BE -3.27 CD +9.81 CE +5.77 DE -0.65 A^2 +3.70 B^2 +1.61 C^2 -4.80 D^2 +4.35 E^2 (5.2)

Predictions about the response of each given level of each factor can be made using the equation. By default, the high levels of the factors are coded as +2 and the low levels of the factors are coded as -2. By comparing the factor coefficients from the coded equation the relative impact of the factors can be identified.

Final Equation in terms of actual factors:

% change in roughness, % ΔRa = 156.26207 +18.52939 I +0.017167 N -5.06651 F +7.74251 A -17.45055 C -0.018828 IN +0.46057 IF +0.14375 IA -0.30804 IC -1.11607E-006 NF -2.56771E-003 NF -2.56771E-003 NA +2.14211E-003 NC -0.065327 FA +0.19616 FC +0.23065 AC -0.65327 I^2 +2.31120E-005 N^2 +0.016086 F^2 -0.19208 A^2 +0.17387 C^2 (5.3)

There are five insignificant model terms (p-value > 0.05) as shown in Table 5.8. The insignificant model terms are dropped which leads to the reduction of model.

The ANOVA analysis after dropping the insignificant terms is presented in Table 5.11 and Table 5.12. The Model F-value of 30.46 implies the model is significant. There is only a 0.01% chance that an F-value this large could occur due to noise. Values of "Prob. > F" less than 0.0500 indicate model terms are significant. In this case A, B, D, E, AB, AC, BD, BE, CD, CE, DE, B^2, D^2, E^2 are significant model terms. The "Pred.

R-Squared" of 0.8240 is in reasonable agreement with the "Adj. R-Squared" of 0.9002; i.e. the difference is less than 0.2. "Adeq. Precision" measures the signal to noise ratio. The ratio of 24.025 indicates an adequate signal as it is larger than the least desirable ratio i.e. 4.

Table 5.11 ANOVA for % change in Ra after dropping the insignificant terms

Source	Sum of Squares	DoF	Mean Square	F Value	p-value Prob. > F	
Model	19319.11	15	1287.94	30.46	< 0.0001	significant
A-I	384.70	1	384.70	9.10	0.0048	
B-N	2951.03	1	2951.03	69.78	< 0.0001	
C-F	43.80	1	43.80	1.04	0.3160	
D-A	501.06	1	501.06	11.85	0.0015	
E-C	5249.55	1	5249.55	124.14	< 0.0001	
AB	1815.03	1	1815.03	42.92	< 0.0001	
AC	678.79	1	678.79	16.05	0.0003	
BD	843.92	1	843.92	19.96	< 0.0001	
BE	587.35	1	587.35	13.89	0.0007	
CD	341.41	1	341.41	8.07	0.0075	
CE	3078.32	1	3078.32	72.79	< 0.0001	
DE	1064.03	1	1064.03	25.16	< 0.0001	
B^2	437.59	1	437.59	10.35	0.0028	
D^2	737.92	1	737.92	17.45	0.0002	
E^2	604.61	1	604.61	14.30	0.0006	
Residual	1437.80	34	42.29			
Lack of Fit	1322.18	27	48.97	2.96	0.0704	not significant
Pure Error	115.62	7	16.52			
Cor Total	20756.91	49				

Table 5.12 Other ANOVA parameters after model reduction

Std. Dev.	6.50	R-Squared	0.9307
Mean	52.93	Adj R-Squared	0.9002
C.V. %	12.29	Pred R-Squared	0.8240
PRESS	3652.98	Adeq Precision	24.025
-2 Log Likelihood	309.84	BIC	372.43
		AICc	358.32

Factor coefficients (coded form) after model reduction are given in Table 5.13 represent the range that the true coefficient should be found in 95% of the time.

Final equation in terms of coded factors:

% change in roughness, % ΔRa= 50.33-3.10 A + 8.59 B - 1.05 C - 3.54 D + 11.46 E - 7.53 AB + 4.61 AC - 5.14 BD + 4.28 BE - 3.27 CD + 9.81 CE + 5.77 DE + 3.70 B^2 - 4.80 D^2 + 4.35 E^2 (5.4)

Final equation terms of actual factors:

%change in roughness, % ΔRa= 158.33551 + 11.32403 I + 0.017134 N - 4.10301 F + 8.17376 A - 18.37466 C - 0.018828 IN + 0.46057 IF - 2.56771E-003 NA + 2.14211E-003 NC - 0.065327 FA + 0.19616 FC + 0.23065 AC + 2.31120E-005 N^2 - 0.19208 A^2 + 0.17387 C^2 (5.5)

Percentage contributions of process parameters on the improvement in surface roughness Ra is presented in Table 5.14.

Table 5.13 Factor coefficients (coded form) after model reduction

Factor	Coefficient Estimate	df	Standard Error	95% CI Low	95% CI High	VIF
Intercept	50.33	1	1.84	46.60	54.07	
A-I	-3.10	1	1.03	-5.19	-1.01	1.00
B-N	8.59	1	1.03	6.50	10.68	1.00
C-F	-1.05	1	1.03	-3.14	1.04	1.00
D-A	-3.54	1	1.03	-5.63	-1.45	1.00
E-C	11.46	1	1.03	9.37	13.55	1.00
AB	-7.53	1	1.15	-9.87	-5.20	1.00
AC	4.61	1	1.15	2.27	6.94	1.00
BD	-5.14	1	1.15	-7.47	-2.80	1.00
BE	4.28	1	1.15	1.95	6.62	1.00
CD	-3.27	1	1.15	-5.60	-0.93	1.00
CE	9.81	1	1.15	7.47	12.14	1.00
DE	5.77	1	1.15	3.43	8.10	1.00
B^2	3.70	1	1.15	1.36	6.03	1.00
D^2	-4.80	1	1.15	-7.14	-2.47	1.00
E^2	4.35	1	1.15	2.01	6.68	1.00

Table 5.14 Percentage contribution of process parameters in final response of Ra

Source	Sum of squares	% contribution
I	384.70	1.98
N	2951.03	15.18
F	43.80	0.23
A	501.06	2.58
C	5249.55	27.01
IN	1815.03	9.34
IF	678.79	3.49
NA	843.92	4.34
NC	587.35	3.02
FA	341.41	1.76
FC	3078.32	15.84
AC	1064.03	5.47
N^2	437.59	2.25
A^2	737.92	3.80
C^2	604.61	3.11
Pure error	115.62	0.59

5.5 Results and Discussion

On the basis of the results of response surface model Eq. 5.5 obtained after regression analysis, the results in terms of effect of tool rotation, current, feed rate, abrasive concentration and CIP concentration on the percentage reduction of surface roughness have been observed and computed. The independent controllable variable effects and interaction effects are found to be significant in ANOVA analysis and therefore discussed below.

5.5.1 Effect of Current

The effect of current on percentage change in roughness with tool rotation at 1500 rpm, feed at 30 mm/min, abrasive concentration at 20% and CIP concentration at 20% is shown in Fig. 5.3. With the increase in the value of current, it can be seen from the Fig. 5.3 that the percentage change in the roughness value decreases.

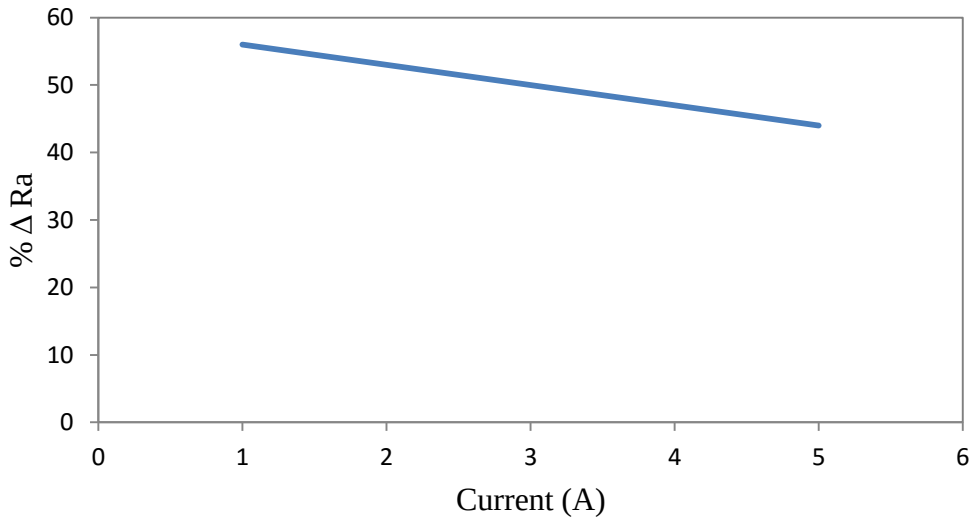

Figure 5.3: Effect of current on percentage change in roughness (% ΔRa)

The sole reason for the same is the high indentation force generated due to high magnetic flux density at the tip surface of tool at higher current. The high indentation force along with tool rotation as 1500 rpm (considerably high as compared with previous literature) generates a very high resultant force. This resultant force is so high that it not only removes the peaks but also removes the surface material which was not to be removed. The resultant finishing force is so large that it starts scratching the surface, which results in pits formation as shown in Fig. 5.4. The roughness value of these pits and scratches is lower than that of initial roughness value and hence it results in some percentage change in roughness, but this percentage change in roughness is lesser than

that obtained with lower value of current. However it was also observed that lower values of current give better reduction as the low current value is not only sufficient enough to form strong CIP chains to chip off the material but also they are not that strong so as to deeply indent the MRP fluid particles inside the workpiece in such a manner that they scratch out the surface material as shown in Fig. 5.5. It was also observed that under the influence of low current values the cracks (formed due to traditional finishing) were also removed and the surface obtained was crack free. However under the influence of high current value, the cracks remained intact. This could have happened because of the high indentation force applied by the abrasive particles. Due to high indentation force the abrasives may have kept on digging the cracks wider and deeper thus leading to lower percentage change in roughness. Though it is a possibility that with high current and higher working time, the crack may be removed.

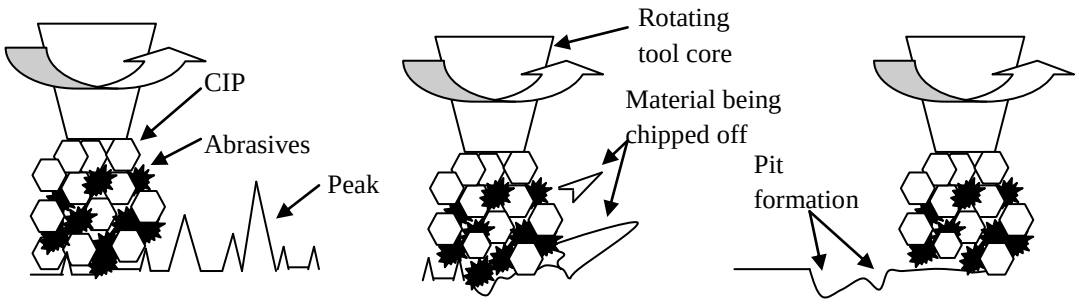

Figure 5.4: Mechanism of material removal with high current (a) rotating tool core with stiffed MRP fluid approaching the rough area, (b) material being chipped off by the MRP fluid and (c) pits formed due to highly stiffed MRP fluid

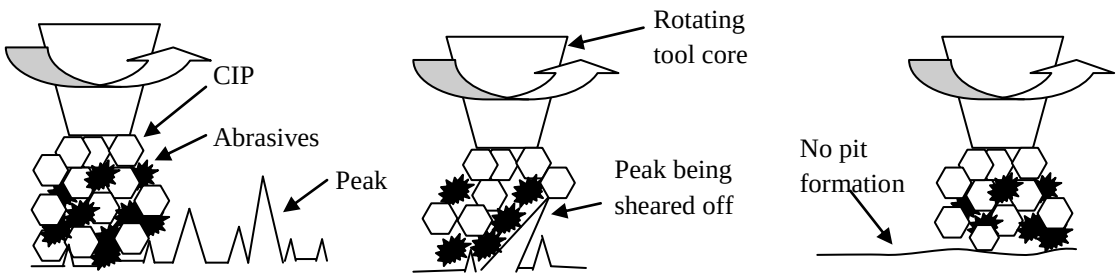

Figure 5.5: Mechanism of material removal with low current, (a) rotating tool core approaching the rough area, (b) peaks being sheared off by the abrasive particles of MRP fluid which is appropriately stiffed and (c) no pit formation on final finished surface

5.5.2 Effect of Tool Rotation

The effect of tool rotation on percentage change in roughness with current at 3A, feed at 30 mm/min, abrasive concentration at 20% and CIP concentration at 20% is shown in Fig. 5.6.

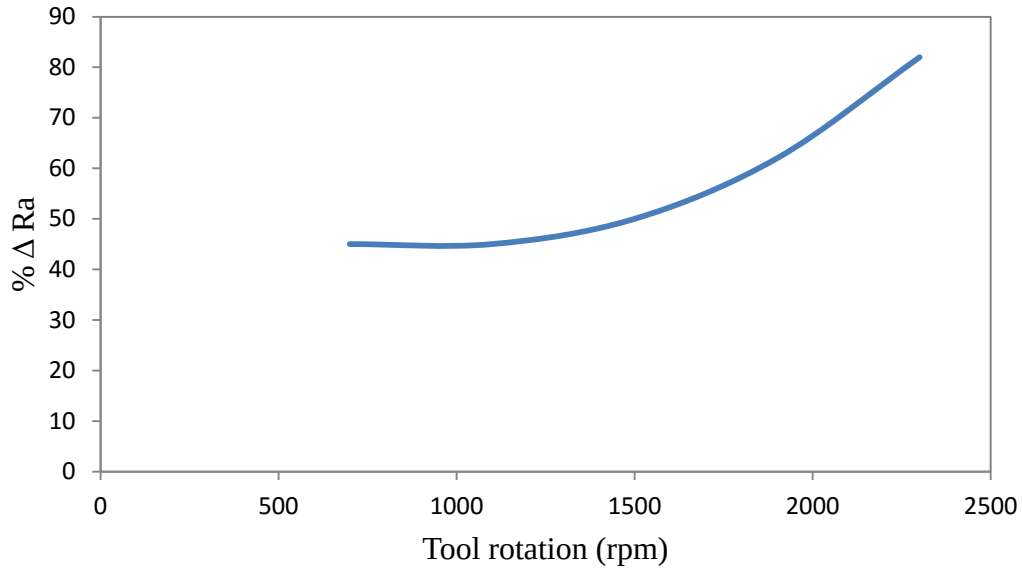

Figure 5.6: Effect of tool rotation speed on the percentage change in roughness (% ΔRa)

It was observed that higher tool rotation values give better finish on the workpiece surface. The trend of percentage reduction increases with increase in tool rotation speed. As the tool rotation force contributes to the resultant force which is responsible for chipping off the material in the form of micro chips from the surface of the workpiece, the tool rotation has a major effect on the surface finishing of the workpiece. Due to increase in tool rotation speed, the abrasives strike the workpiece surface at a very high kinetic energy. This kinetic energy along with indentation force provided by the magnetizing current shear the peaks off the workpiece surface. At lower tool rotation values, the percentage change in roughness is lesser than that at higher tool rotation values. For the same current level (3A), when the tool rotation speed is decreased, the kinetic energy of the abrasive particles reduce and the percentage change in roughness decreases.

5.5.3 Effect of Feed Rate

The effect of feed rate on percentage change in roughness with current at 3A, tool rotation at 1500 rpm, abrasive concentration at 20% and CIP concentration at 20% is shown in Fig. 5.7.

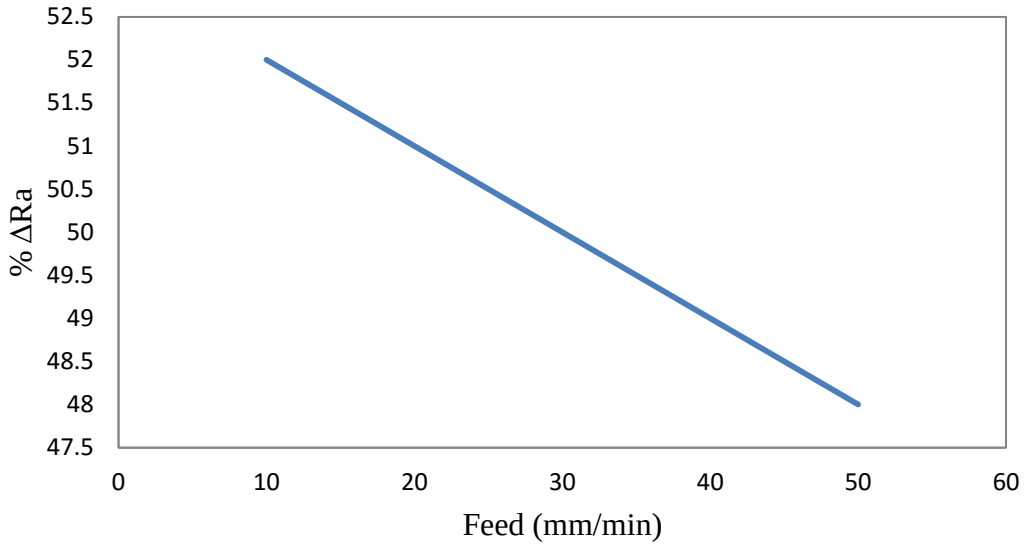

Figure 5.7: Effect of feed rate on percentage change in roughness (% ΔRa)

Higher feed rate values resulted drop in percentage change in roughness values. As the feed value increased, the tool could not get sufficient time to finish a particular area and thus resulted in lower percentage reduction values. However, at lower feed rate values, the tool could get sufficient time to finish the area under it and thus the percentage change in roughness value was more in this case. It was also seen that this trend reversed with certain change in parameters. The shift in trend of percentage change in roughness due to feed has been discussed in later chapters.

5.5.4 Effect of Abrasive Concentration of MRP Fluid

The effect of abrasive concentration on percentage change in roughness with current at 3A, tool rotation at 1500 rpm, feed at 30mm/min and CIP concentration at 20% is shown in Fig. 5.8.

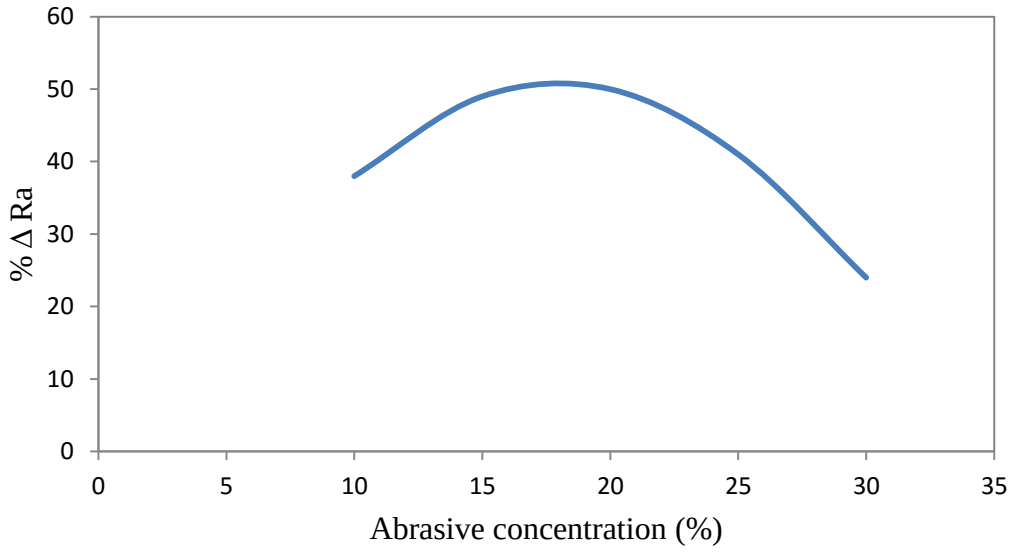

Figure 5.8: Effect of abrasive concentration on percentage change in roughness (% ΔRa)

Abrasive concentration is of high importance as the abrasives are the sole medium of chipping off the material from the surface of the workpiece. For particular CIP concentration, low and high abrasive concentration leads to lesser change in percentage reduction. However there is some particular value for a given CIP concentration which leads to an optimum % composition of the MRP fluid. As the abrasive concentration is low, there are not sufficient abrasives to chip off the material from the workpiece surface. When the abrasive concentration is too high, the CIP chains were not sufficient to grip the abrasives and the excess abrasives were free to move and thus they led to decrease in percentage reduction of roughness value. It is seen that the optimum abrasive concentration is between 15% and 20% for 20% CIP concentration. However with change in other parameters, this optimum value of abrasive concentration will also change for a given CIP concentration. This change has been explained in later part of the chapter.

5.5.5 Effect of CIP Concentration of MRP fluid

The effect of CIP concentration on percentage change in roughness with current at 3A, tool rotation at 1500 rpm, feed at 30mm/min and abrasive concentration at 20% is shown in Fig. 5.9.

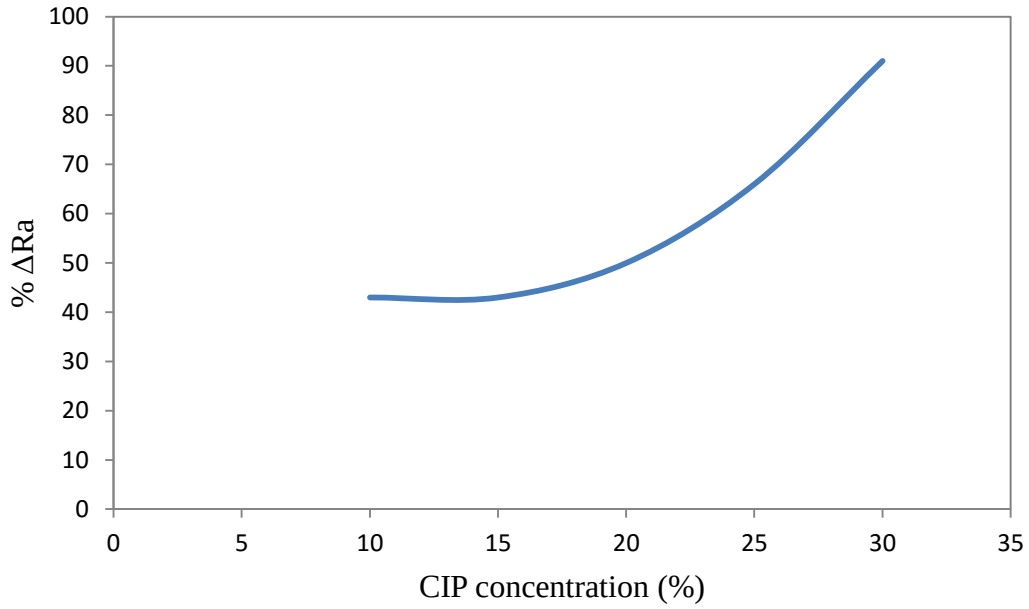

Fig. 5.9: Effect of CIP concentration in percentage change in roughness (% ΔRa)

The CIPs are responsible for gripping the abrasive particles in between them. For a particular value of abrasive concentration as the CIP concentration increases it leads to higher change in percentage reduction of roughness value. However, it is also a possibility outside the design levels that if the concentration of CIP is increased above a certain level the change in percentage reduction of roughness will decrease as the concentration of active abrasive particles at the tip surface will be very low.

5.5.6 Effect of Interaction of Current and Tool Rotation

The effect of interaction of magnetizing current and tool rotation on percentage change in *Ra* value at 30 mm/min feed rate, 20% abrasives concentration and 20% CIP concentration is shown in Fig. 5.10.

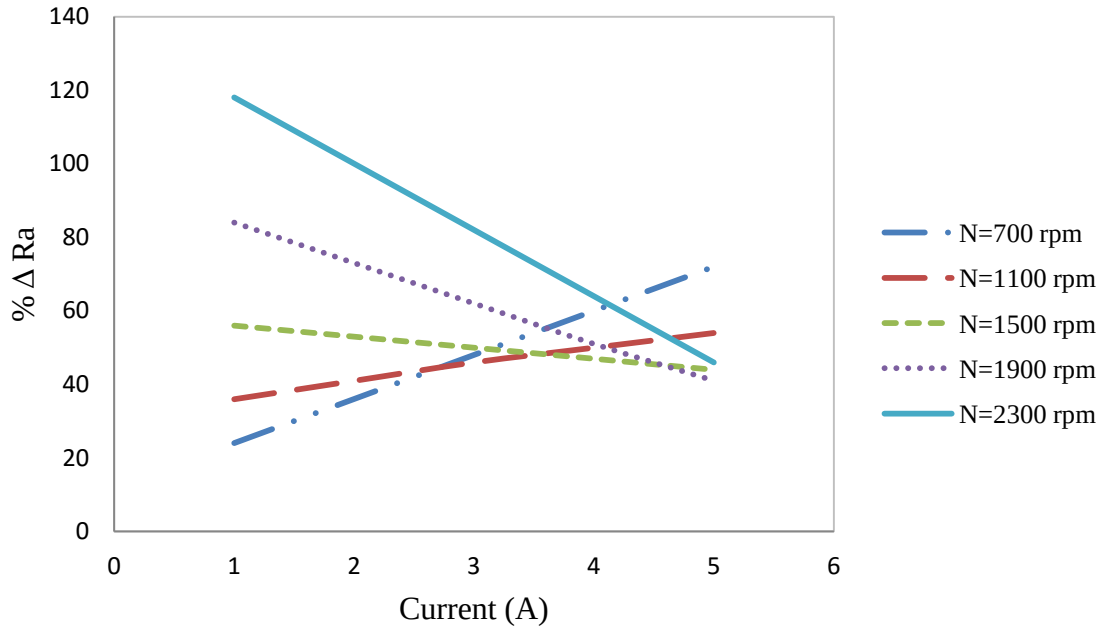

Figure 5.10: Effect of interaction of current and tool rotation on % ΔRa

In this graph it can be clearly observed that high percentage change in roughness can be observed in two cases that are, case 1- low value of current with high tool rotation value and case 2- at high value of current with low value of tool rotation. The percentage change in roughness is more in case 1 i.e. low value of current with high tool rotation value. It was thus concluded that in case 1, the magnetic field generated by the magnetizing current was sufficient enough to form strong CIP chain like structures which could grip the abrasive particles in between them and not let the effect of centrifugal force generated by the tool rotation to overpower it. Also, with high kinetic energy of the abrasive particles due to high tool rotation and appropriate low current, the material contributing to increased roughness value was being sheared off in an almost perfect manner. Hence a very high percentage change in roughness was observed. While in case 2, it was observed that due to high magnetic field generated by high value of current the indentation force (F_i) of the particles became very high. With lower values of tool rotation and high current, the abrasives were also able to chip off the peaks on the surface of the material. But the rotational force (F_r) was not sufficient to take out the deeply indented abrasive particles from the surface of the workpiece due to the high indentation force. The direction of resultant force (F_{rf}) was overpowered by the indentation force as shown in Fig. 5.11 and thus most of the abrasive particles were either indented in the surface of the material or they formed pit on surface of the workpiece which led to drop in percentage change of roughness. A better understanding can be made from Fig. 5.12 which shows the contour and 3D plot of the interaction of

current and tool rotation. It can be seen in Fig. 5.12 (a) that for 1A current and 2300rpm tool rotation the percentage change being shown in more than 100%. This data presented in the 3D plot is based on the model generated i.e. theoretical. According to design, there is no experiment with such parameters i.e. at 1A current and 2300 rpm tool rotation. But during actual experimentation for optimum combination, it was observed that with 1A current and 2300 rpm tool rotation, the magnetic flux was not sufficient to hold the MRP fluid and under the effect of centrifugal force the MRP fluid was being thrown out of action.

Figure 5.11: Line diagram depicting (a) when the resultant force is sufficient to chip off the material from the workpiece (b) when the direction of resultant force is dominated by the indentation force

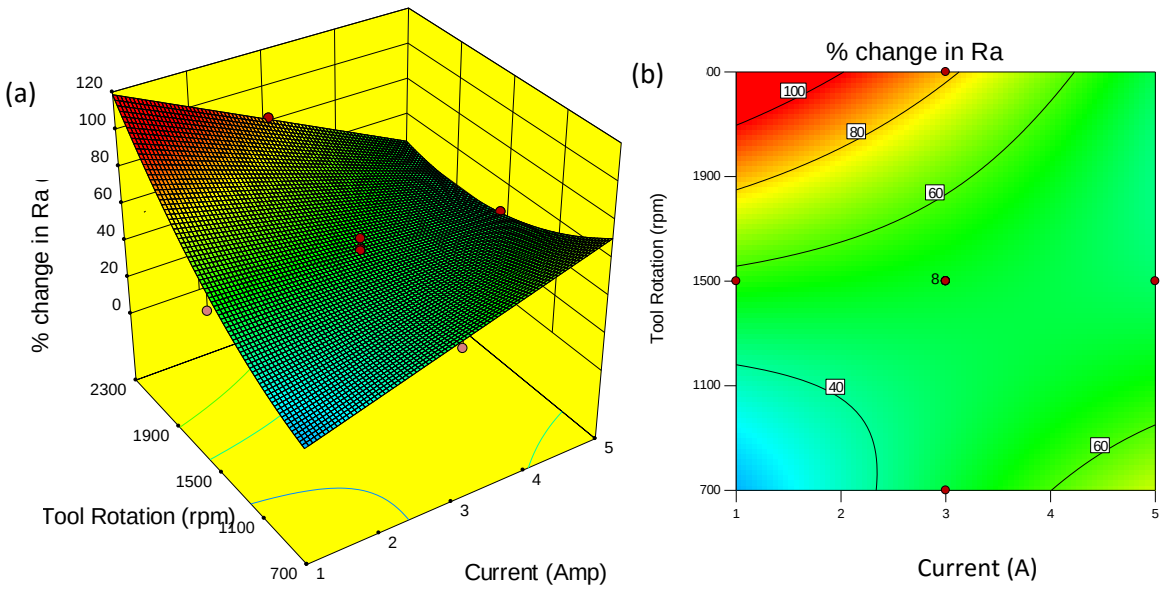

Figure 5.12: (a) 3D plot and (b) contour plot showing the effect of interaction of current and tool rotation

5.5.7 Effect of Interaction of Current and Feed Rate

The effect of interaction of current and feed rate on percentage change in *Ra* value at 1500 rpm tool rotation, 20% abrasives concentration and 20% CIP concentration is shown in Fig. 5.13.

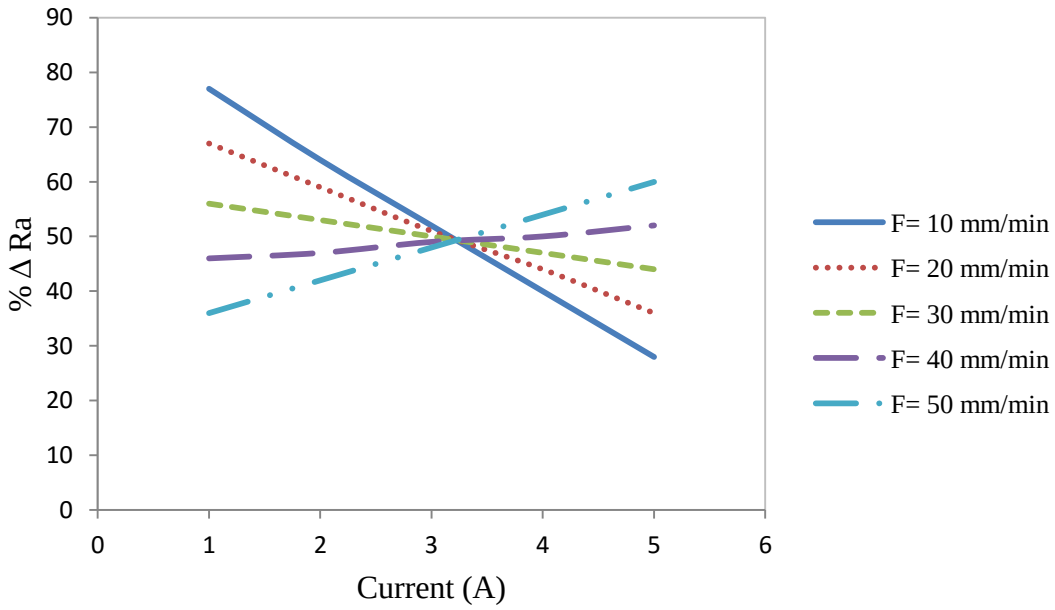

Figure 5.13: Effect of interaction of current and feed on the percent change in roughness

From Fig. 5.13 it is clear that for obtaining required roughness values, lower values of current require lower feed rates while higher values of current require higher feed rates. If feed rate has a higher value that means the tool has lesser time on a particular area of the workpiece surface whereas if the feed rate has a lower value that mean the tool will have more time on a particular area on the workpiece surface. If the value of current is high that means the indentation force is high and it will remove material at a higher rate from the surface of the workpiece and thus higher feed rates are suitable. However for lower values of current the feed required is very low as the time required by the tool on a particular area of workpiece surface is more. Comparing the two cases of higher and lower values of current, it can be observed that lower values of current with lower feed show better reduction as compared with higher values of current with lower feed rates. Another observation that was made from the results was that, the percentage change in roughness was more in case of lower current values as compared with higher current values. The reference for the same can be taken from chapter 5.5.1 and chapter 5.5.6. Better understanding can be made from Fig. 5.14 which shows the 3D plot and

contour plot for the interaction of current and feed rate. It can be clearly observed from Fig. 5.14 (b) that at the lower left corner and at upper right corner areas of the contour plot the percentage change in roughness is more that are the area of low current with low feed and high current with high feed.

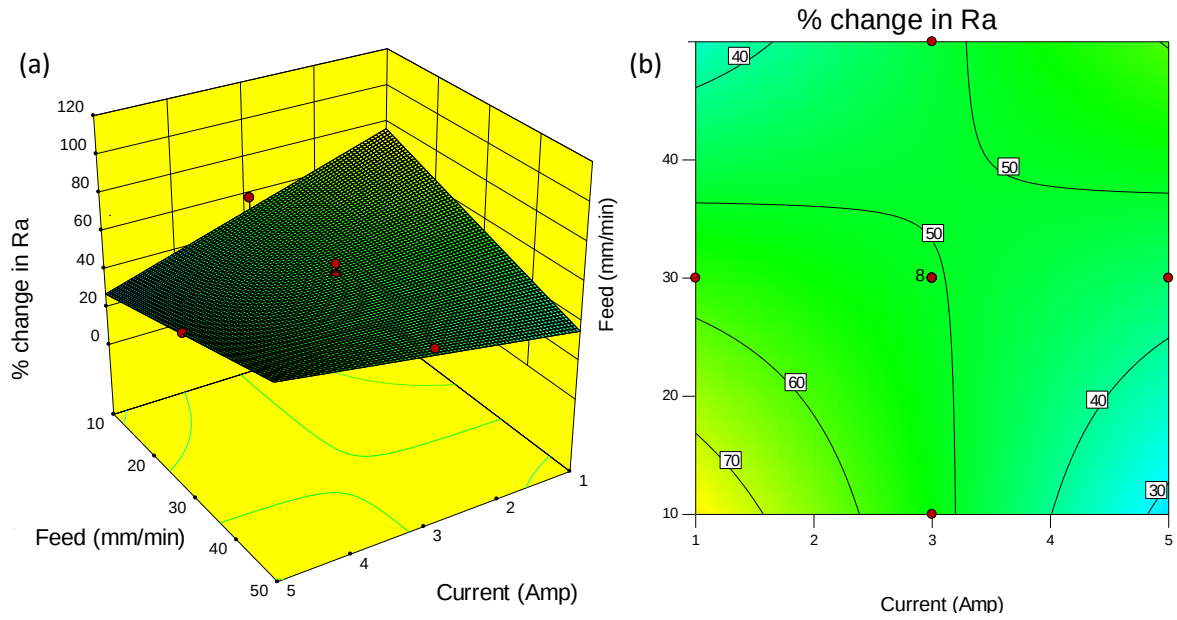

Figure 5.14: (a) 3D plot and (b) contour plot of interaction of current and feed rate

5.5.8 Effect of Interaction of Tool Rotation and Abrasive Concentration

The effect of interaction of tool rotation and abrasive concentration on percentage change in *Ra* value at 3A current, 30 mm/min feed and 20% CIP concentration is shown in Fig. 5.15.

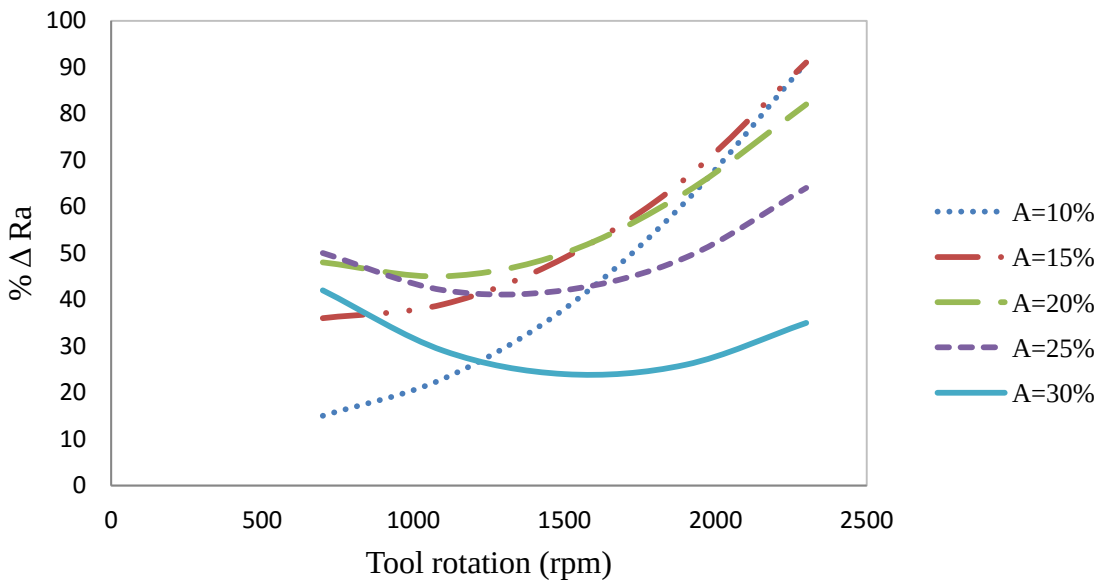

Figure 5.15: Effect of interaction of tool rotation and abrasive concentration on % ΔRa

A very complex effect of abrasive and tool rotation was observed. It was observed that with high values of abrasive concentration (25% and 30%) as the tool rotation speed was increased, the percentage reduction in roughness value first decreased and then increased. This happened because for some range of tool rotation (700 rpm to 1500 rpm) the excess abrasive particles (for 20% CIP concentration) were not leaving the fluid and were scratching the work surface. But when the tool rotation became very high (above 1500 rpm) the excess abrasive particles were thrown out of action and the finishing operation was dominated by the active abrasive particles only. The excess abrasive particles are referred to those which are not properly gripped in the CIP chains because of high concentration of abrasives for a given concentration of CIP. For a particular concentration of CIP in the MR polishing fluid when the abrasive concentration exceeded a certain value, the number of loose abrasive particles increased and with the centrifugal force applied by high tool rotation speed, the value of percentage reduction decreased. However for the same concentration of CIPs, when the concentration of abrasives was low or optimum, the abrasives were tightly gripped in between the CIP chains and with the help of high rotational force generated by the high tool rotation

speed, the active abrasive particles were able to chip off the material from the surface of the workpiece. Thus the percentage change in roughness was high.

5.5.9 Effect of Interaction of Tool Rotation and CIP Concentration

The effect of interaction of tool rotation and CIP concentration on percentage change in R*a* value at 3A current, 30 mm/min feed and 20% abrasive concentration is shown in Fig. 5.16.

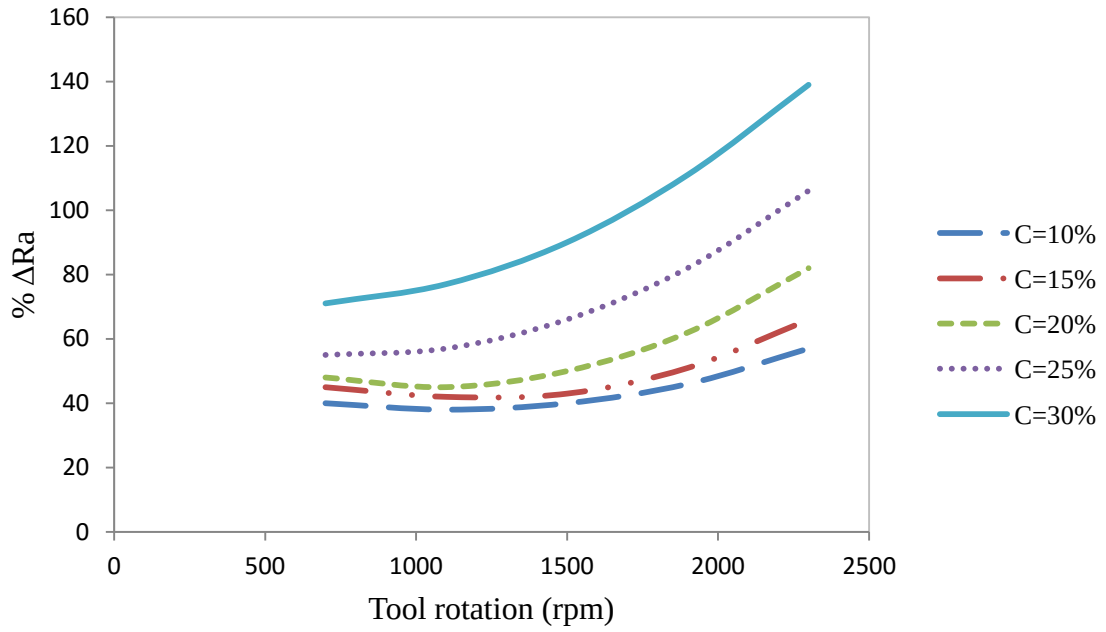

Figure 5.16: Effect of interaction of tool rotation and CIP concentration on % ΔRa

As the CIP concentration increases, the abrasives (fixed concentration for this particular observation) are gripped in a better way in the CIP chains. Now because of better gripping, the number of loose abrasive particles decrease and better finish can be obtained. As the tool rotational speed is increased with increase in CIP concentration, the rotational force generated by high tool rotation speed helps in creating sufficient shearing force and with tightly gripped abrasives (because of increased CIP concentration) the shear strength of the of the fluid increases. Both these factors help in increasing the percentage change in roughness value. A better and easy observation can be made from the 3D and contour plots as shown in Fig. 5.17. It can be clearly observed that the percentage change in roughness is higher at the top right corner of the contour plot where the values of CIP concentration and tool rotation are high.

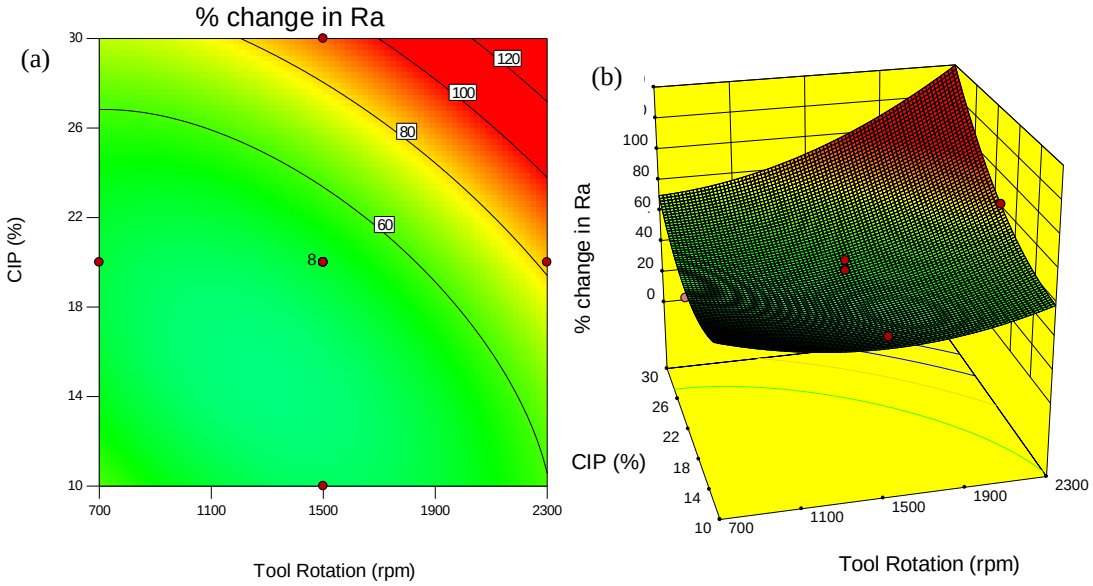

Figure 5.17: (a) contour plot and (b) 3D plot of the effect of interaction of tool rotation and CIP concentration

5.5.10 Effect of Interaction Feed Rate and Abrasives Concentration

The effect of interaction of feed rate and abrasive concentration on percentage change in R*a* value at 3A current, 1500 rpm tool rotation and 20% CIP concentration is shown in Fig. 5.18.

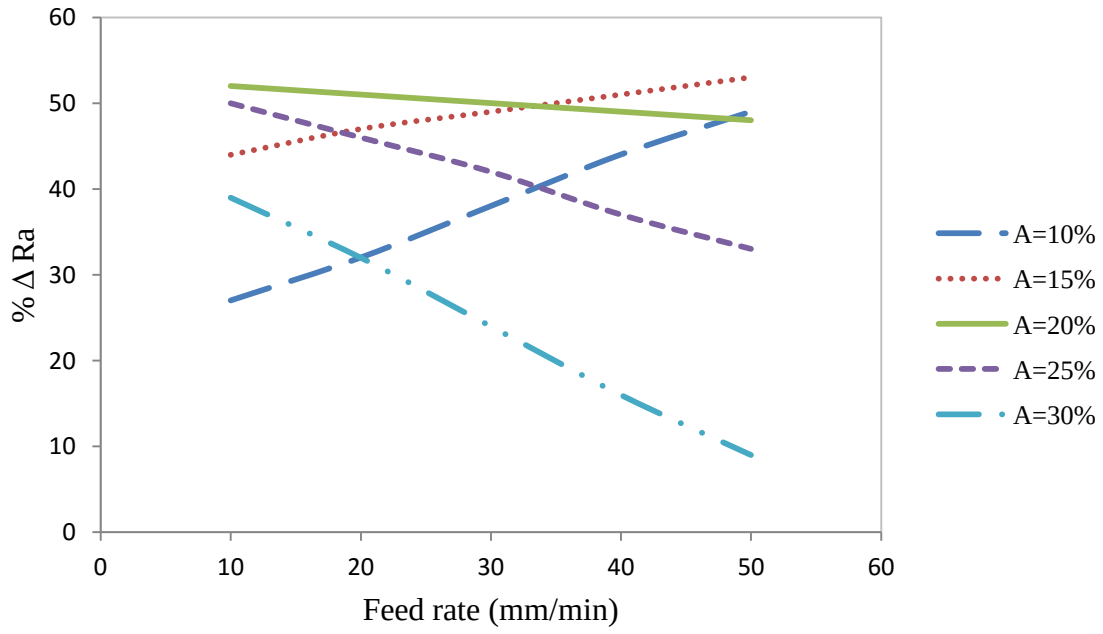

Figure 5.18: Effect of interaction of feed rate and abrasive concentration on % ΔRa

It can be clearly seen from Fig. 5.18 that with increase in feed along with increase in abrasive concentration the percentage reduction in roughness is decreasing. From Table 5.14 it can be observed that the contribution of abrasive concentration is higher than that of feed. So the graph is dominated mostly by the effect of abrasive concentration. When the abrasive concentration and feed were low, the abrasives for a particular amount of CIP concentration were held properly and the tool had sufficient time for finishing on a particular area of workpiece surface. Thus higher percentage change in reduction was obtained. But when the abrasive concentration and feed rate had higher values , neither the abrasives could be help properly for the same value of CIP concentration nor the tool had sufficient time for finishing on a particular area of the workpiece surface, so the percentage change in roughness value decreased.

5.5.11 Effect of Interaction of Feed Rate and CIP Concentration

The effect of interaction of feed rate and CIP concentration on percentage change in *Ra* value at 3A current, 1500 rpm tool rotation and 20% abrasive concentration is shown in Fig. 5.19.

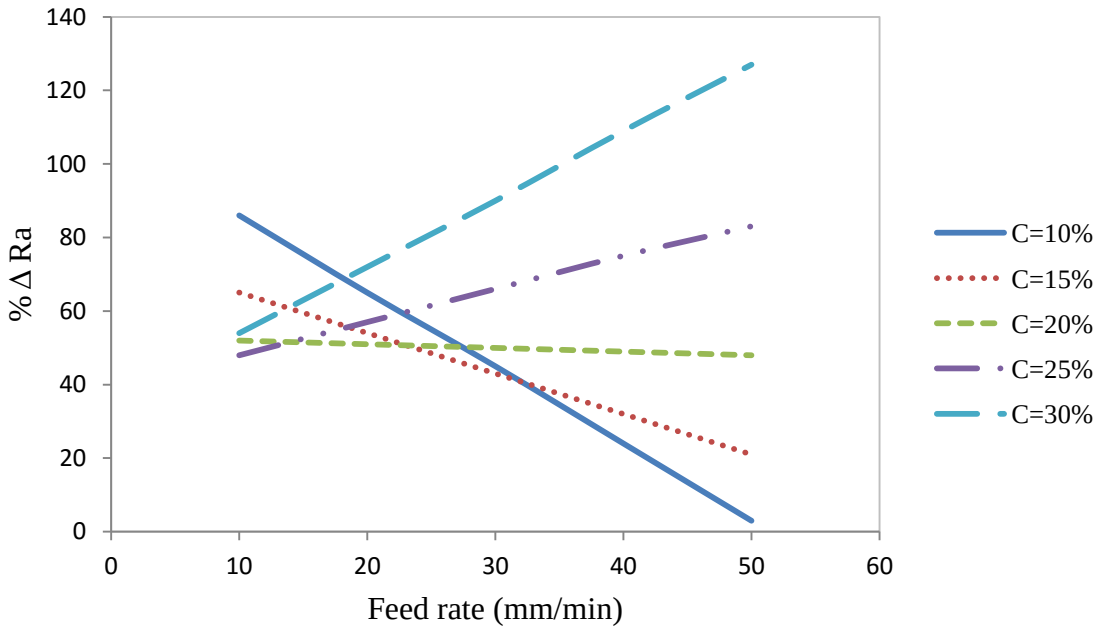

Figure 5.19: Effect of interaction of feed rate and CIP concentration on % ΔRa

For a particular value of abrasive concentration (20% by volume) when the CIPs were too low and the feed rate was high i.e. case of 10% CIP concentration and 50 mm/min feed rate, neither the abrasives could be held properly (because of insufficient CIP concentration) nor the tool had sufficient time to finish a particular area (because of

high feed rate, as discussed in chapter 5.5.3). For the same concentration of abrasives (20% by volume) when the concentration of CIPs was increased; the abrasives were held firmly in the CIP chains and the finishing at higher rates was much better because of tightly gripped active abrasive particles. It must be noted from Table 5.14 that the contribution of feed is almost negligible as compared with that of CIPs. So in this case the effect of abrasives is more predominant than that of feed.

5.5.12 Effect of Interaction of Abrasive Concentration & CIP Concentration

Effect of interaction of abrasive concentration and CIP concentration on percentage reduction in roughness value at 3A current, 1500 rpm tool rotation speed and 30 mm/min feed is shown in Fig. 5.20.

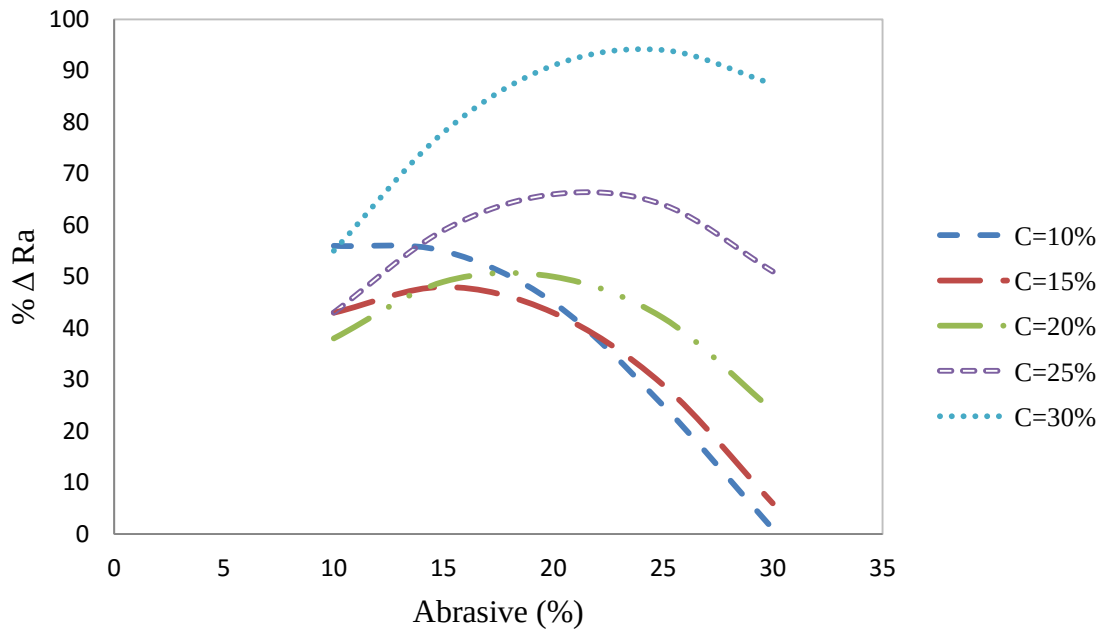

Figure 5.20: Effect of interaction of abrasive concentration and CIP concentration on % ΔRa

Abrasive concentration in the MRP fluid plays a vital role. For obtaining optimum output, the abrasive concentration should be sufficient enough to finish the workpiece surface below the tool tip surface area. For a particular percentage concentration of CIPs, if the abrasive concentration is too high, the CIPs will not be able to hold most of the abrasives particles and thus, the loose abrasive particles form scratches on the surface of workpiece during finishing operation and lead to drop in percentage change in reduction. However, for the same particular percentage concentration of CIPs as in case discussed just now, if the abrasive concentration is too low then the active abrasive particles will be

too low thus resulting in lesser percentage change in reduction of average roughness. For example, with 30 volume % concentration of CIP, if the abrasive concentration is 10 vol. %, then this is a case of too low abrasive concentration whereas with 30 vol. % concentration of CIP and 30 vol. % concentration of abrasive, the case is that of too high abrasive concentration. It is evident from the graph that for obtaining optimum output, as the concentration of CIP is lowered the requirement of abrasives also decreases. For example, for 30 vol. % CIP concentration the abrasive requirement is around 25 vol. % and for 20 vol. % CIP concentration the abrasive concentration requirement is around 17 vol. %.

Among all the experimental parameters the best results were obtained at 2A current, 1900 rpm tool rotation, 40 mm/min feed, 15% abrasive concentration and 25% CIP concentration. The average surface roughness reduced from 330 nm to 30 nm. The percentage change in roughness was observed as 90.81 %. The surface roughness profiles for the initial and final roughness are shown in Fig. 5.21. The workpiece was also examined under SEM as shown in Fig. 5.22.

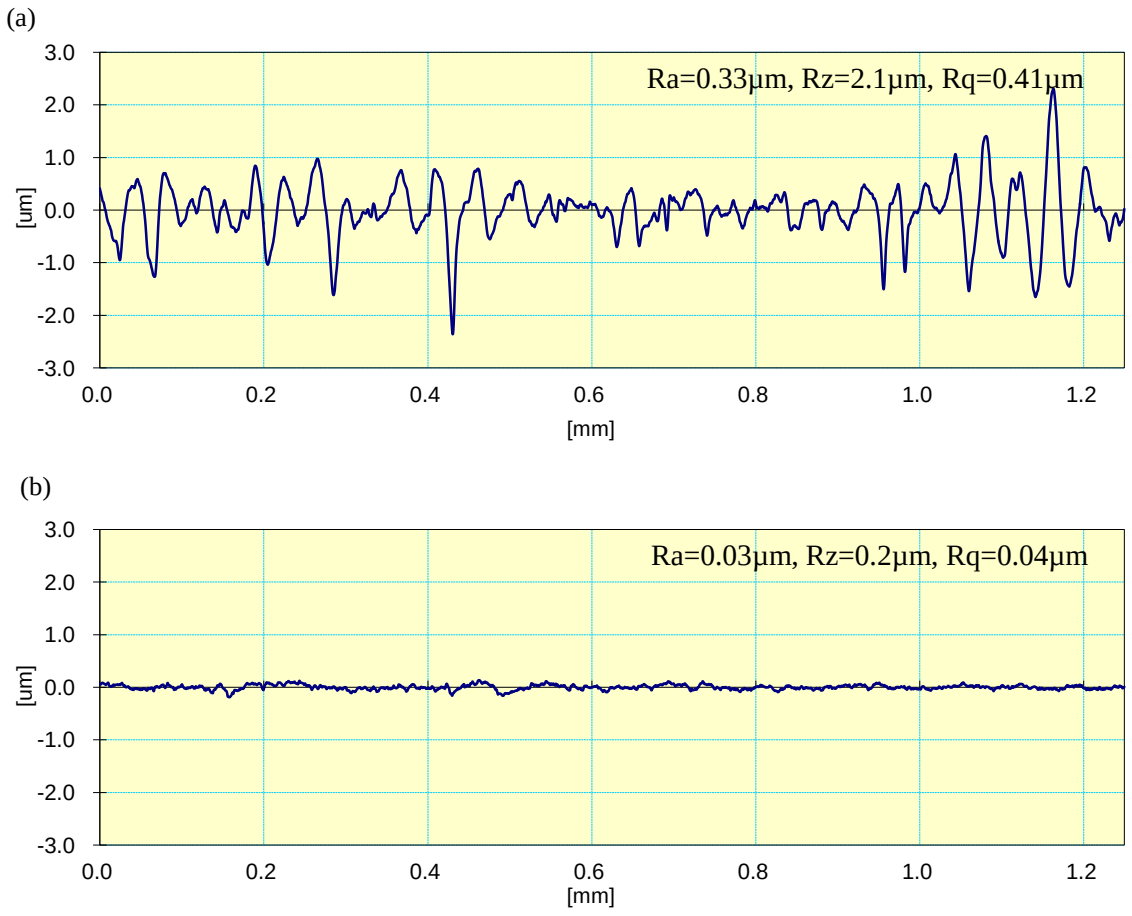

Figure 5.21: Surface roughness profile of the workpiece surface (a) before finishing and (b) after finishing

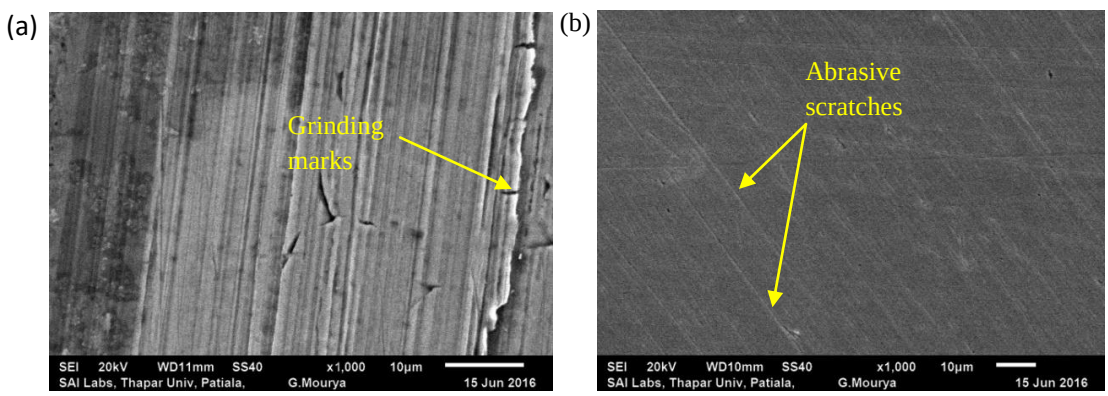

Figure 5.22: Workpiece surface under SEM at 1000X magnification (a) before finishing and (b) after finishing

5.5.13 Confirmation Experiments for Validation of Model

Four experiments were selected from the optimum contour plot for given set of experiments in the design and were compared with the predictions of the formula given in Eq. 5.5. The range of parameters for the experiment and the regression equation generated from the design model is same. Since the equations were derived from quadratic regression fit, therefore confirmation tests were performed to verify their validity. The comparison between the results from the confirmation experiments and the predicted percentage change in surface roughness from the equation is listed in Table 5.15. From the Table 5.15, it can be seen that the error between experimental and predicted values for % ΔRa lie within -7.52 to 6.67%.

Table 5.15: Confirmation tests and the comparison with results

S.No.	Experimental Conditions					Experimental	Predicted	Error
	I	N	F	A	C	ΔRa (%)	ΔRa (%)	(%)
1	2	1100	20	15	25	34.14	32.94	3.51
2	4	1100	20	15	25	30.31	32.59	-7.52
3	2	1900	20	15	25	90.03	84.02	6.67
4	4	1900	20	15	25	51.78	53.54	-3.39

5.5.14 Optimization of Developed Process

As larger percentage change in surface roughness of the finished surface is desired, it is required to maximize the percentage change in surface roughness by optimizing the regression model.

Maximize: % Δ Ra

Subjected to:

$1\ A \leq I \leq 5\ A$

$700\ rpm \leq N \leq 2300\ rpm$

$10 \text{ mm/min} \leq F \leq 50 \text{ mm/min}$

$10\% \leq A \leq 30\%$

$10\% \leq C \leq 30\%$

Using the optimizing tool of the software Design expert 10.0 (trail version), it was found that the best process parameter are 1A current, 2300 rpm tool rotation speed, 50 mm/min feed, 15% abrasive concentration and 30% CIP concentration. Experiment was conducted using the parameters as 1 A current, 2300 rpm tool rotation speed, 50 mm/min feed, 15 % abrasive concentration and 30 % CIP concentration but no significant change was seen. It was observed that at high tool rotational speed such as 2300 rpm, the magnetizing current of 1A was not sufficient enough to hold the MRP fluid at the tip of the surface. The retention force generated by magnetizing current was overpowered by the effect of centrifugal force generated by tool rotation speed. The optimum parameters given by the equation was based on the mathematical model generated, also there was no such experiment in the experimental plan with parameters such as 1A current and tool rotation as 2300 rpm. Thus it seemed like the model was unable to properly calculate the effect of very low current with very high tool rotation on the percentage change in roughness. Thus the new parameters were selected as 2A current, 2300 rpm tool rotational speed, 50 mm/min feed, 15 % abrasive concentration and 30% CIP concentration. These new parameters were selected on the basis of their effect in percentage change in roughness. The data obtained from optimal experimental condition and their comparison with predicted design is listed in Table 5.16. The best average surface finish obtained was 20 nm from 320 nm in just 40 minutes. The minimum roughness value obtained was 20 nm. Figure 5.23 shows the roughness profile before and after finishing the workpiece with optimized parameters. The workpiece before and after applying the BEMRF process were examined under SEM and the have been shown in Fig. 5.24. It was clearly observed that the surface damage done to the workpiece surface due to traditional finishing was completely eliminated. The workpiece surface after finishing appeared free from scratches and cracks.

Table 5.16: Optimal parameter conditions, their response and predicted value as per regression model

S.No.	Process parameters at optimal condition					Predicted	Experimental
	I	N	F	A	C	% Δ Ra	% Δ Ra
1	2	2300	50	15	30	150	92.5

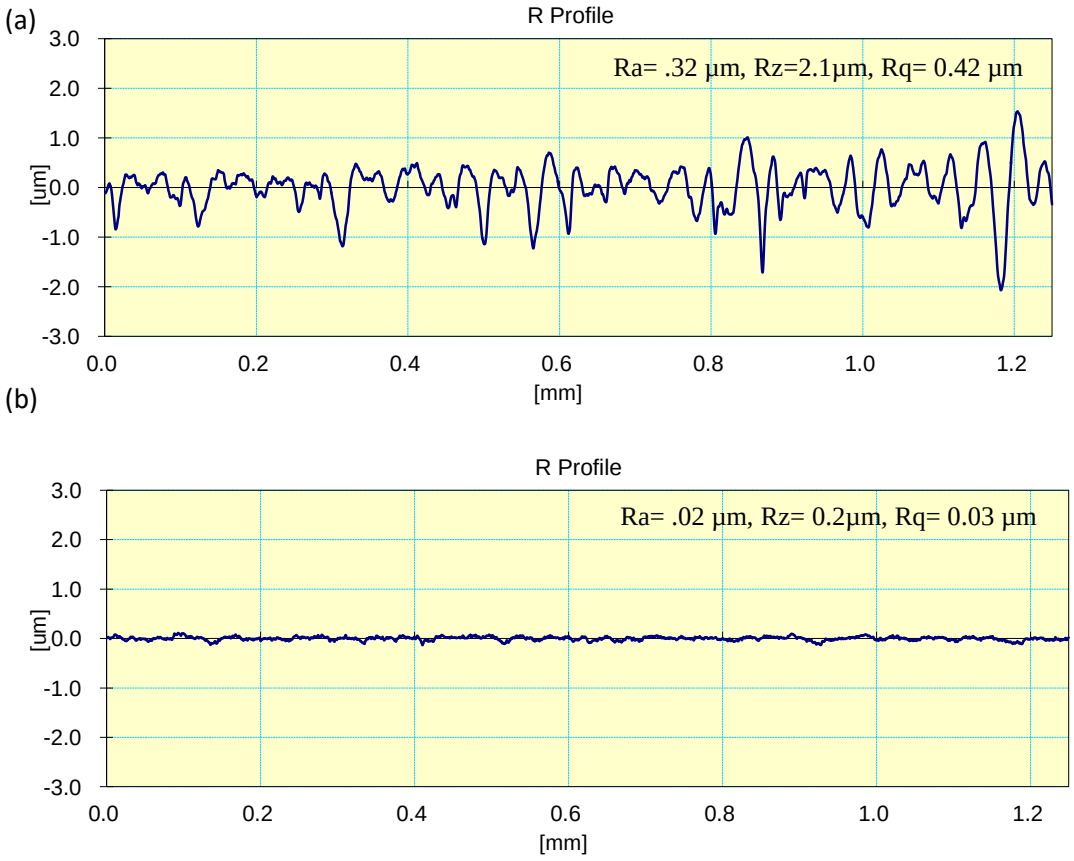

Figure 5.23: Roughness profile from mitutoyo surftest sj-400 (a) before finishing (b) after finishing

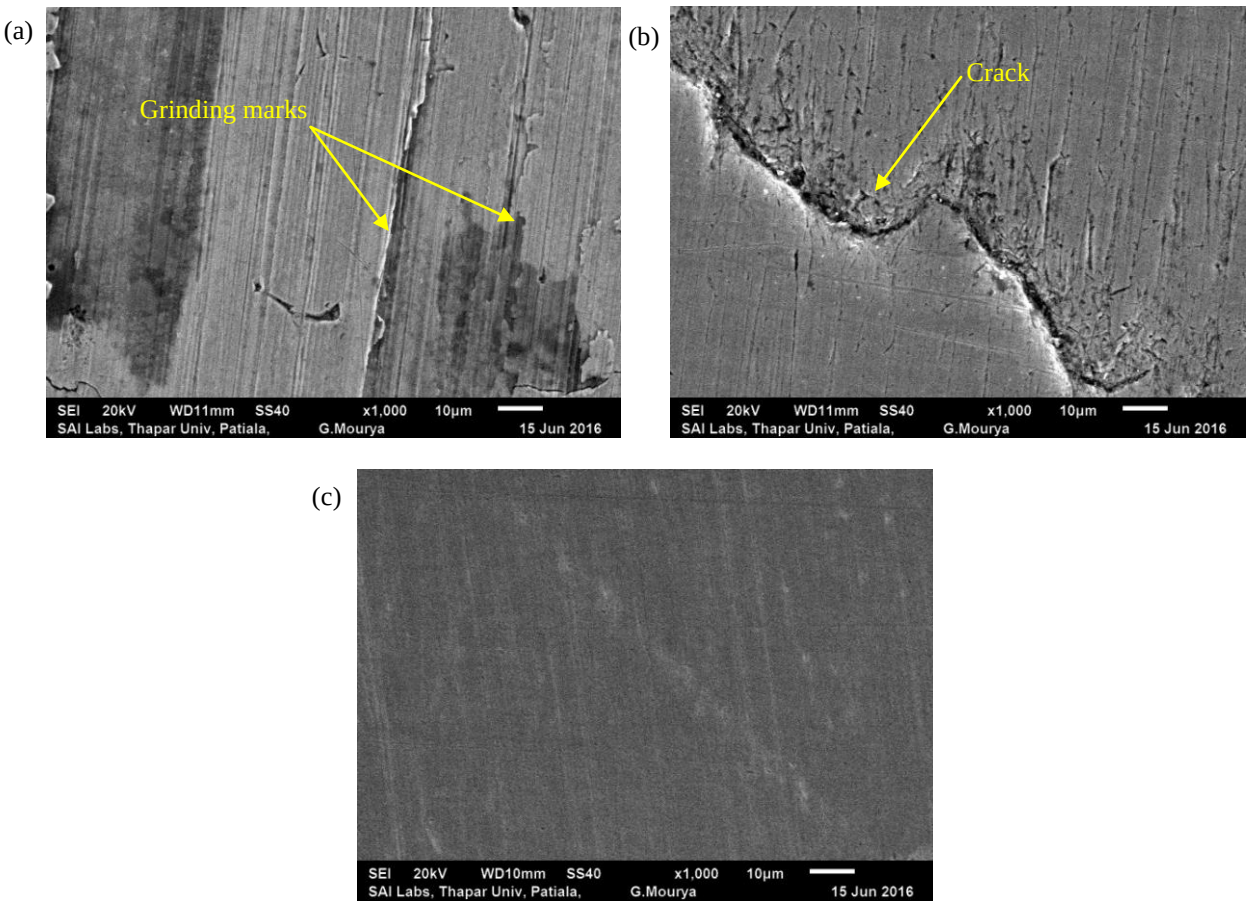

Figure 5.24: SEM images of the workpiece at 1000x magnification (a) after grinding with sub surface damage (b) workpiece surface with cracks due to traditional finishing process and (c) workpiece surface after finishing for 40 minutes with optimized parameters

5.5.15 Performance Evaluation of Ball End Solid Rotating Core Magnetorheological Finishing Process

The performance of ball end solid rotating core magnetorheological finishing process has also been studied. The best finishing conditions of 2 A current, 1900 rpm tool rotation speed, 40 mm/min feed, 15 % abrasive concentration and 25 % CIP concentration was selected for evaluating the performance of this finishing process. Other parameters such as gap, scanning path and temperature were kept constant as similar to the conditions of other experiments. Measurements were taken at fixed intervals of 20 minutes. It is to be noted that same workpiece was used after each successive finishing.

Figure 5.25 shows the effect of finishing time on the roughness value measured every 20 minutes. The initial roughness of the workpiece was found to be 330 nm. It was

found that the surface roughness decreased from 330 nm to 110 nm in first 20 minutes of finishing as shown in Fig. 5.25. After next 20 minutes it was found that roughness value decreased from average roughness of 110 nm to 50 nm. After next 20 minutes, the average surface roughness decreased from 50 nm to 35 nm. After the next interval of 20 minutes it was observed that the roughness value started increasing. The average roughness value increased from 35 nm to 80 nm as shown in Fig. 5.25.

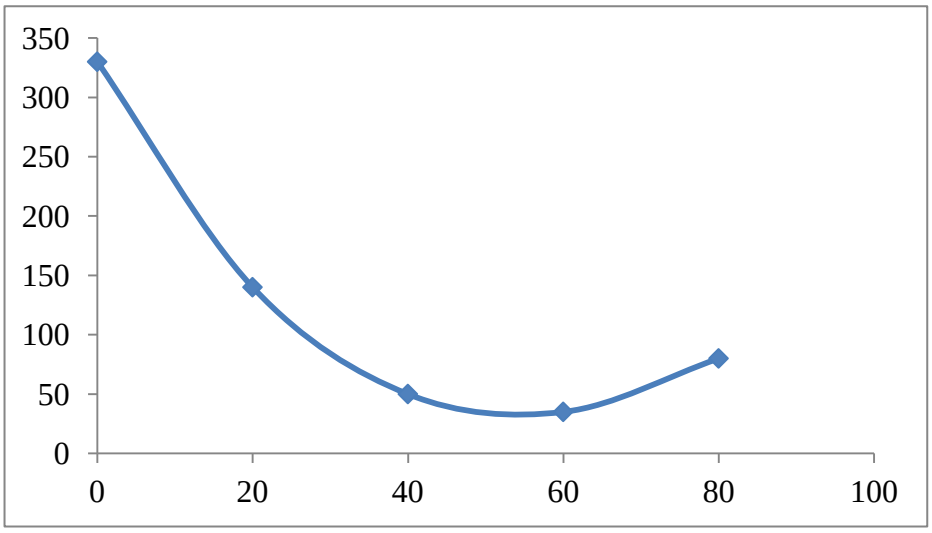

Figure 5.25: Effect of time on % change in roughness of the workpiece surface

5.6 Conclusion

- The effect current, tool rotation, feed rate, abrasive concentration and CIP concentration on the percentage change in roughness was analyzed using response surface methodology.
- Maximum contribution was made by CIP concentration of MRP fluid followed by tool rotation of the core, abrasive concentration of MRP fluid, current and feed rate.
- Maximum percentage change in roughness was observed at 2A current, 1900 rpm tool rotation, 40 mm/min feed, 15% abrasive concentration and 25% CIP concentration. Average roughness of 30 nm was obtained in 60 minutes.
- Optimized parameters within the experimental range were found as 2A current, 2300 rpm, 50 mm/min feed, 15% abrasive concentration and 30% CIP concentration.
- With optimized parameters, the average surface roughness was found as 20 nm in just 40 minutes.

- When the workpiece was subjected to prolonged finishing operation, the surface roughness value increased after achieving a lowest possible surface roughness value at any given parametric condition.

Chapter 6

Conclusions and Scope for Future Work

6.1 Conclusion

Ball end solid rotating core magnetorheological finishing process was used for finishing of hardened EN31 steel. The surface of the workpiece was successfully finished to SPI-A1 standard of society of plastic industries (SPI). Optimisation of process parameters (current, tool rotation, feed, abrasive concentration and CIP concentration) was done using central composite design of response surface method.

- Hardened EN31 steel was finished using ball end solid rotating core magnetorheological finishing process.
- The average surface roughness was obtained as 30 nm in 60 minutes with parameters as 2A current, 1900 rpm tool rotation, 40 mm/min feed, 25 vol. % abrasive concentration and 25 vol. % CIP concentration.
- After optimization, the minimum average surface roughness value was 20 nm in just 40 minutes with process parameters as 2A current, 2300 rpm tool rotation, 50 mm/min feed, 15 vol. % abrasive concentration and 30 vol. % CIP concentration.
- With optimized parameters the working time was minimized by 20 minutes (from 60 minutes to 40 minutes) and the surface roughness of the workpiece also reduced by 10 nm (from 30 nm to 20 nm).
- The grinding marks and cracks generated because of surface grinding were also removed by the present finishing process with optimized parameters and its verification was done using scanning electron microscopy.
- The surface roughness value started increasing after achieving a minimum roughness value as the finishing process was applied for prolonged duration.

6.2 Scope for Future Work

- Effect of abrasive size and CIP size can be studied on the same material using the same process for further better finishing.
- The variation in finishing at the edges of material due to edge effect can be studied.
- The effect of tool scanning path on the surface roughness of a material can also be studied.
- The machine can be utilized for finishing a hardened 3D workpiece by increasing the working axis of machine.

References

Boujelbene, M.; Moisan, A.; Tounsi, N.; Brenier, B. (2004) Productivity enhancement in die and molds manufacturing by use of C^1 continuous tool path. *Internation Journal of Machine Tools and Manufacture,* 44:101-107.

Bedi, T.S.; Singh, A.K. (2015) Magnetorheological methods for nanofinishing-A review, *Particulate Science and Technology,* DOI:10.1080/02726351.2015.1081657.

Chen, M.; Liu, H.;Su, Y.; Yu, B.; Fang, Z. (2016) Design and fabrication of a novel magnetorheological finishing process for small concave surfaces using small ball-end permanent-magnet polishing head. *International Journal of Advance Manufacturing Technology,* 83:823–834.

Harris, D.C. (2011) History of magnetorheological finishing. *Proceedings of the Window and Dome Technologies and Materials, SPIE.* DOI: 10.1117/12.882557.

Das, M.; Jain, V.K.; Ghoshdastidar, P.S. (2008) Fluid flow analysis of magnetorheological abrasive flow finishing process. *International Journal of Machine Tools and Manufacture,* 48: 415-426.

Gheisari, R.; Ghasemi, A.A.; Jafarkarimi, M.; Mohtaram, S. (2014) Experimental studies on the ultra precision finishing of cylindrical surfaces using magnetorheological finishing process. *Production & Manufacturing Research An Open Access Journal,* 2:1, 550-557.

Guo, H.; Wu, Y.; Lu, D.; Fujimoto, M.; Nomura, M. (2014) Effects of pressure and shear stress on material removal rate in ultra-fine polishing of optical glass with magnetic compound fluid slurry. *Journal of Materials Processing Technology,* 214: 2759–2769

Guo, H.; Wu, Y.; Lu, D.; Fujimoto, M.; Nomura, M. (2014) Ultrafine polishing of electroless nickel–phosphorus-plated mold with magnetic compound fluid slurry, *Materials and Manufacturing Processes,* 29:11-12, 1502-1509.

Guo, Y.B.; Liu, C.R. (2002) Mechanical properties of hardened AISI 52100 steel in hard machining process. *Journal of Manufacturing Science and Engineering,* DOI: 10.1115/1.1413775.

Helieby, S.O.A.; Rowe, G.W. (1981) Grinding cracks and microstructural changes in ground steel surfaces. *Metals Technology,* 8: 58-66.

Hong, K.; Cho, Y.; Shin, B.; Cho, M.; Choi, S.; Cho, W.; Jae, J. (2012) Magnetorheological (MR) polishing of alumina-reinforced zirconia ceramics using

diamond abrasives for dental application, *Materials and Manufacturing Processes,* 27:10, 1135-1138.

Jain, V.K. (2008) Abrasive-based nano-finishing techniques. *Machining Science and Technology*, 12: 257-294.

Jain, V.K. (2009) Magnetic field assisted abrasive based micro-/nano-finishing. *Journal of Materials Processing Technology*, 209: 6022-6038.

Jang, K.; Kim, D.; Maeng, S.; Lee, W.; Han, J.; Seok, J.; Je, T.; Kang, S.; Min, B. (2012) Deburring microparts using a magnetorheological fluid, *International Journal of Machine Tools & Manufacture,* 53: 170–175.

Jha, S.; Jain, V.K. (2004) Design and development of magnetorheological abrasive flow finishing process. *International Journal of Machine Tool and Manufacture,* 44(10): 1019-1029.

Jha, S.; Jain, V.K. (2005) Nano finishing techniques. Micro manufacturing and Nano-Technology, 171-195.

Jha, S.; Jain, V.K. (2006) Modelling and simulation of surface roughness in magnetorheological abrasive flow finishing process. *Wear,* 261: 856-866.

Jiang, M.; Komanduri, R. (1998) On the finishing of Si_3N_4 balls for bearing applications. *Wear*, 215: 267-278.

Jiao, L.; Wub,Y.; Wang, X.; Guo, H.; Liang, Z. (2013) Fundamental performance of magnetic compound fluid (MCF) wheel in ultra-fine surface finishing of optical glass. *International Journal of Machine Tools & Manufacture,* 75: 109–118.

Khanna, O.P.; Lal, M. (2010) A text book of Production Technology. Dhanpat Rai publication: New Delhi, India.

Komanduri, R. (1996) On material removal mechanisms in finishing of advanced ceramics and glasses. *CIRP Annals- Manufacturing Technology,*45: 509-514.

Kordonski, W.I.; Jacobs, S.D. (1999) Progress update in magnetorheological finishing. *International Journal of Modern Physics B,* 13: 2205-2212.

Kordonski, W.I.; Golini, D. (1999) Fundamentals of magnetorheological fluid utilization in high precision finishing, *Journal of Intelligent Material Systems and Structures,* 10(9): 683-689.

Kordonski, W. I.; Shorey, A.B.; Tricard, M. (2006) Magnetorheological jet finishing technology. *Transactions of ASME,* 128: 20-26.

Lynah, P.; Hoffman, P.R. (1989) Machining metals handbook, American Society for Metals: Metals Park.

Mateo, M.; Carrion-Vilches, F.J.; Sanes, J.; Bermudez, M.D. (2011) Surface damage of mold steel and its influence on surface roughness of injection molded plastic parts, *Wear*, 271: 2512-2516.

Mori, T.; Hirota, K.; Kawashima, Y. (2003) Clarification of magnetic abrasive finishing mechanism. *Journal of Materials Processing Technology*, 143-144: 682-686.

Monroe, T. (1996) Engine builder's handbook. HP Books, pp-27.

Niranjan, M.S.; Jha, S. (2014) Flow behaviour of bidisperse MR polishing fluid and ball end MR finishing. *Procedia Materials Science*, 6: 798-804.

Niranjan, M.; Jha, S.; Kotnala, R.K. (2014) Ball End magnetorheological finishing using bidisperse magnetorheological polishing fluid. *Materials and Manufacturing Processes*, 29: 487-492.

Owat, S. (2002) Flat surface lapping: Process modeling in an intelligent environment. Doctoral Dissertation, University of Pittsburgh, PA.

Pandey, S.; Kant, S.; Mishra, V.; Khatri, N.; Ramagopal, S.V. (2013) Parametric Optimization of Ball End Magneto Rheological Finishing Process on EN-31. *International Journal of Recent Technology and Engineering*, 2:2, 2277-3878,

Rhoades, L.J. (1988) Abrasive flow machining, *Manufacturing Engineering*, 1: 75-78.

Sadiq, A.; Shunmugan, M.S. (2009*)* Investigation into magnetorheological abrasive honing. *International Journal of Machine Tools and Manufacture*, 49: 554-560.

Sadiq, A.; Shunmugan, M.S. (2010) A novel method to improve finish on non-magnetic surface in magnetorheological abrasive honing process. *Tribology International*, 43: 1122-1126.

Saraeian, P.; Mehr, H.S.; Moradi, B.; Tavakoli, H.; Alrahmani, O.K. (2016) Study of magnetic abrasive finishing for AISI321 stainless steel. *Materials and Manufacturing Processes*, DOI: 10.1080/10426914.2016.1140195.

Saraswathamma, K.; Jha, S.; Rao, P.V. (2015) Experimental investigation into Ball end MagnetorheologicalFinishing of silicon. *Precision Engineering*, 42: 218–223.

Seok, J.; Lee, S.O.; Jang, K.I.; Min, B.K.; Lee, S.J. (2009) Tribological properties of a magnetorheological (MR) fluid in a finishing process. *Tribology Transaction*, 52(4): 460-469.

Schnitzler, G. (2001) What's happening with honing. *Manufacturing Engineering*, 127(5): 70-72, 75-77.

Schmitt, C.; Bahre, D. (2014) Analysis of the process dynamics for the precision honing of bores. *Procedia CIRP*, 17: 692-697.

Shinmura, T.; Takazawa, K.; Hatano, E.; Aizawa, T. (1985) Study on magnetic abrasive process- process principles and finishing possibility. *Bulletin of the Japan Society* of *Precision Engineering,* 19(1): 54-55.

Sidpara, A.; Das, M.; Jain, V.K. (2009) Rheological characterization of magnetorheological finishing fluid. *Materials and Manufacturing Processes,* 24(2): 1467-1478.

Sidpara, A.; Jain, V.K. (2011) Experimental investigations into forces during magnetorheological fluid based finishing process. *International Journal of Machine Tools and Manufacture,* 51: 358-362.

Sidpara, A.; Jain, V.K. (2011) Experimental investigations into forces during magnetorheological fluid based finishing process. *International Journal of Machine Tools and Manufacture,* 51: 358-362.

Singh, A.K.; Jha, S.; Pandey, P.M. (2011) Design and development of nanofinishing process for 3D surfaces using ball end MR finishing tool. *International Journal of Machine Tools and Manufacture,* 51: 142-151.

Singh, A.K.; Jha, S.; Pandey, P.M. (2012) Nanofinishing of fused silica glass using ball end magnetorheological finishing tool. *Materials and Manufacturing Processes,* 27: 1139-1144.

Singh, A.K.; Jha, S.; Pandey, P.M. (2012) Nanofinishing of a typical 3D ferromagnetic workpiece using ball end magnetorheological finishing process. *International Journal of Machine Tools & Manufacture* 63: 21–31.

Singh, A.K.; Jha, S.; Pandey, P.M. (2013) Mechanism of material removal in ball end magnetorheological finishing process. *Wear,* 302: 1180–1191.

Todd, R.; Allen, D.; Alting, L. (1994) Honing. In: Manufacturing Processes, Industrial Press Inc: New York, USA.

Tolinski, M. (2008) High-Performance Honing: Combination of honing process equipment and tooling create highly finished surfaces. *Manufacturing Engineering,* 140(6): 57-68.

Uhlmann, E.; Doits, M.; Schmiedel, C. (2013) Development of a material model for visco-elastic abrasive medium in Abrasive Flow Machining. *Procedia CIRP,* 8: 351-356.

Wang, A.C; Lee, S.J. (2009) Study the characteristics of magnetic finishing with gel abrasive, *International Journal of Machine Tools and Manufactures,* 49: 1063-1069.

Wang, J.; Chen, W.; Han, F. (2015) Study on the magnetorheological finishing method for the WEDMed pierced die cavity. *International Journal of Advance Manufacturing Technology*, 76:1969–1975.

Wang, Y.Q.; Yin, S.H.; Hunag, H.; Chen, F.J.; Deng, G.J. (2015) Magnetorheological polishing using a permanent magnetic yoke with straight air gap for ultra-smooth surface planarization, *Precision Engineering*, 40: 309–317.

Yamaguchi, H.; Shinmura, T. (2004) Internal finishing process for alumina ceramic components by a magnetic field assisted finishing process. *Precision Engineering,* 28: 135-142.

Yin, S.; Shinmura, T. (2004) Vertical-assisted magnetic abrasive finishing and deburring for magnesium alloy. *International Journal of Machine Tools and Manufacture,* 44: 1297-1303.

Web References

http://img.diytrade.com/cdimg/502513/3198071/-1/1246240751/Abaram_Plastic_Mould_Manufacturing_Co_Ltd.jpg